Doctoral Thesis

THE VALUE OF SATELLITE SOIL MOISTURE AND SNOW COVER DATA FOR HYDROLOGICAL MODELLING

submitted in satisfaction of the requirements for the degree of
Doctor of Science
of the Vienna University of Technology, Faculty of Civil Engineering

as part of the
Vienna Doctoral Programme on Water Resource Systems

by

MSc. Bsc. **Rui Tong**
Matrikelnummer 01528750
Karlsplatz 13/222, 1040 Wien, Österreich

Examiner: Univ.Prof. Dipl.-Ing. Dr.techn. **Günter Blöschl**
Institut für Wasserbau und Ingenieurhydrologie
Technische Universität Wien
Karlsplatz 13/222, 1040 Wien, Österreich

Examiner: Prof. Dipl.-Ing. Dr. **Ralf Merz**
Department Catchment Hydrology
Helmholtz-Zentrum für Umweltforschung - UFZ
Theodor-Lieser-Str. 4, 06120 Halle (Saale), Deutschland

Examiner: Prof. Ing. **Ján Szolgay**, PhD.
Department of Land and Water Resources Management
Slovak University of Technology in Bratislava
Radlinského 11, 81005 Bratislava

Vienna, May 2021

Die approbierte gedruckte Originalversion dieser Dissertation ist an der TU Wien Bibliothek verfügbar.
The approved original version of this doctoral thesis is available in print at TU Wien Bibliothek.
TU Bibliothek Your knowledge hub

Vienna Doctoral Programme on Water Resource Systems

Dissertation

DER WERT VON SATELLITEN-BODENFEUCHTE- UND SCHNEEDECKENDATEN FÜR HYDROLOGISCHE MODELLIERUNG

ausgeführt zum Zwecke der Erlangung des akademischen Grades eines
Doktors der technischen Wissenschaften
eingereicht an der Technischen Universität Wien, Fakultät für Bauingenieurwesen

als Teil des
Doktoratskolleg für Water Resource Systems

von

MSc. Bsc. **Rui Tong**
Matrikelnummer 01528750
Karlsplatz 13/222, 1040 Wien, Österreich

Gutachter: Univ.Prof. Dipl.-Ing. Dr.techn. **Günter Blöschl**
Institut für Wasserbau und Ingenieurhydrologie
Technische Universität Wien
Karlsplatz 13/222, 1040 Wien, Österreich

Gutachter: Prof. Dipl.-Ing. Dr. **Ralf Merz**
Department Catchment Hydrology
Helmholtz-Zentrum für Umweltforschung - UFZ
Theodor-Lieser-Str. 4, 06120 Halle (Saale), Deutschland

Gutachter: Prof. Ing. **Ján Szolgay**, PhD.
Department of Land and Water Resources Management
Slovak University of Technology in Bratislava
Radlinského 11, 81005 Bratislava

Wien, Mai 2021

Die approbierte gedruckte Originalversion dieser Dissertation ist an der TU Wien Bibliothek verfügbar.
The approved original version of this doctoral thesis is available in print at TU Wien Bibliothek.
TU Bibliothek Your knowledge hub

Die approbierte gedruckte Originalversion dieser Dissertation ist an der TU Wien Bibliothek verfügbar.
The approved original version of this doctoral thesis is available in print at TU Wien Bibliothek.

Die approbierte gedruckte Originalversion dieser Dissertation ist an der TU Wien Bibliothek verfügbar.
The approved original version of this doctoral thesis is available in print at TU Wien Bibliothek.
TU Bibliothek WIEN Your knowledge hub

Abstract

Knowledge of the factors controlling the spatial and temporal variability of the water balance components at the regional scale is essential for solving a range of practical problems in society, management and planning. One way of improving our understanding of the interactions between runoff generation processes and catchment response is to examine and evaluate new modelling methods and datasets reflecting the ongoing progress in Earth observations. The recent satellite datasets of snow cover and soil moisture have a finer spatial and temporal resolution, including an improved vegetation parameterization in soil moisture retrieval, and allow a more flexible snow cover mapping.

The main objective of this thesis is to examine whether and how the most recent satellite products of snow cover (MODIS) and soil moisture (S1ASCAT) improve the mapping and simulation of water balance components at the regional scale, and the prediction of snow cover, soil moisture and runoff at ungauged sites. The thesis intends to advance the understanding of the spatial and temporal variability of suitable reflectance thresholds for snow cover mapping and to examine to what extent the combined use of satellite products improves the calibration and validation of conceptual hydrologic models and the prediction of runoff hydrographs at ungauged sites.

The thesis is organized into five chapters. Chapter 1 presents the main objectives and introduces the research context for the following chapters. Chapter 2 examines whether and how the new MODIS datasets improve snow cover mapping at the regional scale. The previous versions of MODIS snow cover products had classified snow by globally fixed reflectance thresholds (termed the Normalized Difference Snow Index, NDSI). Chapter 2 investigates the sensitivity and accuracy of varying NDSI thresholds and compares the results of snow cover mapping with a former classification based on a fixed NDSI threshold (NDSI=0.4). The accuracy is tested for Aqua (MYD10A1) and Terra (MOD10A1) daily snow cover products by using daily snow depth observations at 665 climate stations in Austria in 2002 - 2014. The results show that the accuracy of the new mapping approach is greater than 97% (97.4% for Terra and 97.6% for Aqua) in Austria. The new optimized thresholds vary seasonally, decrease with increasing elevation and are lower in forested than in open land cover settings. The results show that the optimized NDSI thresholds improve regional snow cover mapping by 3-10% in forested regions above 900m a.s.l. from January to March.

Chapter 3 examines the potential of new satellite datasets of snow cover (MODIS) and soil moisture (S1ASCAT) for multiple objective calibrations of a conceptual hydrologic model. The analysis is performed in 213 catchments in Austria for the period 2000–2014. The results show that the combined use of snow cover and soil moisture improves hydrological model simulations of soil moisture and snow simulations to almost the same extent and outperforms simulations based on traditional calibration to runoff only. The improvements of both runoff and soil moisture model efficiencies are larger in low elevation and agricultural catchments than in alpine catchments. The results show that the median soil moisture correlation between hydrologic model outputs and ASCAT soil water index is 0.4 to 0.52 (depending on the calibration variant), which is significantly larger than the median of 0.26 found in previous studies using the coarser ERS scatterometer data. This reflects improvements both in the

instrument specifications, i.e. better temporal and spatial sampling, higher radiometric accuracy, and the retrieval algorithm.

Chapter 4 investigates whether and to what extent the spatial transfer of model parameters, calibrated in Chapter 3, impacts the prediction of runoff hydrographs, soil moisture, and snow cover in ungauged catchments. For the transfer of model parameters, eight regionalization methods (global and local variants of arithmetic mean, regression, spatial proximity, and similarity) are examined in two periods, i.e., the period in which the model is calibrated (2000-2010) and an independent validation period (2010-2014). The predictive accuracy is evaluated by leave-one-out cross-validation. The results show that the method by which the model is calibrated in the gauged catchment has a larger impact on runoff prediction accuracy in the ungauged catchments than the choice of the parameter transfer method. The best transfer methods are global and local similarity and the kriging approach. In the lowland catchments, the median of soil moisture correlation ranges between 0.62 and 0.70 for these methods. A comparison of transfer methods based on model parameters calibrated to runoff, snow cover, and soil moisture with those based on parameters calibrated to runoff only indicates that the performance of simulating runoff is similar, but the simulation of soil moisture and snow cover will be further improved if the multi-objective approach is applied for the parameter calibration.

Remotely sensed products have been applied in hydrologic research for decades, and their accuracy is continually improving. The results of this thesis highlight the importance of satellite soil moisture and snow cover data for hydrological applications. There is generally a lot of value in using remotely sensed data in the calibration of the parameters of hydrological models. The improvement in model predictions of snow, soil moisture and runoff in the ungauged catchment is significant. Thus, their use is an important contribution to mitigating water disasters, managing water resources and optimizing water energy benefits.

Die approbierte gedruckte Originalversion dieser Dissertation ist an der TU Wien Bibliothek verfügbar.
The approved original version of this doctoral thesis is available in print at TU Wien Bibliothek.
TU Bibliothek WIEN Your knowledge hub

Kurzfassung

Die Kenntnis der Faktoren, die die räumliche und zeitliche Variabilität der Wasserhaushaltskomponenten auf regionaler Ebene bestimmen, ist für die Lösung einer Reihe praktischer Probleme in Gesellschaft, Management und Planung von wesentlicher Bedeutung. Eine Möglichkeit, unser Verständnis der Wechselwirkungen zwischen Abflussentstehungsprozessen und Einzugsgebietsreaktionen zu verbessern, besteht darin, neue Modellierungsmethoden und Datensätze zu untersuchen und zu bewerten, die den laufenden Fortschritt bei der Erdbeobachtung widerspiegeln. Die neuesten Satellitendatensätze der Schneedecke und Bodenfeuchte haben eine feinere räumliche und zeitliche Auflösung, enthalten eine verbesserte Vegetationsparameterisierung der Bodenfeuchte und ermöglichen eine flexiblere Kartierung der Schneedecke.

Das Hauptziel dieser Arbeit ist es zu untersuchen, ob und in welcher Weise die neuesten Satellitenprodukte der Schneedecke (MODIS) und der Bodenfeuchtigkeit (

ASCAT) die Kartierung und Simulation von Wasserhaushaltskomponenten auf regionaler Ebene und die Prognose von Schneedecke, Bodenfeuchte und Abfluss in Gebieten ohne Messungen verbessern. Die Arbeit soll das Verständnis der räumlichen und zeitlichen Variabilität geeigneter Grenzwerte der Reflexion für die Kartierung der Schneedecke verbessern und untersuchen, inwieweit die kombinierte Verwendung von Satellitenprodukten die Kalibrierung und Validierung konzeptioneller hydrologischer Modelle und die Vorhersage von Abflussganglinien in unbeobachteten Gebieten verbessert.

Die Arbeit ist in fünf Kapitel gegliedert. Kapitel 1 stellt die Hauptziele der Arbeit und den Forschungskontext der folgenden Kapitel vor. In Kapitel 2 wird untersucht, ob und wie die neuen MODIS-Datensätze die Kartierung der Schneedecke auf regionaler Ebene verbessern. In früheren Versionen von MODIS-Schneedeckenprodukten wurde Schnee anhand global festgelegter Grenzwerte der Reflexion (NDSI, Normalized Difference Snow Index) klassifiziert. Kapitel 2 untersucht die Empfindlichkeit und Genauigkeit variierender NDSI-Grenzwerte und vergleicht die Ergebnisse der Schneedeckenkartierung mit einer früheren Klassifizierung auf der Grundlage eines festen NDSI-Grenzwertes (NDSI = 0,4). Die Genauigkeit wird für tägliche Schneedeckenprodukte von Aqua (MYD10A1) und Terra (MOD10A1) anhand täglicher Schneehöhenbeobachtungen an 665 Klimastationen in Österreich in den Jahren 2002 bis 2014 getestet. Die Ergebnisse zeigen, dass die Genauigkeit des neuen Kartierungsansatzes in Österreich größer als 97% ist (97,4% für Terra und 97,6% für Aqua). Die neuen optimierten Schwellenwerte variieren saisonal, nehmen mit zunehmender Höhe ab und sind in bewaldeten Gebieten niedriger als in unbewaldeten Gebieten. Die Ergebnisse zeigen, dass die optimierten NDSI-Grenzwerte die regionale Schneedeckenkartierung in Waldgebieten über 900 m ü.M. in den Monaten Januar bis März um 3-10% verbessern.

Kapitel 3 untersucht das Potenzial neuer Satellitendatensätze der Schneedecke (MODIS) und der Bodenfeuchtigkeit (S1ASCAT) für die Kalibrierung unter Mehrfachzielsetzung eines konzeptionellen hydrologischen Modells. Die Analyse wird in 213 Einzugsgebieten in Österreich für den Zeitraum 2000–2014 durchgeführt. Die Ergebnisse zeigen, dass die kombinierte Verwendung von Schneebedeckung und Bodenfeuchtigkeit die hydrologischen Modellsimulationen von Bodenfeuchtigkeit und Schnee in etwa gleichem Maße verbessert und

Die approbierte gedruckte Originalversion dieser Dissertation ist an der TU Wien Bibliothek verfügbar.
The approved original version of this doctoral thesis is available in print at TU Wien Bibliothek.
TU Bibliothek Your knowledge hub WIEN

eine höhere Genauigkeit erzielt als solche Simulationen, die auf der herkömmlichen Kalibrierung ausschließlich am Abfluss basieren. Die Verbesserung der Genauigkeit der Abfluss- und Bodenfeuchtemodellierung ist in niedrigen und landwirtschaftlich genutzten Einzugsgebieten größer als in alpinen Einzugsgebieten. Die Ergebnisse zeigen, dass die mittlere Korrelation der Bodenfeuchte zwischen den Ergebnissen des hydrologischen Modells und dem ASCAT-Bodenwasserindex 0,4 bis 0,52 beträgt (abhängig von der Kalibrierungsvariante), was signifikant größer ist als der Median von 0,26, der in früheren Studien unter Verwendung der gröberen ERS-Scatterometerdaten gefunden wurde. Dies spiegelt Verbesserungen sowohl in den Instrumentenspezifikationen (d.h. eine bessere zeitliche und räumliche Auflösung, eine höhere radiometrische Genauigkeit) und im den Analysealgorithmus wider.

In Kapitel 4 wird untersucht, ob und in welcher Weise sich die räumliche Übertragung der in Kapitel 3 kalibrierten Modellparameter auf die Berechnung von Abflussganglinien, Bodenfeuchtigkeit und Schneebedeckung in unbeobachteten Einzugsgebieten auswirkt. Für die Übertragung der Modellparameter werden acht Regionalisierungsmethoden (globale und lokale Varianten des arithmetischen Mittelwerts, der Regression, der räumlichen Nähe und der Ähnlichkeit) in zwei Zeiträumen untersucht, d.h. im Kalibrierungszeitraum (2000-2010) und in einem unabhängigen Validierungszeitraum (2010-2014). Die Vorhersagegenauigkeit wird durch Kreuzvalidierung bewertet. Die Ergebnisse zeigen, dass die Methode, mit der das Modell im Einzugsgebiet mit Pegelmessungen kalibriert wird, einen größeren Einfluss auf die Genauigkeit der Abflussberechnung in den unbeobachteten Einzugsgebieten hat als die Wahl der Parameterübertragungsmethode. Die besten Übertragungsmethoden sind globale und lokale Ähnlichkeit und der Kriging-Ansatz. In den Tieflandeinzugsgebieten liegt der Median der Bodenfeuchtigkeitskorrelation für diese Methoden zwischen 0,62 und 0,70. Ein Vergleich der Übertragungsmethoden basierend auf Modellparametern, die an Abfluss, Schneebedeckung und Bodenfeuchtigkeit kalibriert sind, mit denen, die auf Parametern basieren, die nur am Abfluss kalibriert sind, zeigt, dass die Qualität der Abflusssimulationen ähnlich ist, die Simulation der Bodenfeuchtigkeit und der Schneedecke jedoch weiter verbessert wird, wenn eine Mehrfachzielsetzung bei der Parameterkalibrierung zum Einsatz kommt.

Fernerkundungsprodukte werden seit Jahrzehnten in der hydrologischen Forschung eingesetzt und ihre Genauigkeit verbessert sich kontinuierlich. Die Ergebnisse dieser Arbeit unterstreichen die Bedeutung von Satelliten-Bodenfeuchtigkeits- und Schneedeckendaten für hydrologische Anwendungen. Die Verwendung von Fernerkundungsdaten bei der Kalibrierung der Parameter hydrologischer Modelle ist im Allgemeinen von großem Wert. Die Verbesserung der Simulationen von Schnee, Bodenfeuchtigkeit und Abfluss in Einzugsgebieten ohne Messungen ist signifikant. Ihre Verwendung ist daher ein wichtiger Beitrag zum Disastermanagement, zur Bewirtschaftung der Wasserressourcen und zur Optimierung der Wasserkraftnutzung.

Die approbierte gedruckte Originalversion dieser Dissertation ist an der TU Wien Bibliothek verfügbar.
The approved original version of this doctoral thesis is available in print at TU Wien Bibliothek.
TU Bibliothek Your knowledge hub WIEN

Acknowledgment

The financial support for this thesis was provided by the Austrian Science Funds (FWF) as part of the Vienna Doctoral Programme on Water Resource Systems (DK W1219-N28), the Austrian Research Promotion Agency (FFG) through the BMon project (Contract No. 866031), SAIA Project Nr. 2019-10-15-002 and VEGA Scientific Grant Agency Grant No. 1/0632/19, and the China Scholarship Council (CSC, 201506710071).

I would like to express my sincere gratitude to Prof. Günter Blöschl for letting me be involved in the doctoral programme and supervising my research. His thoughtful and encouraging words through the successes and challenges of my research are always beneficial. I am very grateful to Prof. Juraj Parajka for his detailed suggestions at any time with kindness and enthusiasm. I would also like to thank Dr. Jürgen Komma who is always available to discuss the hydrological model with me. Many thanks to the colleagues in the doctoral programme for the good atmosphere and working collaborations, especially to Isabella Pfeil, Dr. Mariette Vreugdenhil, and Prof. Wolfgang Wagner in the geodesy department for their contributions to improve the satellite soil moisture products and the help to my study. A special thank you goes to Dr. Borbála Széles, who helped me a lot with designing the methodologies and validating the results for part of this thesis.

I would like to thank Prof. Liliang Ren from Hohai University of China who recommended me to study hydrology in Austria.

I would like to thank my friends who were studying, travelling, and keeping accompany with me during the happy and difficult times.

I would like to thank my parents for giving me a very good growth environment and letting me freely pursue my dream.

Die approbierte gedruckte Originalversion dieser Dissertation ist an der TU Wien Bibliothek verfügbar.
The approved original version of this doctoral thesis is available in print at TU Wien Bibliothek.
TU WIEN Bibliothek Your knowledge hub

Content

Abstract 4
Kurzfassung 6
Acknowledgment 8
1. Introduction 11
2. Mapping snow cover from daily Collection 6 MODIS products over Austria 14
2.1 Review of MODIS snow cover mapping methods and objective of this chapter 14
2.2 Study area and data 15
2.2.1 Study region 15
2.2.2 MODIS snow cover datasets 16
2.2.3 Daily snow depth measurements at climate stations 16
2.3 Methods 16
2.4 Results 17
2.4.1 Evaluation of the best NDSI threshold 17
2.4.2 Accuracy assessment 24
2.5 Discussion 29
2.6 Conclusions 31
3. The value of ASCAT soil moisture and MODIS snow cover data for calibrating a conceptual hydrologic model 32
3.1 State art of multiple objective calibration of hydrological models and the aim of this chapter 32
3.2 Data 34
3.2.1 ASCAT Soil Water Index product 34
3.2.2 MODIS snow cover product 34
3.2.3 Study area and other data 35
3.3 Methods 37
3.3.1 Conceptual hydrologic model 37
3.3.2 Multiple objective calibration and validation of hydrologic model 39
3.4 Results 41
3.4.1 Performance of multiple objective calibration 41
3.4.2 Variability in calibrated model parameter values 52
3.4.3 Comparison of multiple objective and runoff only calibration efficiencies 55
3.5 Discussion 61
3.6 Conclusions 62

Die approbierte gedruckte Originalversion dieser Dissertation ist an der TU Wien Bibliothek verfügbar.
The approved original version of this doctoral thesis is available in print at TU Wien Bibliothek.
TU Bibliothek Your knowledge hub WIEN

4. The value of satellite soil moisture and snow cover data for the transfer of hydrological model parameters to ungauged sites 64
4.1 Prior knowledge of prediction in ungauged basins and the purpose of this chapter 64
4.2 Method 65
4.2.1 Hydrological model 65
4.2.2 Transfer of model parameters to ungauged sites 67
4.2.3 Evaluation of the prediction accuracy 69
4.3 Data 69
4.3.1 Study region 69
4.3.2 Hydrologic and climate data 70
4.3.3 MODIS snow cover 70
4.3.4 ASCAT soil moisture 71
4.4 Results 71
4.4.1 Efficiency of transfer methods to simulate runoff 71
4.4.2 Efficiency of transfer methods to simulate soil moisture 74
4.4.3 Efficiency of transfer methods to simulate snow cover 77
4.4.4 Improvement of multi objective regionalization vs runoff only regionalization 80
4.5 Discussion 83
4.6 Conclusions 84
5. Overall conclusions and outlook 86
References 89

Die approbierte gedruckte Originalversion dieser Dissertation ist an der TU Wien Bibliothek verfügbar.
The approved original version of this doctoral thesis is available in print at TU Wien Bibliothek.
TU WIEN Bibliothek Your knowledge hub

1. Introduction

Understanding the processes and factors controlling the spatial and temporal variability of water balance components at the regional scale is essential for solving a range of practical problems in society, management, and planning. From the scientific perspective, the interactions between runoff generation processes and catchment response are still part of the unresolved problems in hydrology (Blöschl et al., 2019). One way of improving our knowledge on this topic is to examine and evaluate new modelling methods and datasets reflecting the ongoing progress in Earth observations. There exists a variety of modelling concepts and estimation methods. Notwithstanding their usefulness, the resulting simulations of the water balance components are subject to uncertainty due to uncertainty in model inputs, parameter estimation and model structure.

Previous studies have demonstrated that constraining hydrologic models to multiple objectives can reduce modelling uncertainty and improve prediction accuracy (e.g. Efstratiadis and Koutsoyiannis, 2010). These studies showed that additional information typically improves the spatial and/or temporal patterns of internal state variables and fluxes but does not necessarily improve the efficiency of simulating runoff. Most of the studies reported a minor degradation of runoff model efficiency while the internal consistency of the models improved. Only a few studies examined the value of combining more variables in multiple objective calibrations (Milzow et al., 2011; Kunnath-Poovakka et al., 2016; López et al., 2017; Nijzink et al., 2018; Demirel et al., 2019; Szeles et al., 2020, 2021). Their results indicate that the multi-source combination of different characteristics can reduce the parameter uncertainty, particularly in data-poor regions. However, the exact characteristics and spatial and temporal resolutions needed to improve the estimation of the water balance components are still not well understood.

The recent advances in remote sensing and new satellite missions have improved the spatial and temporal resolutions of satellite datasets and their regional accuracy. Moderate Resolution Imaging Spectroradiometer (MODIS) snow cover products have been applied in hydrological modelling and snow cover mapping. The long observation period, daily temporal and 500m spatial resolutions make them very attractive for global or regional hydrological applications. Yet, the previous studies indicate that the mapping algorithm can still be improved and adjusted to regional conditions (Wang et al., 2010; Zhang et al., 2019; Da Ronco et al., 2020). The latest version (MODIS, V006) aims to make the snow cover mapping more flexible, providing the user with the original retrieval indices based on reflectance observations on different bands. Such improvement allows to regionally or seasonally adjust the snow cover mapping instead of using a fixed snow classification approach globally. The new satellite datasets therefore allow but also require the examination and identification of thresholds for the detection of snow cover.

Recent advances in soil moisture mapping allow improvements in soil moisture estimation under vegetation and provide soil moisture estimates with higher spatial and temporal resolutions (Bauer-Marschallinger et al., 2019; Hahn et al., 2020; Beck et al., 2021). While the former spatial resolution of the scatterometer was 25km, the recent satellite Sentinel missions allow downscaling of Advanced Scatterometer (ASCAT) observations to finer scale (i.e. 500m), as well as to implement a new vegetation correction parameterization (Hahn et al., 2020). It is interesting to examine whether and how these advances can be applied to improve hydrological modelling.

The main objective of this thesis is to examine the value of the most recent satellite products of snow cover and soil moisture for mapping and simulating water balance components at the regional scale and the prediction of snow cover, soil moisture and runoff at ungauged sites. The specific research aims are to understand:

Die approbierte gedruckte Originalversion dieser Dissertation ist an der TU Wien Bibliothek verfügbar.
The approved original version of this doctoral thesis is available in print at TU Wien Bibliothek.
TU Bibliothek Your knowledge hub WIEN

1. Whether and how the new MODIS datasets improve snow cover mapping at the regional scale;
2. The potential of using the new MODIS snow cover and ASCAT Soil Water Index for multiple objective calibration and validation of a conceptual hydrologic model; and
3. The value of using satellite data of snow cover and soil moisture to predict runoff hydrographs in ungauged catchments.

The research part of the thesis is organized into three chapters (Chapter 2-4). Chapter 2 examines the snow cover mapping accuracy of the new version of MODIS datasets. The new daily snow cover products provide a normalized snow difference index instead of a fixed snow cover classification used in the previous versions. The aim of Chapter 2 is to find the optimal thresholds of the snow index for snow cover classification and to understand how the optimal thresholds vary in time and space. The accuracy of new snow cover maps is evaluated for two satellite products (Terra and Aqua) by using daily snow depth observations at 665 climate stations in Austria.

The research question of Chapter 3 is how to include the new satellite soil moisture and snow cover dataset in calibrating a hydrologic model. The idea is to test different calibration strategies that use soil moisture or snow cover data or their combination in a multiple-objective calibration. The aim is to investigate how different weights of runoff, soil moisture and snow cover in the objective function impact the performance of the hydrologic model. The model efficiency is evaluated not only in terms of daily runoff but also in terms of soil moisture correlation or snow cover model efficiency. The analysis is carried out for a large sample of 213 catchments situated in different physiographic settings in Austria.

Chapter 4 builds on the results of Chapter 3 and investigates whether and how the model parameters calibrated in Chapter 3 can improve the prediction of daily hydrographs in ungauged catchments (i.e. at locations without runoff measurements). The main aim is to test various methods for transferring model parameters from gauged to ungauged sites and evaluate how parameters obtained by different multiple-objective strategies impact the prediction accuracy of runoff, soil moisture, and snow cover. The analysis is performed for the same dataset of 213 catchments in Austria as examined in Chapter 3.

In all chapters, for the purpose of improving the simulation of hydrological variables from a hydrological model, a new method for mapping snow cover from MODIS satellites is adopted; the new snow cover maps and the latest satellite soil moisture maps with finer spatial resolution are integrated in the calibration of the model parameters; the performance of regionalization methods for the prediction in ungauged basins with the newly derived parameters are investigated. The value of the satellite soil moisture and snow cover data for hydrological modelling is hence examined from different perspectives in the three main chapters (Chapters 2-4) of the thesis.

Finally, Chapter 5 concludes the thesis with a summary of the key findings and a discussion of potential future extensions of the research work and implications for hydrology and water resources management.

The three main chapters of the thesis are based on papers that have been published in or have been submitted to scientific journals as follows:

Die approbierte gedruckte Originalversion dieser Dissertation ist an der TU Wien Bibliothek verfügbar.
The approved original version of this doctoral thesis is available in print at TU Wien Bibliothek.
TU Bibliothek Your knowledge hub WIEN

Tong, R., Parajka, J., Komma, J., Blöschl, G. (2020). Mapping snow cover from daily Collection 6 MODIS products over Austria. *Journal of Hydrology*, 590, 125548. doi:https://doi.org/10.1016/j.jhydrol.2020.125548

Tong, R., Parajka, J., Salentinig, A., Pfeil, I., Komma, J., Széles, B., Kubáň, M., Valent, P., Vreugdenhil, M., Wagner, W., Blöschl, G. (2021). The value of ASCAT soil moisture and MODIS snow cover data for calibrating a conceptual hydrologic model. Hydrol. *Earth Syst. Sci.*, 25(3), 1389-1410. doi:10.5194/hess-25-1389-2021

Tong, R., Parajka, J., Széles, B., Pfeil, I., Vreugdenhil, M., Komma, J., Valent, P., Blöschl, G. (2021). The value of satellite soil moisture and snow cover data for the transfer of hydrological model parameters to ungauged sites. *Hydrol. Earth Syst. Sci. Discuss.* [preprint], https://doi.org/10.5194/hess-2021-189, in review.

Die approbierte gedruckte Originalversion dieser Dissertation ist an der TU Wien Bibliothek verfügbar.
The approved original version of this doctoral thesis is available in print at TU Wien Bibliothek.
TU Bibliothek Your knowledge hub WIEN

2. Mapping snow cover from daily Collection 6 MODIS products over Austria

The present chapter corresponds to the following scientific publication in its original form:

Tong, R., Parajka, J., Komma, J., & Blöschl, G. (2020). Mapping snow cover from daily Collection 6 MODIS products over Austria. Journal of Hydrology, 590, 125548. doi:https://doi.org/10.1016/j.jhydrol.2020.125548

2.1 Review of MODIS snow cover mapping methods and objective of this chapter

Spatial and temporal patterns of snow cover help to improve our understanding of snowmelt processes, and hence improve runoff prediction during snowmelt (Grayson and Blöschl, 2001). Due to the shortage of in-situ snowpack information for water resource management at the catchment scale, remotely sensed snow cover could be a substitute for in-situ data (Dong, 2018). Optical remote sensing effectively classifies snow cover based on different reflectance of snow and land cover in the visible and shortwave infrared spectrum. The recent satellites (such as Sentinel, Landsat, Terra, Aqua, Meteosat) provide snow cover maps in high temporal (sub-daily to 3 weekly) and spatial (30m – 5km) resolution and are one of the most attractive remote sensed datasets used for hydrological applications (Parajka and Blöschl, 2008a; Parajka et al., 2012).

The MODIS (Moderate Resolution Imaging Spectroradiometer) instrument mounted on board Terra and Aqua satellites has been mapping daily snow cover at 500m spatial resolution globally since 2000 (Terra) and 2002 (Aqua). Hundreds of research papers (https://nsidc.org/data/modis/research.html) have shown that MODIS datasets provide accurate snow cover maps which can be used for mapping of snow cover characteristics and their changes and/or for calibration, validation and assimilation in land surface and hydrologic models. Numerous studies have been conducted to evaluate the MODIS accuracy, either based on comparisons with other satellite-derived products, reanalyses of regional climate simulations or based on comparisons with point ground-based (in situ) snow depth measurements (Parajka et al., 2012). The results of these studies demonstrate that the MODIS overall accuracy during clear sky conditions usually is within the range of 85-99%, and the accuracy is related mainly to land cover (Hall and Riggs, 2007; Coll and Li, 2018), season (Simic et al., 2004; Parajka and Blöschl, 2006), persistency of snow cover (Pu et al., 2007) and snow depth (Xu et al., 2017). Coll and Li (2018) recently found that the foremost control factor of the snow cover mapping accuracy is the land cover type. Some of the validation studies, such as Simic et al. (2004), Ault et al. (2006) and Wang et al. (2008) indicate that the accuracy assessment tends to be sensitive to the snow depth threshold used to determine snow cover in the neighborhood of climate stations. In order to account for the scale gap between the MODIS pixel value and in situ measurements, snow depth thresholds between 1 cm and 4 cm have been used in accuracy assessments. Some of the studies presented a sensitivity analysis investigating the impact of snow depth threshold on the accuracy (Liang et al., 2008; Wang et al., 2008; Gao et al., 2010; Marchane et al., 2015; Yang et al., 2015, Da Ronco et al.,2020), but few have investigated different seasons or land cover categories.

The snow cover mapping algorithm and thus also its accuracy has changed since the launch of the Terra satellite (Hall et al., 2019). The original mapping version (V001) has been replaced

Die approbierte gedruckte Originalversion dieser Dissertation ist an der TU Wien Bibliothek verfügbar.
The approved original version of this doctoral thesis is available in print at TU Wien Bibliothek.
TU Bibliothek Your knowledge hub WIEN

by version (V003) in 2003. The changes include processing refinements, instrument, and calibration stabilization (https://nsidc.org/data/modis/data_versions.html). In the next versions (V004 and V005), further changes of cloud mask, metadata extensions and data format have been implemented. More significant changes were introduced in 2016. These include revisions in atmospheric calibration (Lyapustin et al., 2014), improvements in surface temperature screening (Riggs et al., 2017) and extending the overall quality flagging. From a practical perspective, the most significant change is that C6 (also known as V006) snow cover products do not include binary snow cover information (i.e. whether the pixel is snow covered or not), but Normalized Difference Snow Index (NDSI) values. As indicated in the users' guide, NDSI values from 0.00-1.00 are within the theoretically possible range of snow (Riggs et al., 2016). However, clouds may also have positive NDSI values, which normally ranges from -0.4 to 0.4 (Stillinger et al., 2019). Hence, a lower NDSI value will increase the difficulty of distinguishing cloud from snow. This means that for hydrological applications, the NDSI threshold value indicating whether a pixel is snow covered or not needs to be determined. User defined NDSI thresholds that are suited for the study area, could result in better mapping accuracy. Wang et al. (2010) compared the MODIS snow cover map from Terra using different NDSI thresholds with the Landsat-ETM+ snow cover maps, and found that the relevant NDSI threshold is about 0.36 for the upper Heihe river basin in northwestern China. Zhang et al. (2019) suggested taking different NDSI threshold would improve the accuracy of snow cover data, and they demonstrated that the NDSI threshold 0.10 was more reasonable than 0.40 for use in China. Da Ronco et al. (2020) compared MODIS snow cover maps with 3 NDSI thresholds, 0.10, 0.20 and 0.40, at 7 stations in Italian Alpine catchments, and found that an NDSI threshold of 0.20 is optimal for this region from November to April. However, the fixed NDSI threshold prevented detection of snow cover that had lower NDSI value caused by the seasonally varying canopy or by the complex landscape in the mid-latitude regions.

The main objective of this Chapter is thus to investigate the accuracy and sensitivity of different NDSI thresholds for snow cover mapping from daily C6 MODIS datasets. The aim is to evaluate the spatial and seasonal patterns of the NDSI thresholds in Austria and to analyze the factors that control the mapping accuracy. The results are compared with the assessment based on a fixed NDSI threshold (NDSI=0.4) used in previous versions of the datasets. The snow cover accuracy is evaluated against daily snow depth measurements at 665 climate stations which allows discussing and transferring the findings to similar physiographic mountain and flatland regions. We therefore propose a spatiotemporally dynamic NDSI thresholding method to improve the mapping accuracy of MODIS snow cover products and other NDSI derived products.

2.2 Study area and data

2.2.1 Study region

The study area is Austria. Austria is located in Central Europe and has an area of about 84000 km^2. Topography is characterized by flat or undulating topography in the East and North, and Alpine terrain in the West and South (Figure 2.1). Elevations vary from 115 m a.s.l. to 3800 m a.s.l.. Climatically, Austria is located in a temperate zone, where mean annual precipitation is less than 400 mm/year in the East and more than 2800 mm/year in the West. Land use is mainly agricultural land in the lowlands, mixed and coniferous forests in the medium elevation ranges and alpine vegetation and rocks in elevations above 2000 m a.s.l.. Such diverse physiographic and landscape characteristics allows to consider territory of Austria to be representative for a wider spatial domain with similar physiographic characteristics.

Die approbierte gedruckte Originalversion dieser Dissertation ist an der TU Wien Bibliothek verfügbar.
The approved original version of this doctoral thesis is available in print at TU Wien Bibliothek.
TU Bibliothek Your knowledge hub WIEN

2.2.2 MODIS snow cover datasets

The MODIS snow cover datasets tested in the Chapter are MOD10A1 (Terra) and MYD10A1 (Aqua) products. These are daily snow cover data with 500m spatial resolution available from Aqua (Hall and Riggs, 2016a) and Terra (Hall and Riggs, 2016b) satellites. The study region is covered by two tiles: h18v04 and h19v04 which have been merged and re-projected by MODIS Reprojection Tool (Dwyer and Schmid, 2006). The analysis is based on all available daily images from September 2002 to August 2014.

The MOD10A1 and MYD10A1 datasets provide information about the snow cover in the form of Normalized Difference Snow Index (NDSI) values (Hall and Riggs, 2011). This index compares the difference in the reflectance in the visible (band 4) and shortwave infrared (band 6) part of the spectrum and is estimated as:

NDSI = ((band 4-band 6) / (band 4 + band 6))

If a pixel has NDSI larger than 0.0 then it indicates the presence of some snow. In the former Collection 5 version of the dataset a pixel is identified as snow if NDSI is larger than 0.4. In the previous version of MYD10A1, band 7 was used instead of band 6 because part of the detectors in Aqua band 6 were either nonfunctional or noisy. The newly developed mapping technique (Gladkova et al., 2012) allows relating Aqua MODIS band 6 data to the estimation quality, so in version C6 Aqua and Terra uses the same snow detection method. Compared to version C5, the most recent version of MYD10A1 does not use band 7 to calculate the NDSI.

2.2.3 Daily snow depth measurements at climate stations

The daily snow depths used for validating the MODIS datasets are taken from observations at 665 climate stations (Figure 2.1). The observations are available at the data portal of the Hydrographic Service of Austria (https://ehyd.gv.at/). The snow depth readings represent point measurements at permanent staff gauges (permanently mounted snow stake) daily at 7:00 AM, and total snow depths are reported as centimeter integer values (HZB, 1992). Such measurements represent new snow that has fallen combined with snowpack already covering the ground. The spatial arrangement of the stations indicates that the snow depth measurements cover a wide range of elevation zones of the country, but in the high alpine regions the stations tend to be located at lower elevations, typically in the valleys. As indicated in Parajka and Blöschl (2006), the highest climate station used in this Chapter is at 2290 m a.s.l. which means that approximately 6% of the region is higher and not represented by any climate station. Most of the stations (i.e. n=602) have complete observational records and gaps longer than 5 years occur only for 10 stations.

2.3 Methods

The selection of the best NDSI threshold (BT_{NDSI}) is based on finding the NDSI threshold (T_{NDSI}) that has the maximum snow cover mapping accuracy expressed by the overall accuracy index (OA_T). The OA_T compares snow depth observations at climate stations with pixel values of NDSI and estimates the overall accuracy as:

$$\mathbf{OA_T} = \frac{A+D}{A+B+C+D} \cdot 100\% \qquad (2.1)$$

where A,B,C,D represent the number of cloud-free days in each of the category of confusion matrix (Table 2.1). We tested 100 different T_{NDSI} from 0.01 to 1.0 with a step of 0.01. BT_{NDSI} represents the value with the highest mapping accuracy. The procedure is repeated for five different snow depth thresholds T_{SD} (1cm, 2cm, 3cm, 4cm and 5cm).

Die approbierte gedruckte Originalversion dieser Dissertation ist an der TU Wien Bibliothek verfügbar.
The approved original version of this doctoral thesis is available in print at TU Wien Bibliothek.
TU Bibliothek WIEN Your knowledge hub

The assessment of the best BT_{NDSI} is performed for all individual climate stations, as well as for different groups of stations representing different physiographic conditions. The classification of different elevation, aspect and land use groups is based on previous snow cover and hydrological evaluations in Austria (Parajka et al., 2006, 2009). The assessment is also applied for finding the best BT_{NDSI} for all the stations in the entire time period (September 2002 to August 2014) or for individual stations and individual months of the selected time period.

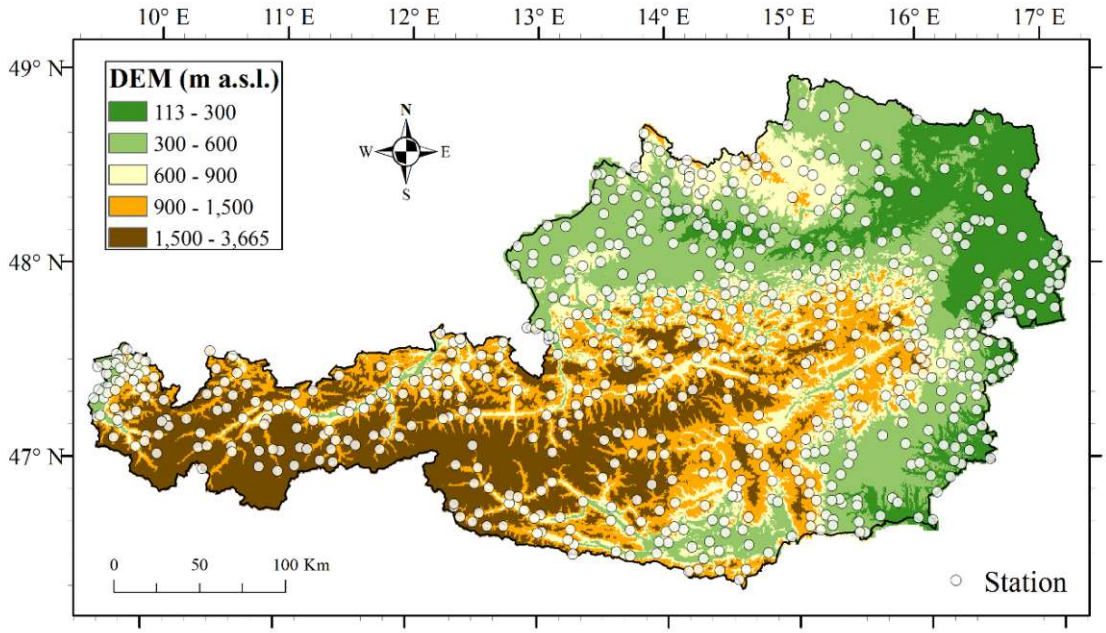

Figure 2.1 Topography of Austria and spatial distribution of the 665 climate stations with daily snow depth measurements.

Table 2.1. Confusion matrix defining the snow cover mapping accuracy index (OA_T). T_{NDSI} represents the MODIS NDSI threshold and T_{SD} indicates the snow depth threshold at the climate stations.

	MODIS NDSI>=T_{NDSI} (SNOW)	MODIS NDSI<T_{NDSI} (LAND)
Station snow depth >=T_{SD} (SNOW)	A	B
Station snow depth<T_{SD} (LAND)	C	D

2.4 Results

2.4.1 Evaluation of the best NDSI threshold

The distribution of the Terra and Aqua NDSI values stratified by snow depth categories is presented in Figure 2.2. The box-whiskers plot shows the distribution of NDSI pixel values for the locations of climate stations in the period September 2002 to August 2014. It is clear that the NDSI values tend to increase and their variability tends to decrease with increasing snow depth. Interestingly, even if the snow depth at the climate stations exceeds 1 m of snow, the median of the NDSI values is about 30% lower (0.71 for Terra and 0.73 for Aqua) than the theoretically possible maximum NDSI value (NDSI=1.00). On the other hand, during snow-

Die approbierte gedruckte Originalversion dieser Dissertation ist an der TU Wien Bibliothek verfügbar.
The approved original version of this doctoral thesis is available in print at TU Wien Bibliothek.
TU Bibliothek Your knowledge hub WIEN

free conditions at the climate stations, only 3 % of MODIS pixels values have NDSI larger than 0. A comparison of the Aqua and Terra satellites indicates that the median and variability of the Terra NDSI values is somewhat smaller than those of Aqua. This is likely related to the different processing chain used for snow detection in the Aqua product (Kraatz et al.,2017). The snow reflectance is slightly lower in band 7 than in band 6 (Wang et al., 2006). This results in higher NDSI value of Aqua, which band 6 value used for NDSI calculation is retrieved from Band 7. The most noticeable difference between Aqua and Terra occurs for patchy snow conditions (snow depth in range 1-5cm). The median of the Aqua NDSI values is about 0.11 smaller and the variability is about 50% larger than the variability of Terra NDSI values. The main reason for the difference is that the Aqua images the same area approximately three hours later than Terra, the patchy snow covered area shrinks between this gap.

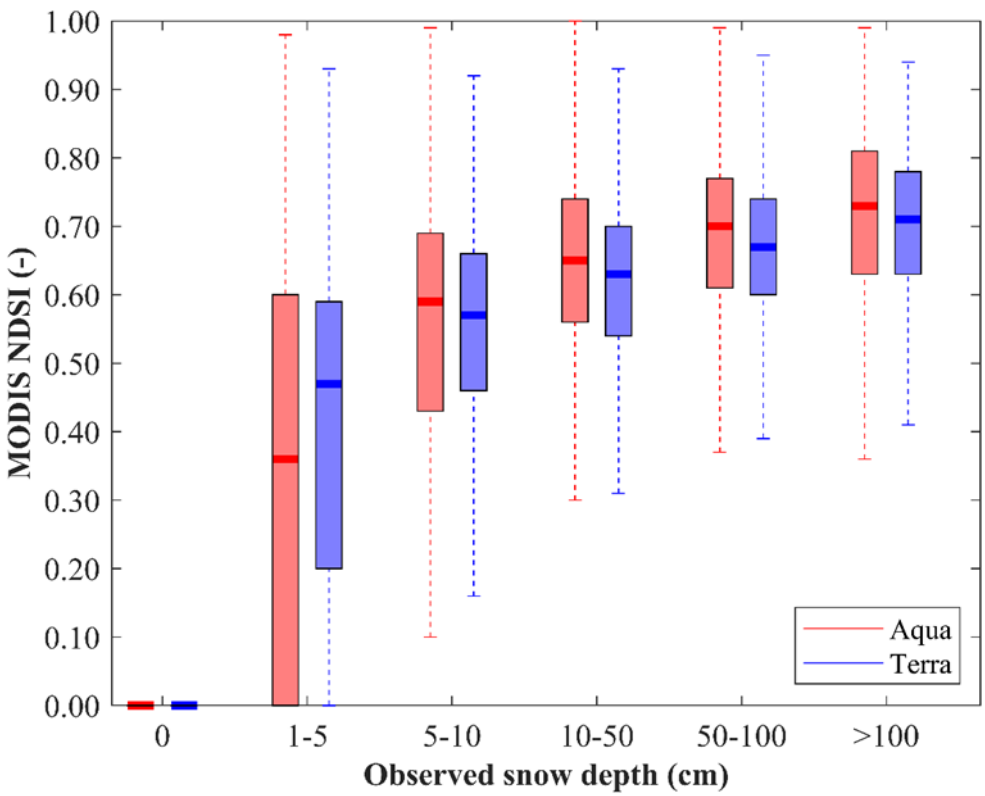

Figure 2.2 Distribution of NDSI values for different categories of observed daily snow depth at 665 stations in the period September 2002 – August 2014. Red and blue boxes show the space-time variability (i.e. 75%- and 25%- percentiles) in the Aqua (MYD10A1) and Terra (MOD10A1) snow cover products.

The best threshold for snow cover mapping (BT_{NDSI}) fitted for each individual climate station is evaluated in Figure 2.3. The cumulative distribution functions of the BT_{NDSI} are presented for different snow depth thresholds T_{SD} indicating the limit above which the ground (neighborhood of climate station) is considered as snow covered. The results show that the BT_{NDSI} tends to increase with increasing snow depth threshold T_{SD}. The variability of BT_{NDSI} caused by different T_{SD} is somewhat larger for the Terra than the Aqua products, mainly for shallow snowpack described by smaller thresholds (i.e. T_{SD}=1cm and 2cm). The median of BT_{NDSI} over 665 climate stations (Table 2.2) varies between 0.34 (T_{SD}=1cm) to 0.45 (T_{SD}=5cm) for Terra and between 0.37 (T_{SD}=1cm) and 0.45 (T_{SD}=5cm) for the Aqua daily dataset.

Die approbierte gedruckte Originalversion dieser Dissertation ist an der TU Wien Bibliothek verfügbar.
The approved original version of this doctoral thesis is available in print at TU Wien Bibliothek.
TU Bibliothek Your knowledge hub WIEN

An analysis of the relationship between BT_{NDSI} fitted for each individual climate station and selected physiographic characteristics of pixels where climate stations are located is presented in Figure 2.4 using a snow depth threshold T_{SD}=1cm. The evaluation shows that the BT_{NDSI} tends to decrease with increasing altitude of climate stations (Figure 2.4, left panel). The median of BT_{NDSI} for stations below 300m a.s.l. and above 1500 m a.s.l. ranges from 0.45 to 0.35 for Aqua, and from 0.43 to 0.27 for Terra. The thresholds fitted for each individual station are generally larger for non-forest land cover (i.e. urban areas and grassland) than for coniferous and other forests (Figure 2.4, middle panel). Interestingly, there is no large difference between different forest type categories in Austria. The variability of BT_{NDSI} between different aspects of 500 m pixels (Figure 2.4, right panel) indicates smaller BT_{NDSI} values for pixels with S and SW aspects in the Terra dataset. The difference in the median between S-SW and W-N aspects is 0.07 for Aqua and 0.10 for Terra. Interestingly, the Aqua BT_{NDSI} values are larger in all aspect categories and the median of the southern aspects has a similar magnitude as the median of the pixels with northern aspects in the Terra dataset. The best threshold represents a tradeoff between minimizing under- and overestimation errors. Larger Aqua BT_{NDSI} values are affected by a larger frequency of clouds and an approximately 10% lower mapping accuracy during shallow snowpack conditions (snow depth between 1 and 5cm), which has likely an impact on the determination of the final thresholds. The spatial patterns of the BT_{NDSI} for different snow depth thresholds are presented in Fig 2.5.

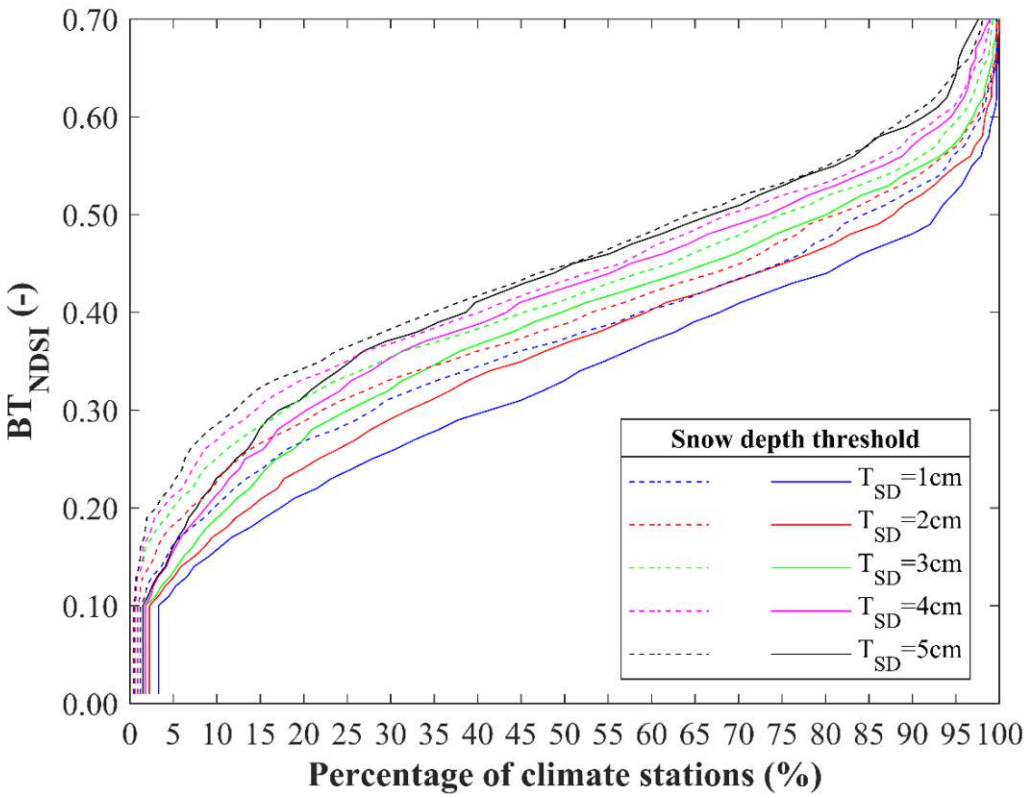

Figure 2.3 Cumulative distribution functions of the best NDSI threshold BTNDSI estimated for Aqua (dashed line) and Terra (solid line) snow cover products by using different (1cm, 2cm, 3cm 4cm and 5cm) snow depth thresholds at 665 stations in the period September 2002 to August 2014.

Die approbierte gedruckte Originalversion dieser Dissertation ist an der TU Wien Bibliothek verfügbar.
The approved original version of this doctoral thesis is available in print at TU Wien Bibliothek.
TU Bibliothek Your knowledge hub WIEN

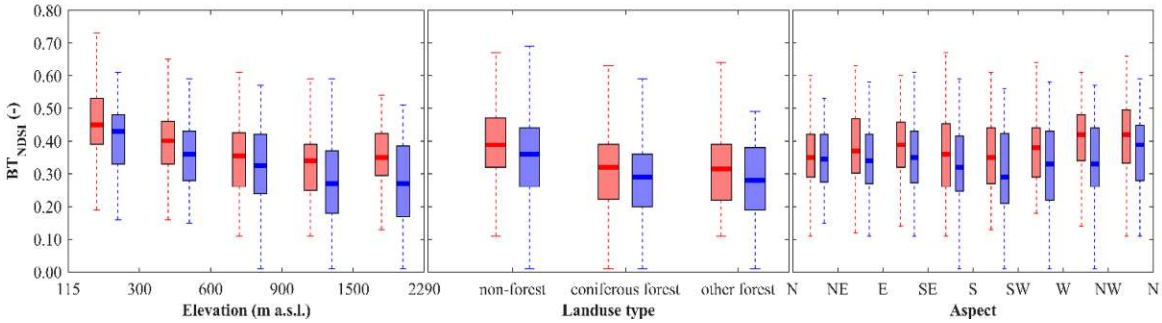

Figure 2.4 Boxplots of the best NDSI threshold estimated for MYD10A1 (Aqua, red) and MOD10A1 (Terra, blue) products stratified by elevation, aspect and landuse of 665 climate stations in the period September 2002 to August 2014. Snow cover at climate stations is defined by 1-cm snow depth threshold.

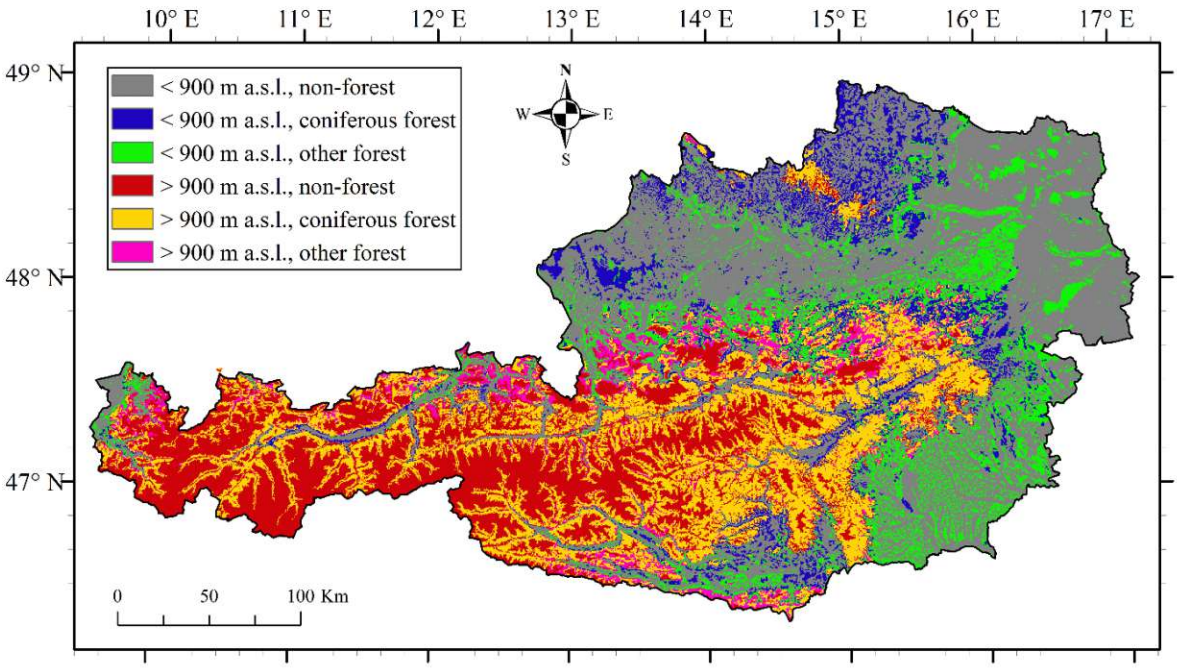

Aqua		Jan	Feb	Mar	Apr	May	Jun	Jul	Aug	Sep	Oct	Nov	Dec
below 900 m a.s.l.	non-forest	0.36	0.34	0.36	0.67	0.98	0.97	0.89	0.96	0.84	0.67	0.43	0.41
	coniferous forest	0.17	0.24	0.34	0.50	0.63	0.66	0.79	0.77	0.92	0.47	0.42	0.26
	other forest	0.32	0.29	0.29	0.82	0.70	0.78	0.75	0.89	0.90	0.80	0.47	0.30
over 900 m a.s.l.	non-forest	0.22	0.18	0.28	0.49	0.67	0.91	0.89	0.91	0.71	0.43	0.45	0.26
	coniferous forest	0.20	0.14	0.29	0.49	0.74	0.86	0.82	0.87	0.82	0.49	0.43	0.25
	other forest	0.17	0.12	0.13	0.50	0.83	0.74	0.77	0.58	0.69	0.44	0.46	0.20

Terra		Jan	Feb	Mar	Apr	May	Jun	Jul	Aug	Sep	Oct	Nov	Dec
below 900 m a.s.l.	non-forest	0.32	0.30	0.37	0.57	0.74	0.78	0.82	0.85	0.82	0.52	0.41	0.36
	coniferous forest	0.30	0.19	0.29	0.34	0.72	0.80	0.65	0.93	0.61	0.56	0.31	0.34
	other forest	0.22	0.19	0.29	0.86	0.78	0.64	0.78	0.74	0.65	0.65	0.40	0.31
over 900 m a.s.l.	non-forest	0.21	0.16	0.20	0.44	0.60	0.90	0.77	0.70	0.84	0.54	0.35	0.27
	coniferous forest	0.16	0.12	0.22	0.40	0.65	0.78	0.80	0.76	0.78	0.47	0.37	0.20
	other forest	0.10	0.11	0.10	0.17	0.53	0.16	0.26	0.69	0.67	0.31	0.31	0.22

Figure 2.5. Spatial distribution of the threshold classifications for Austria in this study and the optimized NDSI threshold values by below/above 900 m a.s.l and 3 landuse types in each month for MYD10A1 (Aqua) and MOD10A1 (Terra).

Die approbierte gedruckte Originalversion dieser Dissertation ist an der TU Wien Bibliothek verfügbar.
The approved original version of this doctoral thesis is available in print at TU Wien Bibliothek.
TU Bibliothek Your knowledge hub WIEN

The seasonal variability of BT_{NDSI} fitted for each individual station in individual months is presented in Figure 2.6. The results indicate that there is a distinct difference between larger BT_{NDSI} values fitted for the winter months (i.e. November to March) and almost zero threshold values in the summer months (i.e. June to September). An exception is the BT_{NDSI} threshold for the Aqua dataset in September and October, which, for most of the stations, is significantly larger than the thresholds fitted for the Terra dataset. This is likely related to the fitting procedure of the best thresholds, where a wide range of thresholds has a very similar mapping accuracy and thus only few cases influence the final estimate. Time shifts between Terra and Aqua during the onset of the snow cover, which can be one of the reasons for a higher Aqua threshold, are very rare (only 7 cases for all stations in the selected time period), so it is unlikely that the difference in overpass time has a significant effect on the estimated best thresholds in Austria.

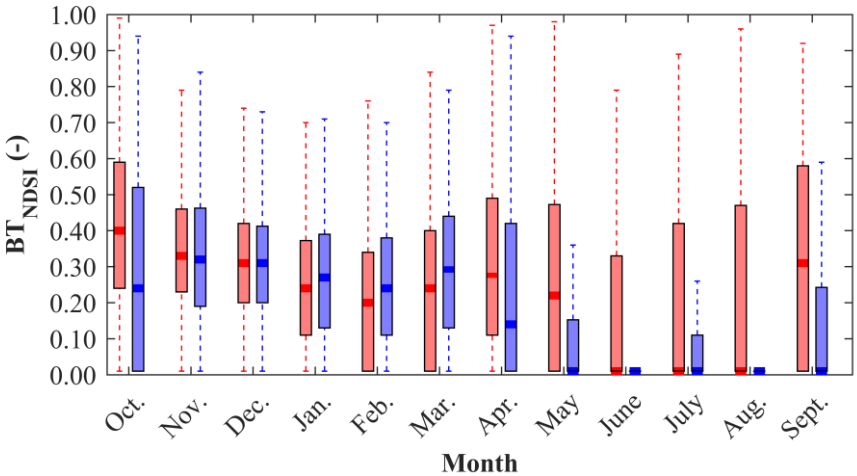

Figure 2.6 Seasonal variability of the best NDSI threshold for MYD10A1 (Aqua, red) and MOD10A1 (Terra, blue) products estimated at 665 climate stations in the period September 2002 to August 2014. Snow cover at climate stations is defined by 1-cm snow depth threshold.

A different strategy is evaluated in Table 2.2 and Figure 2.7. In contrast to the previous assessment that evaluates the thresholds fitted for individual stations (and months), Table 2.2 presents a summary of thresholds fitted as a single value representative of all stations in Austria. Table 2.2 shows that, if the MODIS threshold is fitted to all stations, the NDSI threshold value is somewhat smaller than the median BT_{NDSI}. The exception is BT_{NDSI} fitted for the Aqua product and snow depth threshold T_{SD}=1cm, which has the same value of 0.37.

Die approbierte gedruckte Originalversion dieser Dissertation ist an der TU Wien Bibliothek verfügbar.
The approved original version of this doctoral thesis is available in print at TU Wien Bibliothek.
TU Bibliothek Your knowledge hub WIEN

Table 2.2. The best NDSI threshold optimized from the overall accuracy using all stations and the median value of the best NDSI threshold selected for individual stations.

Snow depth threshold T_{SD}/Station groups with T_{SD}=1cm		Best NDSI threshold for all stations		Best NDSI threshold for median stations	
		Aqua	Terra	Aqua	Terra
Snow depth threshold T_{SD}	T_{SD}=1cm	0.37	0.30	0.37	0.34
	T_{SD}=2cm	0.37	0.32	0.39	0.37
	T_{SD}=3cm	0.38	0.34	0.41	0.40
	T_{SD}=4cm	0.40	0.37	0.43	0.43
	T_{SD}=5cm	0.40	0.38	0.45	0.45
Elevation	<300 m a.s.l.	0.48	0.40	0.45	0.43
	300-600 m a.s.l.	0.40	0.34	0.40	0.36
	600-900 m a.s.l.	0.35	0.31	0.36	0.33
	900-1500 m a.s.l.	0.34	0.24	0.34	0.27
	>1500 m a.s.l.	0.35	0.19	0.35	0.27
Landuse type	non-forest	0.38	0.32	0.39	0.36
	coniferous forest	0.34	0.27	0.32	0.29
	other forest	0.33	0.26	0.32	0.28
Aspect	N-NE	0.36	0.32	0.35	0.35
	NE-E	0.37	0.32	0.37	0.34
	E-SE	0.36	0.32	0.39	0.35
	SE-S	0.35	0.32	0.36	0.32
	S-SW	0.32	0.24	0.35	0.29
	SW-W	0.34	0.29	0.38	0.33
	W-NW	0.43	0.32	0.42	0.33
	NW-N	0.42	0.37	0.42	0.39
Month	November	0.43	0.39	0.33	0.32
	December	0.34	0.32	0.31	0.31
	January	0.29	0.28	0.24	0.27
	February	0.26	0.24	0.20	0.24
	March	0.31	0.25	0.24	0.29

A different pattern is observed for single thresholds fitted separately for six groups of stations. The thresholds in each group are fitted to maximize the overall accuracy in individual months.

Die approbierte gedruckte Originalversion dieser Dissertation ist an der TU Wien Bibliothek verfügbar.
The approved original version of this doctoral thesis is available in print at TU Wien Bibliothek.
TU Bibliothek WIEN Your knowledge hub

The groups split stations into two elevation and three land cover groups. While the left panels (Figure 2.7) show thresholds for the group of stations situated at altitudes equal or lower than 900 m a.s.l. (i.e. are representative for lowland and hilly regions), the right panels show stations situated in the mountains (i.e. stations above 900 m a.s.l.). Three land cover classes represent the main vegetation types in Austria. The results show a clear seasonal pattern of the best thresholds. Interestingly, compared to thresholds fitted for each station in individual months (Figure 2.6), the best thresholds for all groups are significantly larger in the summer months. This is likely the result of fitting procedure to minimize overestimation of snow cover due to misclassification of clouds as snow (Parajka and Blöschl, 2006). The thresholds are fitted to maximize the overall accuracy, so thresholds exceeding 0.65 in the summer months help to eliminate the relatively higher possibility of overestimation of snow cover in the summer months. The thresholds fitted for the mountain groups (all vegetation classes) are generally smaller than those fitted for flatland stations. The thresholds tend to be larger for non-forest classes, and the difference between the coniferous and other forest classes is obvious in the mountain groups. The thresholds are the smallest (less than 0.15 in January to March) in the mountains for the other forest group. In this group there are also the largest differences between the Terra and Aqua datasets, particularly in the period between April and July. Aqua and Terra show a similar variance tendency in the winter, but disagreement in the summer, for the other forest group.

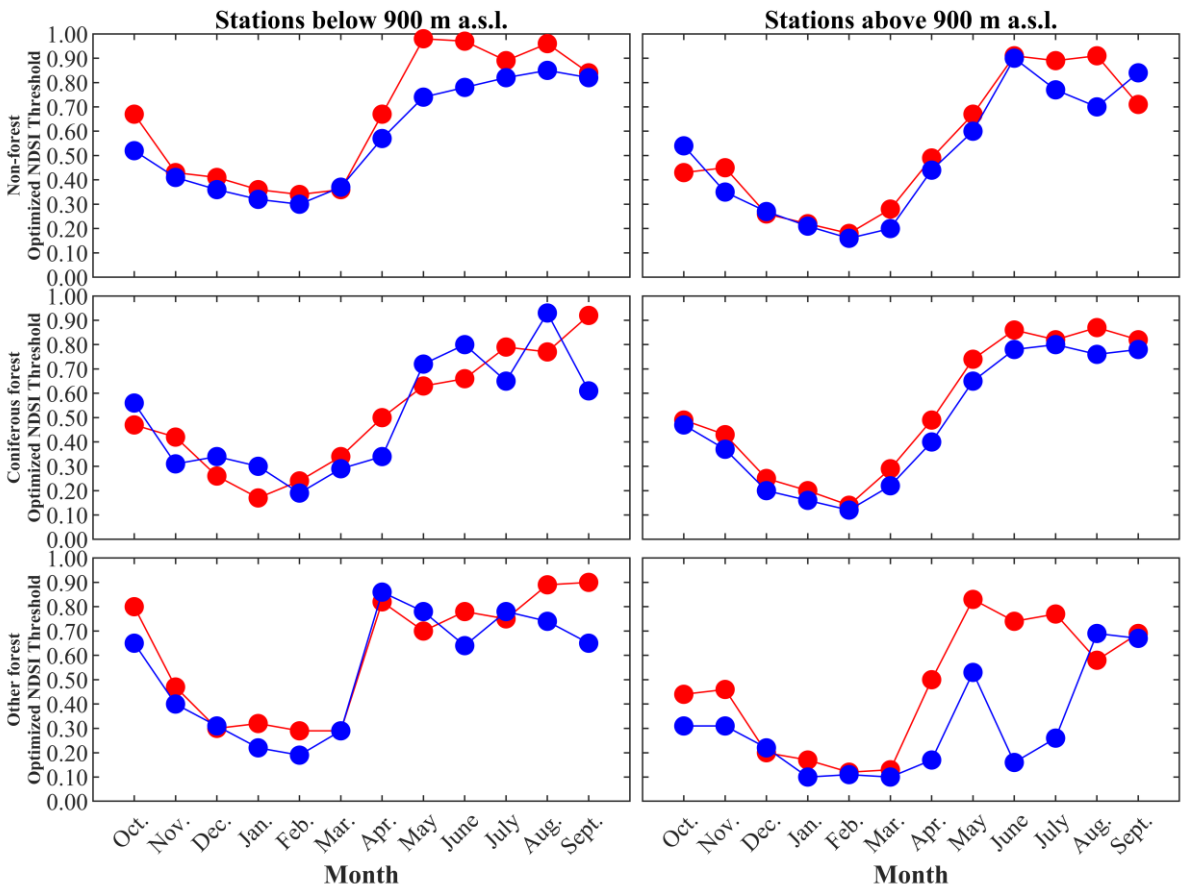

Figure 2.7 Optimized NDSI threshold for 6 classification of 665 Austrian stations by below/above 900 m a.s.l and 3 landuse types in each month for MYD10A1 (Aqua, red) and MOD10A1 (Terra, blue) in the period September 2002 to August 2014.

Die approbierte gedruckte Originalversion dieser Dissertation ist an der TU Wien Bibliothek verfügbar.
The approved original version of this doctoral thesis is available in print at TU Wien Bibliothek.
TU Bibliothek Your knowledge hub WIEN

2.4.2 Accuracy assessment

The mapping accuracy of the snow cover maps classified by using the fitted BT_{NDSI} thresholds is evaluated in Figures 2.8 to 2.12 and Table 2.3. Figure 2.8 shows cumulative distribution functions of the overall accuracy (OA) for five different snow depth thresholds applied to the Aqua and Terra datasets. The results demonstrate a very high snow cover mapping accuracy and very similar accuracy values obtained for different snow depth thresholds. This indicates that, for a given snow depth threshold, one can fit NDSI thresholds that give similar mapping accuracies. The median of OA over all stations is very high and similar for the Terra and Aqua datasets. The median overall accuracy slightly decreases with increasing snow depth threshold for Terra (from 98.1% to 97.6%) but the median OA slightly increases for increasing thresholds between 1 and 3 cm for Aqua (from 98.2% to 98.4%). The variability of OA for different snow depth thresholds is slightly larger for the Terra dataset, which reflects also a slightly larger variability of BT_{NDSI} thresholds (Figure 2.3). Interestingly, the relative variability of mapping accuracy is smaller than the relative variability of the BT_{NDSI} thresholds, which means that a similar overall accuracy can be obtained by different NDSI and snow depth thresholds.

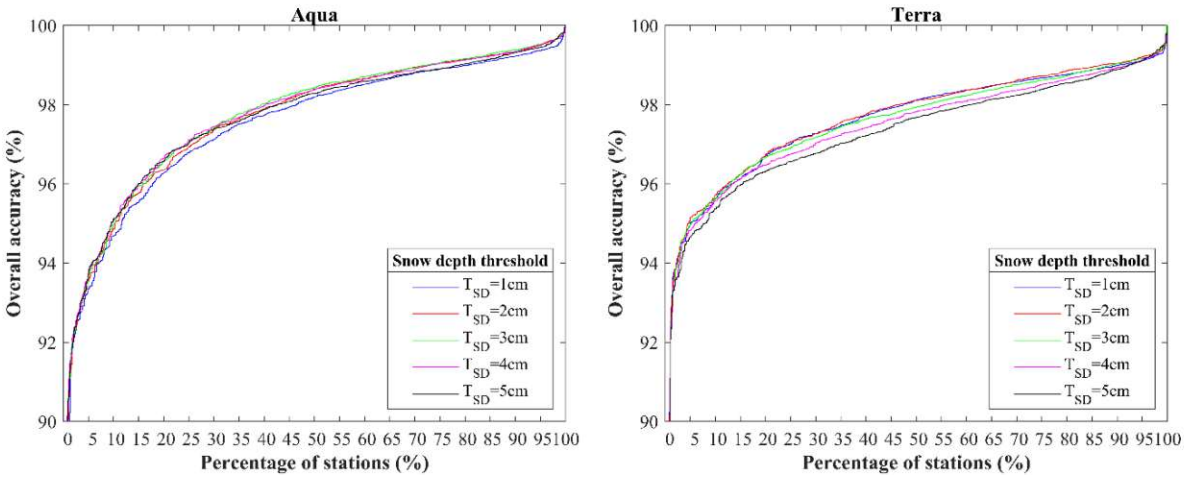

Figure 2.8 Cumulative distribution functions of the overall accuracy of Aqua (left panel) and Terra (right panel) snow cover products estimated for best NDSI thresholds in individual stations and for 5 snow depth (SD) thresholds (Table 2.1). Overall accuracy is estimated for all 665 stations in the period September 2002 to August 2014.

The relationships between the overall accuracy and the physiographic characteristics of the pixels the stations are located (Figure 2.9) show that the OA tends to decrease with increasing elevation of the stations and is larger for open (non-forest) areas than for stations situated in coniferous forest. There are no significant relationships between OA and the aspect of the pixels, the medians of OA for 8 different aspect classes vary between 97.55% and 98.53 (Table 2.3). The variability of OA is larger for northern than for southern and eastern slopes. Overall, the accuracies and relationships are very similar for the Terra and Aqua datasets.

The mapping accuracy has a strong seasonal variability. Figure 2.10 shows the seasonal variability of OA for thresholds fitted in each station for each month. The results indicate that the accuracy is similar for Terra and Aqua and is the lowest in December. The median of OA in December is 92.31% (Aqua) and 91.67% (Terra), and in 10% of stations it is less than 80%. In the spring months (March, April) the median accuracy increases to over 95%.

Die approbierte gedruckte Originalversion dieser Dissertation ist an der TU Wien Bibliothek verfügbar.
The approved original version of this doctoral thesis is available in print at TU Wien Bibliothek.
TU Bibliothek Your knowledge hub WIEN

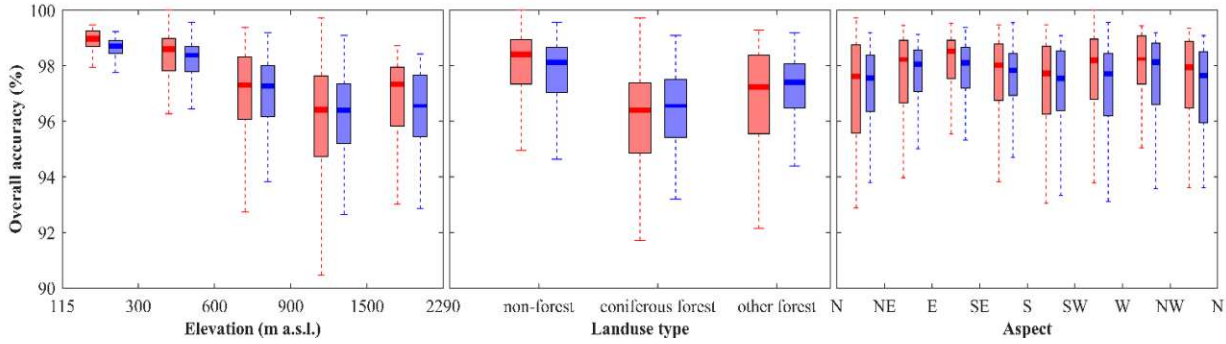

Figure 2.9 Boxplots of overall accuracy for MYD10A1 (Aqua, red) and MOD10A1 (Terra, blue) with using the optimized NDSI threshold showing in Figure 2.7 for different groups (elevation, aspect, landuse type) of the 665 Austrian stations in the period September 2002 to August 2014.

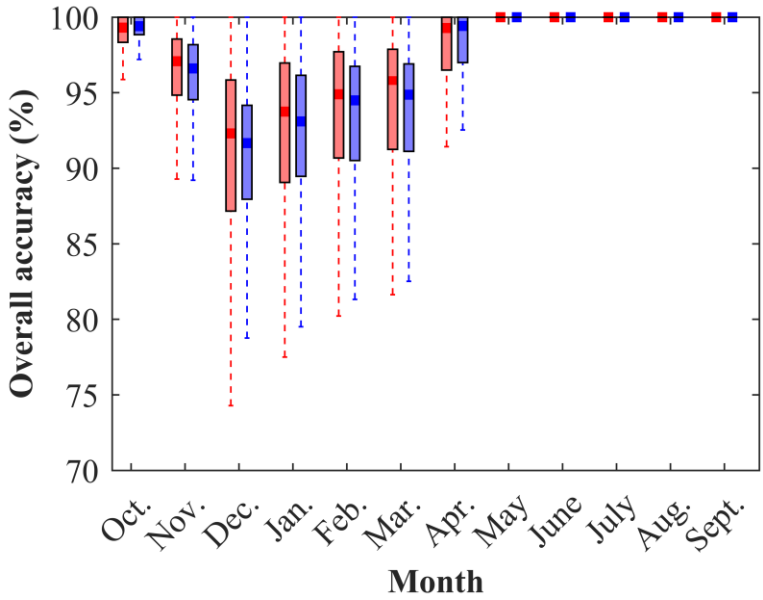

Figure 2.10 Boxplots of overall accuracy for MYD10A1 (Aqua, red) and MOD10A1 (Terra, blue) with using the optimized NDSI threshold showing in Figure 2.7 for different months at 665 Austrian stations in the period September 2002 to August 2014.

Die approbierte gedruckte Originalversion dieser Dissertation ist an der TU Wien Bibliothek verfügbar.
The approved original version of this doctoral thesis is available in print at TU Wien Bibliothek.
TU Bibliothek Your knowledge hub WIEN

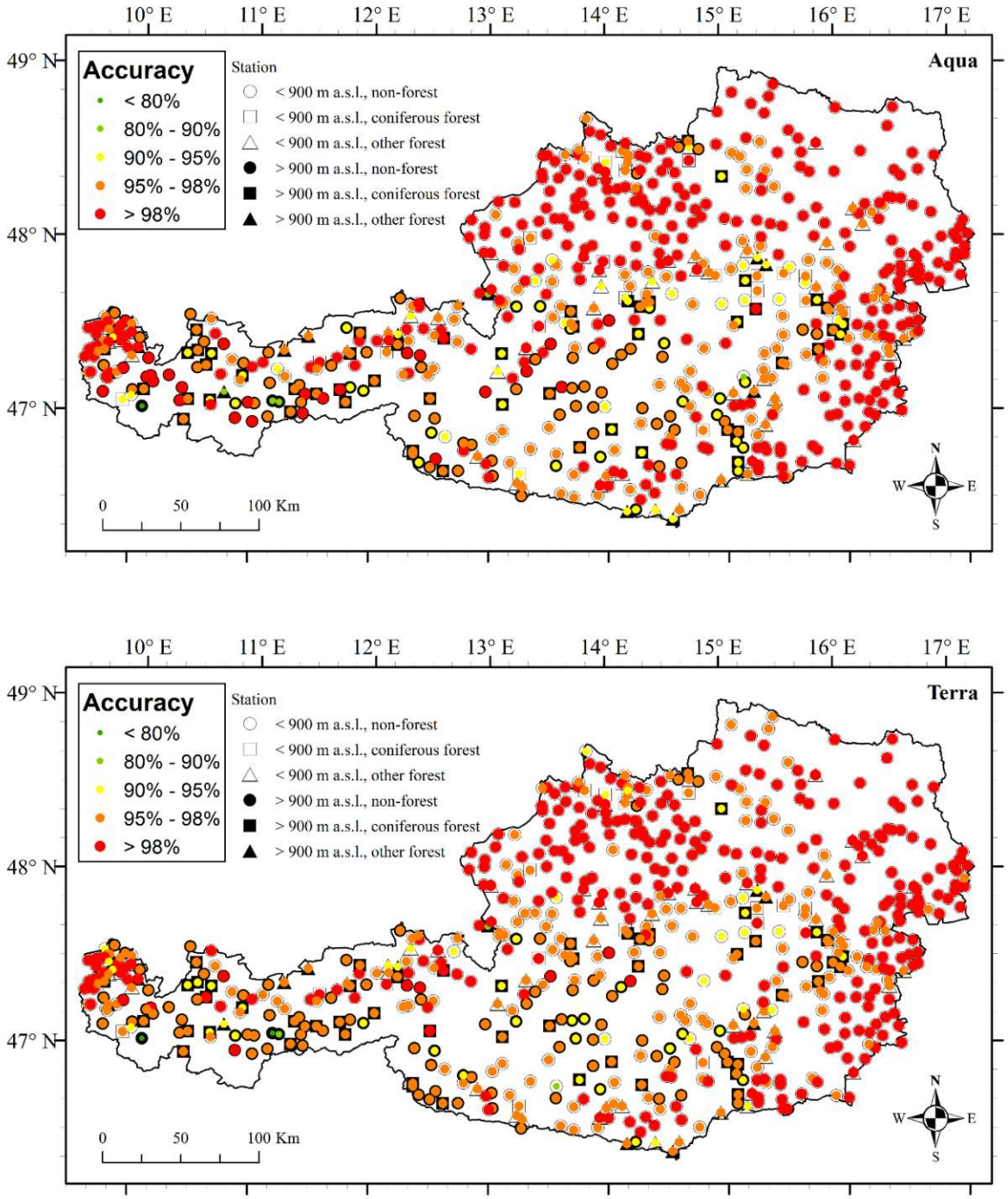

Figure 2.11 Overall accuracy for MYD10A1 (Aqua, upper panel) and MOD10A1 (Terra, lower panel) with using the optimized NDSI threshold showing in Figure S.1. at 665 Austrian stations in the period September 2002 to August 2014.

Die approbierte gedruckte Originalversion dieser Dissertation ist an der TU Wien Bibliothek verfügbar.
The approved original version of this doctoral thesis is available in print at TU Wien Bibliothek.
TU Bibliothek Your knowledge hub WIEN

Table 2.3. Mapping accuracy obtained for different snow depth stations and different groups of stations. The NDSI threshold applied here is using the best NDSI threshold for all stations as shown in Table 2.2 for snow depth threshold T_{SD} 1-5 cm; using the optimized NDSI threshold with 6 classification as shown in Figure 2.7 for the station groups with snow depth threshold T_{SD}=1cm.

Snow depth threshold T_{SD}/Station groups with T_{SD}=1cm		OA for all stations (%)		OA for median stations (%)	
		Aqua	Terra	Aqua	Terra
Snow depth threshold T_{SD}	T_{SD}=1cm	97.17	97.23	97.90	97.78
	T_{SD}=2cm	97.32	97.21	98.10	97.77
	T_{SD}=3cm	97.35	97.02	98.12	97.51
	T_{SD}=4cm	97.30	96.82	98.02	97.28
	T_{SD}=5cm	97.20	96.61	97.91	97.08
Elevation	<300 m a.s.l.	98.90	98.60	98.98	98.71
	300-600 m a.s.l.	98.31	98.11	98.60	98.36
	600-900 m a.s.l.	96.96	96.91	97.30	97.27
	900-1500 m a.s.l.	95.79	96.01	96.42	96.40
	>1500 m a.s.l.	96.58	96.39	97.34	96.60
Landuse type	non-forest	97.84	97.58	98.41	98.13
	coniferous forest	95.92	96.34	96.41	96.60
	other forest	96.79	97.06	97.23	97.41
Aspect	N-NE	97.05	97.05	97.63	97.57
	NE-E	97.67	97.58	98.24	98.06
	E-SE	97.95	97.74	98.53	98.11
	SE-S	97.45	97.36	98.02	97.84
	S-SW	97.35	97.21	97.73	97.55
	SW-W	97.63	97.39	98.20	97.71
	W-NW	98.01	97.81	98.29	98.13
	NW-N	96.97	96.81	97.95	97.64
Month	November	95.96	95.67	97.09	96.61
	December	90.43	90.56	92.31	91.67
	January	92.45	92.32	93.75	93.10
	February	93.43	93.15	94.90	94.50
	March	93.65	93.23	95.76	94.87

Die approbierte gedruckte Originalversion dieser Dissertation ist an der TU Wien Bibliothek verfügbar.
The approved original version of this doctoral thesis is available in print at TU Wien Bibliothek.
TU Bibliothek Your knowledge hub WIEN

The thresholds fitted to individual stations can be considered as a baseline for comparison but are difficult to apply in a regional use of MODIS snow cover maps. So, best thresholds for groups of stations in different elevation and land cover classes are representative (Figure 2.7). The accuracy of these thresholds is evaluated in Figure 2.12. The results show that a median accuracy over 90% is found in all three land cover groups for elevations below 900 m a.s.l. and for open (non-forest) land cover above 900 m a.s.l.. The lowest accuracy is found for stations above 900 m a.s.l. for other forest group, particularly in December, February and March. The median accuracy in this group is lower for the Aqua than the Terra dataset and varies between 80-85% for Aqua and 86-90% for Terra.

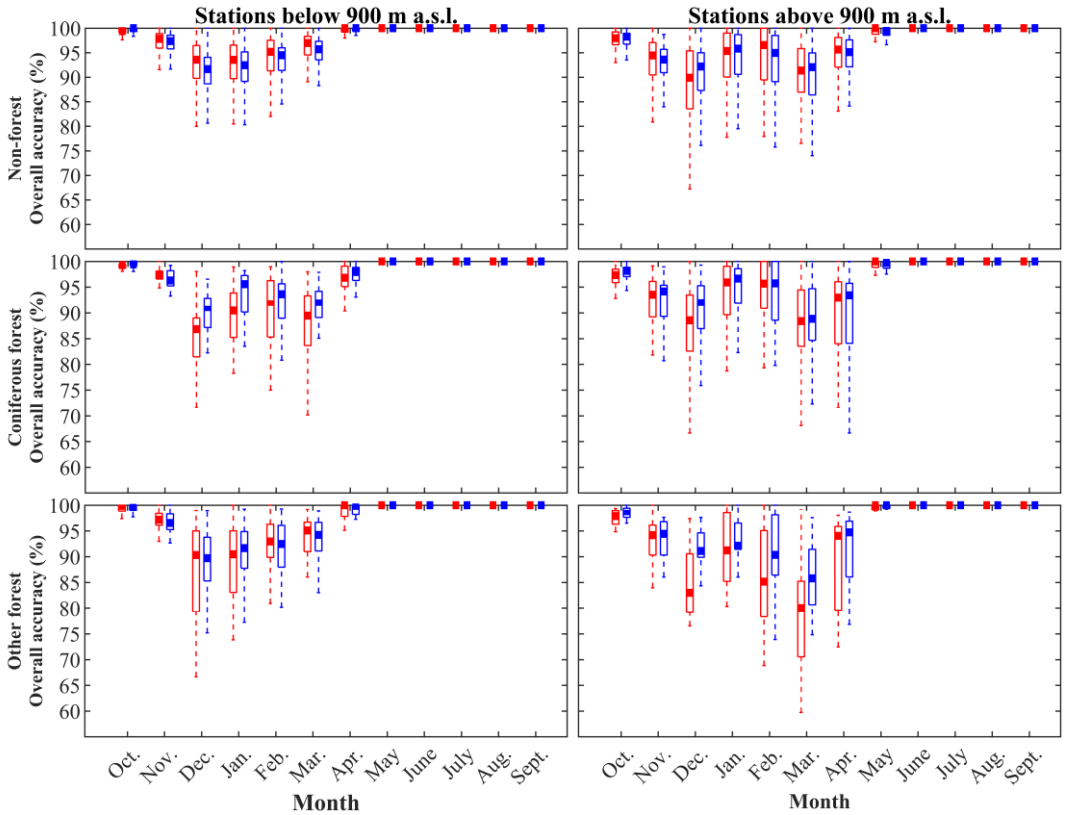

Figure 2.12 Accuracy of MODIS snow cover maps MYD10A1 (Aqua, red) and MOD10A1 (Terra, blue) (with optimized NDSI threshold as shown above, snow depth threshold 1cm) for different classifications (elevation, aspect, landuse type) of the 665 Austrian stations in the period September 2002 to August 2014.

As can be seen from Table 2.4, the mapping accuracy for snow free condition increased but not significant with the optimized T_{NDSI} comparing to T_{NDSI}=0.40. For patchy snow (1-5 cm) conditions the accuracy increased 4.29% for Aqua and 7.53% for Terra. There is also approximate 3% accuracy improvement for thick snow condition. If one is interested in the accuracy of snow classification, it can be improved to 88.08% and 92.03% for Aqua and Terra, respectively with the optimized T_{NDSI}.

Die approbierte gedruckte Originalversion dieser Dissertation ist an der TU Wien Bibliothek verfügbar.
The approved original version of this doctoral thesis is available in print at TU Wien Bibliothek.
TU Bibliothek Your knowledge hub WIEN

Table 2.4. The mapping accuracy (shown in percentage) for different snowpack conditions based on in-situ snow depth with NDSI threshold (T_{NDSI}) 0.40 and optimized T_{NDSI} (Figure 2.7) in this Chapter.

Snowpack condition	Snow free		Patchy snow		Thick snow		Snow covered		Overall	
In-situ snow depth SD (cm)	0		1-5		>5		>0		~	
T_{NDSI}	0.40	Opt.	0.40	Opt.	0.40	Opt.	0.40	Opt.	0.40	Opt.
Aqua	98.78	98.91	52.67	56.96	91.61	94.15	85.25	88.08	97.14	97.59
Terra	98.56	98.32	64.52	72.05	92.26	96.17	87.50	92.03	96.97	97.42

2.5 Discussion

The main objective of this Chapter is to evaluate the accuracy and applicability of the new MODIS snow cover datasets, i.e. Collection 6, for regional snow cover mapping in Austria. The key improvement of the new datasets are the NDSI values instead of binary snow-land-cloud classes based on fixed NDSI value (NDSI=0.4). This provides some flexibility for users to create their own regional snow cover map, but requires selection of the NDSI thresholds, which can vary in time and/or space. Some of the previous studies (Härer et al., 2018) found a fixed threshold T_{NDSI}=0.4 to be accurate, but this Chapter shows that the thresholds, if allowed to vary in space and time, can be fitted to maximize the mapping accuracy. Our results show that the best NDSI thresholds in Austria have a strong seasonality and tend to decrease with increasing elevation. The best thresholds are lower in forested regions than in an open land cover setting and in these locations are generally lower than the fixed threshold (T_{NDSI}=0.4). This is consistent with the recent results of Da Ronco et al. (2020) who quantified and compared optimal NDSI thresholds for 7 stations in the Central Apennines (Italy). They found that the optimal NDSI threshold for this region was 0.20, which resulted in a 15% increase in the snow-cover extent in all seasons. The snow cover mapping accuracy of the new dataset is very high. The median over 665 stations in Austria is larger than 97%, which is approximately 2% larger than that of the previous version (Parajka and Blöschl, 2006). The results indicate a similar decrease of mapping accuracy with increasing elevation and somewhat smaller accuracies in forested regions similar to previous assessments (Parajka et al., 2012; Arsenault et al., 2014). We found that the selection of the NDSI threshold is sensitive to the selection of snow depth threshold indicating snow coverage around the at site measurements. The analysis demonstrates that the different NDSI thresholds can be fitted to obtain very similar mapping accuracies. The question of how to select the NDSI threshold for regional snow cover mapping then depends on the snow depth threshold and land cover and topography of the region. Figure 2.13 shows that, if a single threshold is fitted to all of Austria, a wide range of thresholds, i.e. between 0.2 and 0.4, results in a very similar mapping accuracy. The difference between the originally used threshold 0.4 and somewhat smaller thresholds is very small. If one refines the thresholds in different seasons and elevation and land cover groups (Figure 2.14), the mapping accuracy can be increased for the period January to March by approximately 3-10% in forested regions above 900 m a.s.l..

Die approbierte gedruckte Originalversion dieser Dissertation ist an der TU Wien Bibliothek verfügbar.
The approved original version of this doctoral thesis is available in print at TU Wien Bibliothek.
TU Bibliothek Your knowledge hub WIEN

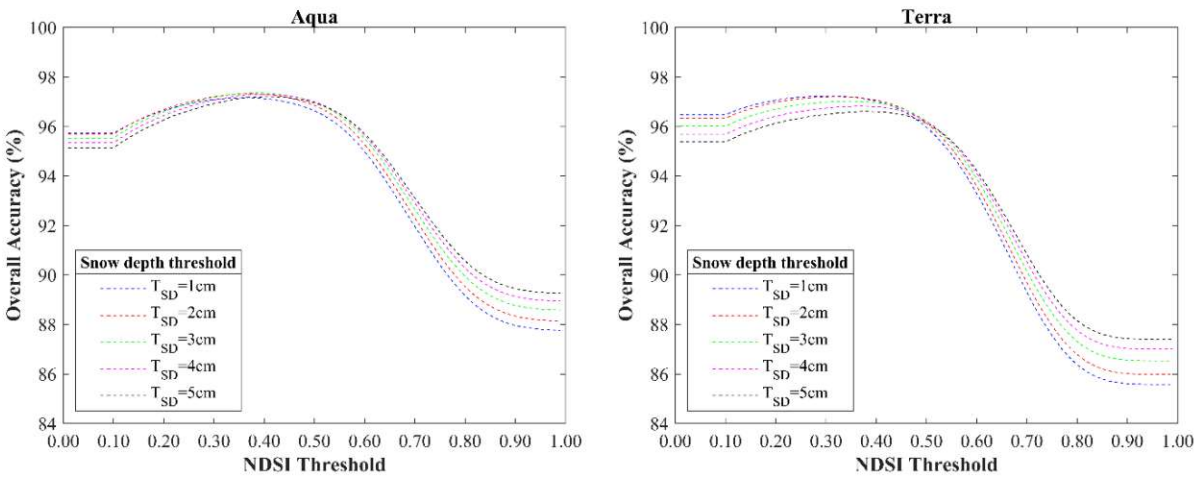

Figure 2.13 Overall accuracy of Aqua (left panel) and Terra (right panel) snow cover products estimated for different NDSI and snow depth (SD) thresholds (Table 2.1). Overall accuracy is estimated for all 665 stations in the period September 2002 to August 2014.

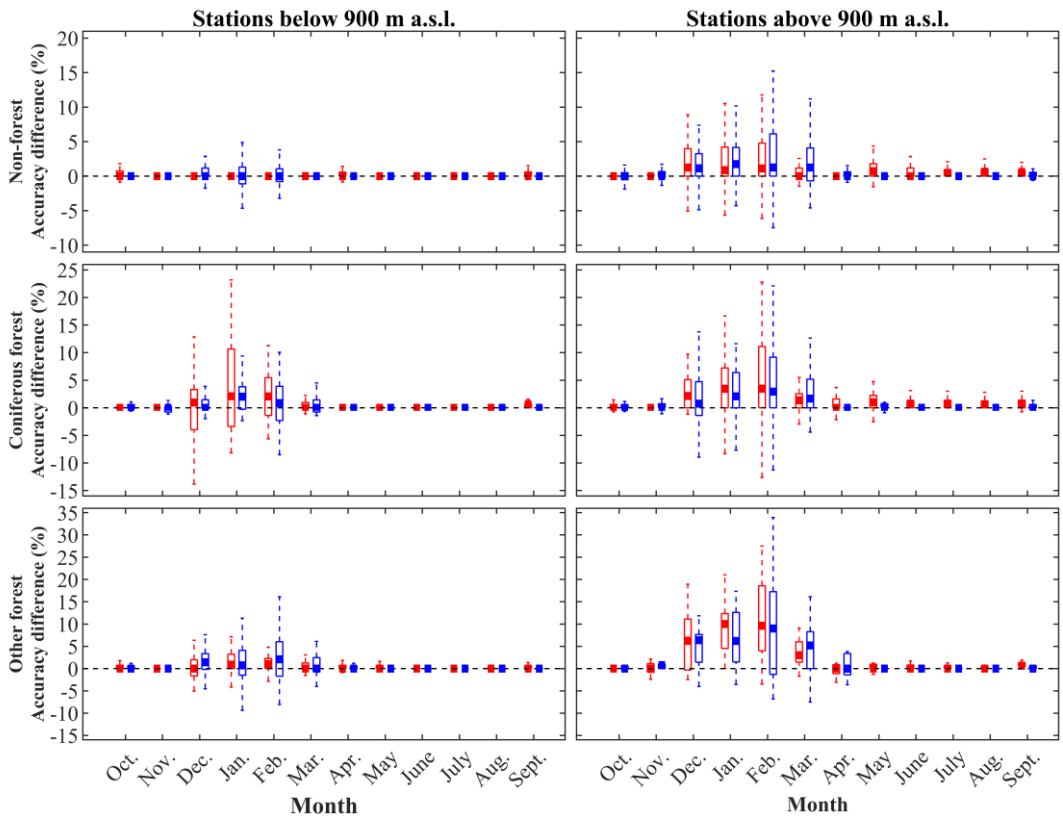

Figure 2.14 Boxplot of accuracy difference between using NDSI threshold optimized and 0.40 for MYD10A1 (Aqua, red) and MOD10A1 (Terra, blue) over Austria according to the elevation of the stations.

Die approbierte gedruckte Originalversion dieser Dissertation ist an der TU Wien Bibliothek verfügbar.
The approved original version of this doctoral thesis is available in print at TU Wien Bibliothek.
TU Bibliothek Your knowledge hub WIEN

2.6 Conclusions

Our results demonstrate that the new MODIS Collection 6 daily products have improved in comparison to the previous version and allow a flexible regional adjustment of mapping accuracy. The accuracy assessment particularly indicates an improvement of the mapping accuracy in spring which is expected to improve hydrological predictions during snowmelt events. In January to March, a lower NDSI threshold could reduce the MODIS underestimation error. While higher NDSI thresholds were found to avoid the MODIS overestimation error in the summer, accuracy improvements were not obvious. We therefore suggest that for future snow cover mapping applications in regions with similar physiographic conditions the previously used threshold (NDSI=0.4) can be, in general, used for robust estimates of snow cover from MODIS (C6) datasets. In forested alpine regions, however, the lower threshold will improve snow cover mapping particularly during spring months. For fitting of such thresholds additional snow cover, snow depth or snow fraction data can be used.

We found that NDSI values provided in new MODIS snow cover product allow a flexible estimation of snow cover area. The uncertainties related to fitting of the best thresholds include the selection of snow depth threshold, particularly when the snow is patchy, or there is large topographical variability within a MODIS pixel or under the dense forest vegetation (Parajka et al., 2012). As it is indicated in Parajka and Blöschl (2006) time shift between snow depth and MODIS observations can also lead to some differences and uncertainty in the mapping of final thresholds. Such uncertainties can be reduced by using satellite products with finer resolution or by using new mapping algorithms that use vegetation characteristics (Wang et al., 2018). In future studies we plan to implement and evaluate different regionalization methods for regional snow cover mapping and to test their value and uncertainty for calibration and validation of rainfall-runoff models as well as for potential assimilation of new MODIS products in operational snowmelt forecasting methods.

Die approbierte gedruckte Originalversion dieser Dissertation ist an der TU Wien Bibliothek verfügbar.
The approved original version of this doctoral thesis is available in print at TU Wien Bibliothek.
TU Bibliothek Your knowledge hub WIEN

3. The value of ASCAT soil moisture and MODIS snow cover data for calibrating a conceptual hydrologic model

The present chapter corresponds to the following scientific publication in its original form:

Tong, R., Parajka, J., Salentinig, A., Pfeil, I., Komma, J., Széles, B., Kubáň, M., Valent, P., Vreugdenhil, M., Wagner, W., Blöschl, G. (2021). The value of ASCAT soil moisture and MODIS snow cover data for calibrating a conceptual hydrologic model. Hydrol. Earth Syst. Sci., 25(3), 1389-1410. doi:10.5194/hess-25-1389-2021

3.1 State art of multiple objective calibration of hydrological models and the aim of this chapter

Estimating the spatial and temporal variability of water balance components at the regional scale is important for solving a range of practical issues in water resources management and planning, as well as for understanding catchment functioning in terms of how runoff generation processes interact to produce catchment response. One estimation approach is by hydrologic models. There is a variety of model types and model parameter estimation methods. Notwithstanding their usefulness, the resulting simulations of the water balance components are subject to uncertainty due to uncertainty in model inputs, parameter estimation and model structure (Kavetski et al., 2006; Parajka et al., 2007; Wagener and Montanari, 2011).

Previous studies have demonstrated that multiple objective calibration helps to constrain hydrologic models and hence to reduce uncertainty and to improve predictions in hydrological modelling (e.g. Efstratiadis and Koutsoyiannis, 2010). Most of these studies examined the value of constraining hydrologic models by combining different runoff signatures (e.g. by simultaneous calibration of the models to low and high flows or timing) or calibrating hydrologic models to runoff and some additional hydrological variable such as snow cover (e.g. Udnæs et al., 2007; Parajka and Blöschl, 2008b; Franz and Karsten, 2013; Duethmann et al., 2014; Finger et al., 2015, Han et al., 2019, Sleziak et al., 2020), soil moisture (e.g. Parajka et al., 2009; Sutanudjaja et al., 2014; Wanders et al., 2014; Rajib et al., 2016; Kundu et al., 2017, Li et al., 2018), evaporation (e.g. Immerzeel and Droogers, 2008; Zhang et al., 2009), groundwater level data (Seibert, 2000) or total water storage (e.g. Lo et al., 2010; Werth and Güntner, 2010; Rakovec et al., 2016; Bai et al., 2018; Trautmann et al., 2018). These studies showed that the use of additional information typically improves the spatial and/or temporal patterns of internal state variables and fluxes, but does not necessarily improve the efficiency of simulating runoff. Most of the studies reported a small degradation of runoff model efficiency while the internal consistency of the models improved. A few studies also tested the combination of more variables in multiple objective calibration (e.g. Milzow et al., 2011; Kunnath-Poovakka et al., 2016; López et al., 2017; Nijzink et al., 2018; Demirel et al., 2019; Szeles et al., 2020, 2021) and found that the combination of different variables generally reduced the parameter uncertainty particularly in data poor regions. For example, Nijzink et al. (2018) demonstrated that constraining hydrologic models profited from an increased number of data sources. Interestingly, the use of different soil moisture products had a positive impact on the identifiability of not only soil but also snow module parameters.

Die approbierte gedruckte Originalversion dieser Dissertation ist an der TU Wien Bibliothek verfügbar.
The approved original version of this doctoral thesis is available in print at TU Wien Bibliothek.
TU Bibliothek Your knowledge hub WIEN

The factors that control these improvements are less well understood. Snow cover data improved snow and runoff simulations in small catchments without precipitation observations (Parajka and Blöschl, 2008b). They helped to reduce snow underestimation errors in flatland catchments in changing climate conditions (Sleziak et al., 2020). Including evapotranspiration estimates improved regionalization and simulations of daily and monthly runoff particularly in drier regions with lower runoff volumes (Zhang et al., 2009). The use of total water storage data from GRACE improved runoff simulations on monthly or longer time scales, particularly in wet catchments (Rakovec et al. 2016). Only a few studies examined the factors that control the changes in soil moisture efficiency when using soil moisture information (Rajib, et al., 2016). Parajka et al., (2006) showed that soil moisture efficiency of a model calibrated to runoff and satellite soil moisture was lower in hilly and alpine regions with large topographical variability as compared to the flatlands. Nijzink et al. (2018) reported that the AMSR-E soil moisture product improved the identifiability of model parameters in peaty lowland catchments.

Recent advances in the observation techniques of soil moisture, particularly in passive and active microwave remote sensing, increases the availability of regional and global soil moisture datasets (Babaeian et al., 2019). Passive microwave sensors operating in the 1-10 GHz frequency range suitable for soil moisture retrieval include the L-band radiometers flown on board the Soil Moisture Active Passive (SMAP) and Soil Moisture and Ocean Salinity (SMOS) missions, and the multi-frequency radiometer Advanced Microwave Scanning Radiometer 2 (AMSR-2). In the active domain, soil moisture retrievals from the C-band Advanced Scatterometer (ASCAT) have found widespread use in geoscientific applications (Brocca et al. 2017). All these satellites have a rather coarse spatial resolution in the order of tens of kilometres (10-50 km). Various validation studies have shown that ASCAT soil moisture data sets (Wagner et al. 2013) are less accurate than corresponding SMAP soil moisture data sets (Kim et al. 2020), but overall, comparable in quality with SMOS and AMSR-2 (Chen et al., 2018; El Hajj et al., 2018; Mousa and Shu 2020). Nonetheless, there are important regional differences in the quality of the satellite soil moisture data sets, with ASCAT performing in general poorest over arid environments and best over more densely vegetated regions. Over the United States and Europe, comparisons with in-situ soil moisture data from dense networks have revealed the presence of seasonal biases in the ASCAT soil moisture time series (Wagner et al., 2014). Pfeil et al. (2018) and Hahn et al. (2020) have demonstrated that these seasonal biases can be much reduced by enhancing the vegetation parameterization of the TU Wien change detection model introduced by Wagner et al. (1999a,b). The launch of the Sentinel-1 series provides observations at a high spatial resolution of 5x20 m. Over mountainous environments, soil moisture retrievals from all microwave sensors are in general much less reliable than over flatland regions due to significant topographic variations within the coarse-resolution satellite footprints and the presence of rocks, ice, snow, and dense vegetation. Nonetheless, in the snow- and frost-free summer months, the satellite retrievals may have some skill as demonstrated by Brocca et al. (2013) for an alpine catchment in northern Italy.

The objective of this Chapter is to test the value of a new ASCAT Soil Water Index (SWI) data product for multiple objective calibration and validation of a conceptual hydrologic model. Compared to the operational ASCAT SWI product as distributed by the Copernicus Global Land Service, this experimental SWI data product mainly benefits from a new vegetation parameterization of the ASCAT surface soil moisture retrieval algorithm and an improved spatial representation due to the application of a new directional resampling method based on Sentinel-1 Synthetic Aperture Radar (SAR) data. The main aims are: (1) to evaluate the performance of a conceptual hydrologic model calibrated to satellite soil moisture and runoff, (2) to test the impact of weight on the runoff objective in model calibration, (3) to compare the multiple objective calibrations to three different calibration variants – (i) traditional calibration

Die approbierte gedruckte Originalversion dieser Dissertation ist an der TU Wien Bibliothek verfügbar.
The approved original version of this doctoral thesis is available in print at TU Wien Bibliothek.
TU Bibliothek Your knowledge hub WIEN

to runoff only, (ii) multiple objective calibration to satellite snow cover and runoff and (iii) multiple objective calibration to satellite snow cover, soil moisture and runoff; (4) to examine factors that control the model performance at the regional scale. The analysis is performed by confronting a conceptual hydrologic model with ASCAT SWI soil moisture data for 213 catchments in Austria, which represent a wide range of physiographic settings typical of Central European conditions.

3.2 Data

3.2.1 ASCAT Soil Water Index product

For producing a new, experimental version of the ASCAT Soil Water Index (SWI) data set, we deployed the same algorithms as used within the EUMETSAT H SAF and Copernicus Global Land Service. The novelty is the application of a new parameterization for the vegetation correction (Hahn et al., 2020) and a new approach for disaggregating the ASCAT soil moisture retrievals to a finer grid. This approach is currently under review by H SAF for producing the planned Metop ASCAT Disaggregated Surface Soil Moisture Near Real Time 1 km sampling (ASCAT DIS SSM NRT 1 km - H28) data product. The main steps in the processing are: (i) retrieving surface soil moisture from ASCAT backscatter time series using the TU Wien change detection algorithm adopted to ASCAT (Naeimi et al., 2009) and using the vegetation parameterization as recommended by Pfeil et al. (2018), (ii) disaggregating the ASCAT surface soil moisture data to a regular 500 m grid using the directional resampling method as described in the Algorithm Theoretical Baseline Document (ATBD) for the planned H SAF H28 data product, and (iii) computing the Soil Water Index (SWI) using the iterative implementation of the exponential filter introduced by Wagner et al. (1999a,b) and Albergel et al. (2008) with a characteristic time value of T = 10 days, representing root zone soil moisture. This last processing step makes the ASCAT soil moisture data better comparable to the modelled soil moisture data as it filters out high-frequency fluctuations of the ASCAT surface soil moisture retrievals and samples the data at regular time intervals. The disaggregation step is based on the analysis of Sentinel 1 backscatter time series sampled to 500 m. It essentially looks for the best direction from which the ASCAT data are interpolated to the 500 m grid. Thereby it improves the resampling especially near large lakes or near large urban areas. The ASCAT product used in this research is the same product which is used as the active product in the ESA-CCI. The study of Dorigo et al. (2017) demonstrated the quality of the active ESA-CCI product over temperate climates such as Austria. Considering that the spatial sampling of the ESA-CCI dataset is 0.25 degree, whereas the ASCAT product has a sampling of 12.5 km, the ASCAT product was chosen to be applied in this Chapter. In addition, the algorithm of the ASCAT product which improved vegetation parameters performed better over Austria (Pfeil et al., 2018).

To exclude invalid ASCAT measurements of snow and frozen ground, soil moisture was masked using soil temperature and snow cover from ECMWF Copernicus Climate Service (C3S) ERA5-Land. Soil moisture was masked when soil temperatures at a soil depth of 0-7 cm were below 1°C or snow cover exceeded 30 % of the pixel.

3.2.2 MODIS snow cover product

Snow cover is mapped by combining the MODIS products from the Terra (MOD10A1) and Aqua (MYD10A1) satellites (Hall and Riggs, 2016a, b). Version 6 of the MOD10A1 and MYD10A1 datasets provide daily maps of Normalized Difference Snow Index (NDSI) at a 500 m spatial resolution. The NDSI values range between 0.0 and 1.0, and snow cover is considered to be present if NDSI is larger than a threshold. Former MODIS versions used a fixed threshold

Die approbierte gedruckte Originalversion dieser Dissertation ist an der TU Wien Bibliothek verfügbar.
The approved original version of this doctoral thesis is available in print at TU Wien Bibliothek.
TU Bibliothek Your knowledge hub WIEN

(0.4), but Tong et al. (2020) found that in Austria, this threshold can be seasonally optimized for different altitudes and land cover classes. In this Chapter, we use a threshold that varies seasonally, decreases with increasing elevation and is lower in forested than open land cover settings (see Fig 2.5). Such a varying threshold improves the regional snow cover mapping by 3-10%, mainly in forested regions above 900m a.s.l. (Tong et al., 2020). The classified snow cover maps from Terra and Aqua are then combined to reduce the effect of clouds. Pixels classified as clouds or missing in Terra are replaced by pixels from Aqua if these are classified as snow-covered or snow-free (Parajka and Blöschl, 2008b).

3.2.3 Study area and other data

The value of satellite data for the calibration of hydrologic models is evaluated in 213 catchments in Austria (Fig. 3.1, Table 3.1). This set of catchments has been selected in previous studies (Viglione et al., 2013, Sleziak et al., 2020) to represent diverse physiographic, landscape and hydrologic characteristics which are not significantly affected by human impact. Selected catchment characteristics of this dataset are presented in Table 3.1. The size of the catchments varies from 13.7 to 6214 km^2, and their mean elevation ranges from 353 m a.s.l. to 2940 m a.s.l.. Topographical characteristics are derived from a digital elevation model with 500m spatial resolution. Land cover in Austria is mainly agricultural crops and meadows in the lowlands and forest in the medium elevation ranges. Alpine vegetation and rocks prevail in catchments in the Alps. Land cover characteristics are derived from the CORINE land cover mapping (CLC2006 dataset, EEA, 2013, https://land.copernicus.eu/), and Normalized Difference Vegetation Index (MOD13A3v006) is generated from MODIS C6 1km monthly data (Didan, 2015). Austria has a warm temperate climate, except for the Alps. The largest precipitation rates (more than 2000 mm/year) occur in the west, mainly due to orographic lifting of northwesterly airflows at the rim of the Alps. Mean annual catchment precipitation is lower (less than 800mm/year) in the lowlands in the east, and the contrast with the Alps is reinforced by the higher air temperature and much higher evaporation in the lowlands. Soil characteristics are derived from a 1km global map of soil hydraulic properties (Zhang et al., 2018). This dataset provides the mean and standard deviations of selected soil hydraulic parameters based on the Kosugi water retention model (Kosugi 1994, 1996) at a 1 km resolution for surface soils (0-5cm).

Hydrological and meteorological data are obtained from Central Hydrographical Bureau (HZB, ehyd.gv.at) and Zentralanstalt für Meteorologie und Geodynamik (ZAMG). Model inputs (i.e. mean daily precipitation and air temperature) are derived from the gridded SPARTACUS dataset (Hiebl and Frei, 2016, 2018). This dataset provides long-term daily gridded (1km spatial resolution) maps, which are consistently interpolated by using a consistent station network throughout the entire period (Duethmann et al., 2020). Mean daily potential evaporation is derived from gridded maps of mean daily air temperature and potential sunshine duration index by using a modified Blaney–Criddle approach (Parajka et al., 2003). Daily runoff data from 213 catchments are used for calibrating and 208 catchments for validating the hydrologic model.

The precipitation, air temperature, runoff and MODIS snow cover data are available from September 2000 to August 2014. The concurrently available period for the soil moisture ASCAT SWI data is January 2007 to August 2014.

Die approbierte gedruckte Originalversion dieser Dissertation ist an der TU Wien Bibliothek verfügbar.
The approved original version of this doctoral thesis is available in print at TU Wien Bibliothek.
TU Bibliothek Your knowledge hub WIEN

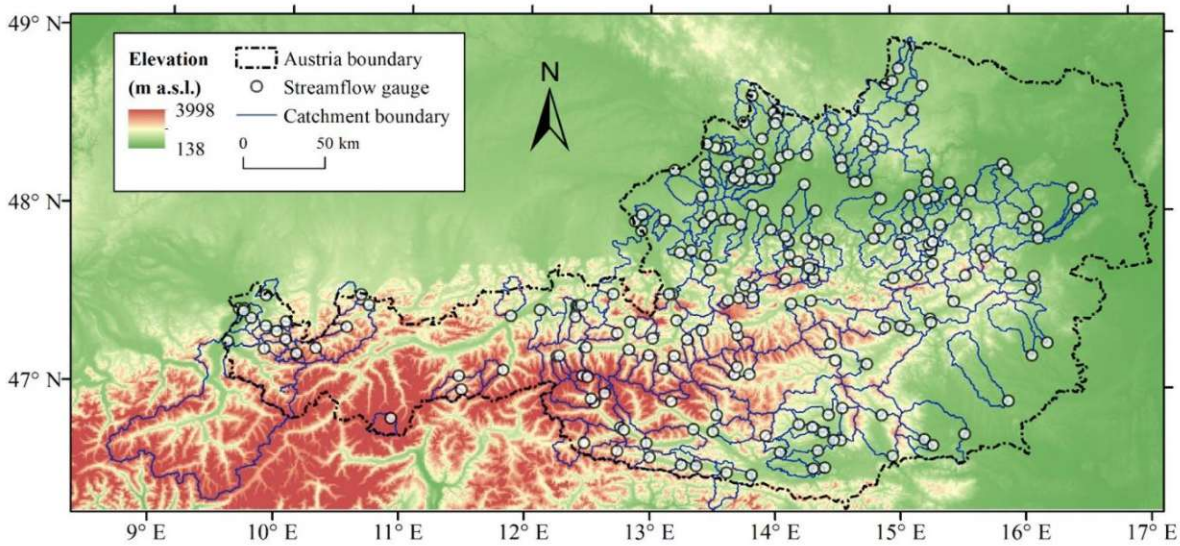

Figure 3.1 Topography of Austria and the location of the 213 catchments.

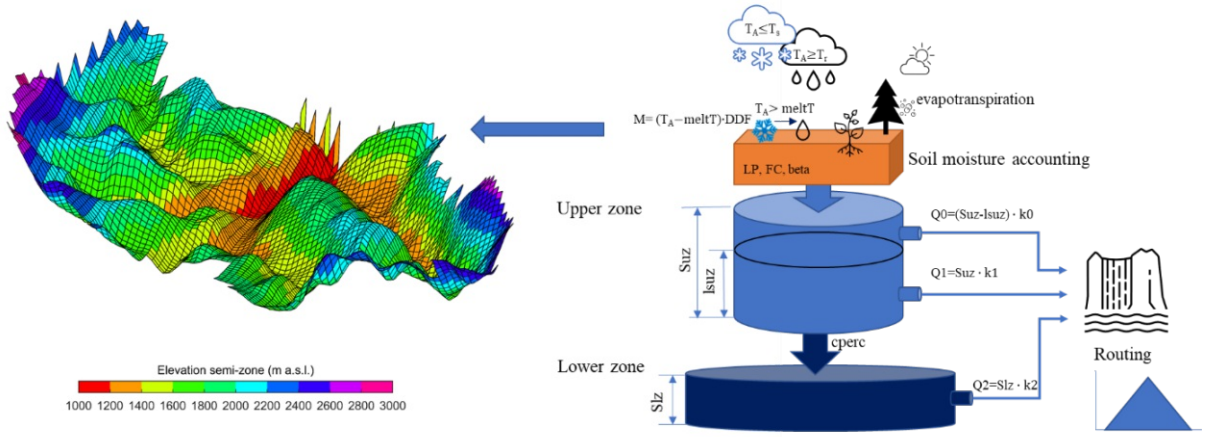

Figure 3.2 Conceptual description of TUWmodel structure.

Die approbierte gedruckte Originalversion dieser Dissertation ist an der TU Wien Bibliothek verfügbar.
The approved original version of this doctoral thesis is available in print at TU Wien Bibliothek.
TU Bibliothek Your knowledge hub WIEN

Table 3.1. Statistics of the catchment attributes of the 213 catchments in Figure 3.1 with abbreviation, unit, minimum, maximum, and median. The standard deviations refer to spatial variability within each catchment.

Information	Attribute	Abbrev.	Unit	Min.	Max.	Median
Size	Area	A	km^2	13.70	6214.00	167.30
Elevation	Mean elevation	MELE	m a.s.l.	353.01	2939.76	1010.73
	Minimum elevation	MiELE	m a.s.l.	200.00	1939.00	561.00
	Maximum elevation	MxELE	m a.s.l.	509.00	3760.00	1861.00
	Elevation range	ER	m	80.00	3072.00	1279.00
	Roughness index (MELE-MiELE)/ER	RI	-	0.15	0.65	0.38
	Mean slope	SL	%	1.74	43.91	18.84
	Mean daily potential global radiation	MGR	$kW \cdot m^{-2} \cdot day$	4.73	6.26	5.19
	Standard deviation of MGR	SDGR	$kW \cdot m^{-2} \cdot day$	0.02	1.10	0.39
Land cover	Coverage of forest	FP	%	0.00	94.59	46.88
	Coverage of agricultural areas	AP	%	0.00	92.86	16.30
	Mean monthly normalized difference vegetation index	MNDVI	-	0.00	0.71	0.60
	Standard deviation of MNDVI	SDNDVI	-	0.02	0.19	0.06
Climate	Mean annual precipitation	MAP	mm	728.13	2301.84	1274.40
	Standard deviation of annual MAP	SDAP	mm	10.79	367.57	124.70
	Mean air temperature	MAT	°C	-2.83	10.30	7.36
	Standard deviation of MAT	SDAT	°C	0.06	3.55	1.26
	Mean annual potential evaporation	MEPI	mm	233.49	740.45	629.57
	Standard deviation of MEPI	SDEPI	mm	4.33	162.07	60.17
	Catchment aridity index (MEPI/MAP)	CAI	-	0.18	0.98	0.47
	Standard deviation of aridity index	SDAI	-	0.01	0.31	0.08
	Proportion of day with temperature below 0 °C	MTL0	-	0.12	0.62	0.20
Soil	Mean field capacity	MFC	$cm^3 \cdot cm^{-3}$	0.29	0.43	0.36
	Standard deviation of MFC	SDFC	$cm^3 \cdot cm^{-3}$	0.01	0.05	0.02
	Mean saturated hydraulic conductivity	MKS	$cm \cdot day^{-1}$	24.88	327.77	161.17
	Standard deviation of MKS	SDKS	$cm \cdot day^{-1}$	6.43	76.03	40.35

3.3 Methods

3.3.1 Conceptual hydrologic model

The hydrologic model used in this Chapter is a semi-distributed version of TUW model, following the structure of the HBV model (Bergström 1992; Parajka et al., 2007). A simple

Die approbierte gedruckte Originalversion dieser Dissertation ist an der TU Wien Bibliothek verfügbar.
The approved original version of this doctoral thesis is available in print at TU Wien Bibliothek.
TU Bibliothek WIEN Your knowledge hub

illustration of the model structure is presented in Fig. 3.2. The model consists of three routines, i.e. snow accumulation and melt, soil moisture accounting and runoff routine. The snow part has five model parameters and is based on a simple degree-day method: the snow correction factor SCF to account for errors in measurement of snowfall due to gauge undercatch, the degree-day factor DDF, and three threshold temperatures Ts, Tr, meltT. The soil moisture routine has three parameters: the maximum soil moisture storage in the root zone FC, a limit that controls the actual evapotranspiration LP and a nonlinear parameter for runoff production beta. The routing involves two parts, within-catchment routing and stream routing. The within-catchment routing has five parameters: three storage coefficients k0, k1 and k2 for three conceptual reservoirs representing overland flow, interflow and base flow, a threshold for very fast response lsuz and a constant percolation rate cperc connecting the fast and slow reservoirs. The stream routing uses a triangular transfer function with two parameters: bmax and croute. The total number of model parameters that are calibrated is 15 (Table 3.2). The model is run in a semi-distributed way, i.e. model inputs and outputs are estimated for elevation zones of 200m while the model parameters are assumed to be lumped (i.e. constant) in each catchment. In order to match the model simulations to the dimensionless satellite soil water index, the simulated soil moisture is scaled by the field capacity (i.e. the model parameter FC), to obtain a relative root zone moisture ranging from 0 to 1. More details about the model can be found in the Appendix of Parajka et al. (2007).

Table 3.2. Parameters of the hydrologic model (TUWmodel) and ranges used in model calibration. A suitable parameter range may vary by climate and land cover regions and is usually set by expert judgement. The range used here is based on the previous experience of Merz et al. (2011) and Viglione et al. (2013) in the study area.

Parameter	Explanation [Unit]	General Range
SCF	snow correction factor [-]	0.9-1.5
DDF	degree day factor [mm/ °C/day]	0.0-6.0
Ts	threshold temperature below which precipitation is snow [°C]	-3.0-1.0
Tr	threshold temperature above which precipitation is rain [°C]	1.0-3.0
meltT	threshold temperature above which melt starts [°C]	-2.0-2.0
LP	parameter related to the limit for potential evaporation [-]	0.0-1.0
FC	field capacity, i.e., max soil moisture storage [mm]	0-600
beta	the nonlinear parameter for runoff production [-]	0-20
k0	storage coefficient for very fast response [day]	0-2.0
k1	storage coefficient for fast response [day]	2-30
k2	storage coefficient for slow response [day]	30-250
lsuz	threshold storage state, i.e., the very fast response starts if exceeded [mm]	1-100
cperc	constant percolation rate [mm/day]	0.0-8.0
bmax	maximum base at low flows [days]	0.0-30.0
croute	free scaling parameter [days^2/mm]	0.0-50.0

Die approbierte gedruckte Originalversion dieser Dissertation ist an der TU Wien Bibliothek verfügbar.
The approved original version of this doctoral thesis is available in print at TU Wien Bibliothek.
TU Bibliothek Your knowledge hub WIEN

3.3.2 Multiple objective calibration and validation of hydrologic model

The value of using satellite soil moisture (SSM) data for multiple objective calibration of conceptual hydrologic models is compared to three other calibration variants: (1) traditional calibration to runoff only, (2) multiple objective calibration to satellite snow cover (SSC) and runoff and (3) multiple objective calibration to SSM, SSC and runoff. The general form of the calibration objective function F used in this Chapter consists of minimizing the weighted sum of individual objectives related to runoff (O_Q), soil moisture (O_{SM}) and snow cover (O_{SC}):

$$F = w_Q \cdot O_Q + w_{SM} \cdot O_{SM} + w_{SC} \cdot O_{SC} \qquad (3.1)$$

where w_Q, w_{SM} and w_{SC} are the weights of the respective objectives. In each multiple objective calibration variant, 11 runoff weights (from 0.0 to 1.0 with a step of 0.1) are tested (Table 3.3). The soil moisture and snow weights are assumed to be equal for symmetry, and are calculated by setting the sum of all weights to 1.0.

Table 3.3. Weights given to runoff, satellite soil moisture (SSM) and satellite snow cover (SSC) in the multiple objective calibration (Eq.3.1) for different calibration variants. a set of 11 w_Q weights in the range 0.0 and 1.0 is tested for each multiple objective calibration variant. The sum of weights is always 1.0.

Calibration variant	Weight of runoff (w_Q)	Weight of soil moisture (w_{SM})	Weight of snow cover (w_{SC})
Runoff only	$w_Q = 1.0$	$w_{SM} = 0.0$	$w_{SC} = 0.0$
SSM+runoff (Var1)	$w_Q = \{k/10\}_{k=0}^{10}$	$w_{SM} = 1 - w_Q$	$w_{SC} = 0.0$
SSC+runoff (Var2)	$w_Q = \{k/10\}_{k=0}^{10}$	$w_{SM} = 0.0$	$w_{SC} = 1 - w_Q$
SSM+SSC+runoff (Var3)	$w_Q = \{k/10\}_{k=0}^{10}$	$w_{SM} = w_{SC}$	$w_{SC} = w_{SM}$

The individual objectives O_Q, O_{SM} and O_{SC} are defined as follows. The runoff objective O_Q consists of a combination of two variants of the Nash-Sutcliffe coefficient *NSE* and NSE_{log} (Nash and Sutcliffe, 1970):

$$O_Q = 0.5 \cdot NSE + 0.5 \cdot NSE_{log} \qquad (3.2)$$

$$NSE = 1 - \frac{\sum_{i=1}^{n}\left(Q_{obs,i} - Q_{sim,i}\right)^2}{\sum_{i=1}^{n}\left(Q_{obs,i} - \overline{Q_{obs}}\right)^2} \qquad (3.3)$$

$$NSE_{\log} = 1 - \frac{\sum_{i=1}^{n}\left(\log(Q_{obs,i}) - \log(Q_{sim,i})\right)^2}{\sum_{i=1}^{n}\left(\log(Q_{obs,i}) - \log(\overline{Q_{obs}})\right)^2} \qquad (3.4)$$

where $Q_{obs,i}$ and $Q_{sim,i}$ represent observed and simulated daily runoff of day i, respectively and Q_{obs} is the average of observed daily runoff over the calibration (or verification) period of n

Die approbierte gedruckte Originalversion dieser Dissertation ist an der TU Wien Bibliothek verfügbar.
The approved original version of this doctoral thesis is available in print at TU Wien Bibliothek.
TU Bibliothek WIEN Your knowledge hub

days. The choice of the equal weighting of *NSE* and NSE_{log} is based on previous studies in the study region (e.g. Parajka and Blöschl, 2008b) to emphasize both the high and low flow conditions.

The soil moisture objective function (O_{SM}) is expressed by the correlation coefficient *r* between relative soil moisture estimated from the ASCAT and simulated by the hydrologic model:

$$O_{SM} = \frac{\sum_{i=1}^{n}\left((\theta_{sim,i} - \overline{\theta_{sim}})(\theta_{obs,i} - \overline{\theta_{obs}})\right)}{\sqrt{\sum_{i=1}^{n}\left((\theta_{sim,i} - \overline{\theta_{sim}})^2(\theta_{obs,i} - \overline{\theta_{obs}})^2\right)}} \qquad (3.5)$$

where θ_{sim} is the relative root zone soil moisture simulated by the model and θ_{obs} is the ASCAT SWI. The correlation coefficient is selected as a measure of similarity because it allows a comparison of the temporal dynamics irrespective of the respective magnitudes and possible intercepts in the relationship between observed and simulated soil moisture.

The snow cover objective function O_{SC} involves the sum of snow overestimation S_O and underestimation S_U errors:

$$O_{SC} = 1 - (S_O + S_U) \qquad (3.6)$$

The estimation of S_O and S_U follows the strategy proposed and evaluated in Parajka and Blöschl (2008b). The snow overestimation error indicates the relative number of days when the hydrologic model simulates snow but the satellite (MODIS) does not observe snow cover:

$$S_O = \frac{1}{\sum_{i=1}^{N_{days}}\sum_{j=1}^{N_{zones}} A_{i,j}} \sum_{i=1}^{N_{days}}\sum_{j=1}^{N_{zones}} A_{i,j} \cap (SWE_{i,j} > \xi_{SWE}) \cap (\mathrm{SCA}_{i,j} = 0) \qquad (3.7)$$

where $A_{i,j}$ is the area of zone *j* on the day *i* which is cloud-free from MODIS. $SWE_{i,j}$ is the simulated snow water equivalent in elevation zone *j* larger than 10mm (Parajka and Blöschl, 2008b), $SCA_{i,j}$ is the snow covered area estimated from MODIS within this zone, N_{days} is the number of days i, where MODIS images are available with cloud cover less than a threshold (ξ_C) 50%.

The snow underestimation error indicates the relative number of days when the hydrologic model does not simulate snow in a zone, but MODIS indicates that snow covered area greater than a threshold 25% is present in the zone, i.e.:

$$S_U = \frac{1}{\sum_{i=1}^{N_{days}}\sum_{j=1}^{N_{zones}} A_{i,j}} \sum_{i=1}^{N_{days}}\sum_{j=1}^{N_{zones}} A_{i,j} \cap (SWE_{i,j} = 0) \cap (\mathrm{SCA}_{i,j} > \xi_{SCA}) \qquad (3.8)$$

The snow covered area, *SCA*, within each zone is calculated from the MODIS data as

$$\mathrm{SCA}=\mathrm{S}/(\mathrm{S}+\mathrm{L}) \qquad (3.9)$$

where S and L represent the number of pixels mapped as snow and snow free, respectively, for a given day and a given elevation zone.

Die approbierte gedruckte Originalversion dieser Dissertation ist an der TU Wien Bibliothek verfügbar.
The approved original version of this doctoral thesis is available in print at TU Wien Bibliothek.
TU Bibliothek Your knowledge hub WIEN

The thresholds ξ_{SWE}, ξ_{SCA} and ξ_C are chosen on the basis of the sensitivity analysis performed by Parajka and Blöschl (2008b).

The procedure of model parameters calibration is carried out for each calibration variant and each catchment independently. All calibration variants are automatically calibrated by using the shuffled complex-self adaptive hybrid evolution (SC-SAHEL) developed by Naeini et al. (2018). It combines four evolutionary algorithms (EA) with the self-selected scheme and hence the evolution process of generating parameter values is more robust. The number of complexes is set to 8, allowing the four EAs to be automatically changed by each evolution generation. The optimization is stopped at any of the following three criteria: if the parameters converge to a space of geometric size less than 0.01; if the best objective function value has not improved by 0.1% over the last 10 loops; if the total number of runs reaches 1,000,000 (see. Chu et al., 2011; Naeini et al., 2018).

The calibration period used in all variants is from September 1, 2000 to August 31, 2010. The validation period is from September 1, 2010 to August 31, 2014. The warmup period is one year before the start of the calibration or validation period. Since soil moisture satellite data are available only from January 2007, the soil moisture simulation efficiency for the calibration period is calculated for a shorter time period.

3.4 Results

3.4.1 Performance of multiple objective calibration

The calibration model performance of three multiple objective calibration variants is presented in Fig. 3.3 and Table 3.4. The objective function involves a runoff component weighted by w_Q and additional soil moisture and snow components (Table 3.3). The limiting case is w_Q=1 where only the runoff component is used and this case represents a typical calibration to runoff only. The case where w_Q=0 represents calibration only to SSM and/or SSC without the use of runoff data. The median runoff efficiency over the 213 catchments (Fig. 3.3, top; Table 3.4) ranges between 0.74 and 0.79 for w_Q larger than 0.3 irrespective of the calibration variants. Using SSM and SSC with runoff for model calibration results in a similar pattern of model performance to the case when only SSM and runoff are used, but the former variant has a smaller regional variability (scatter) of runoff model efficiency for w_Q less than 0.6. Interestingly, when no runoff is involved (w_Q=0), using only SSC results in slightly better runoff simulations than when using only SSM, while for w_Q from 0.1 to 0.3 the opposite is the case.

The correlation between ASCAT and simulated soil moisture (Fig. 3.3, centre) has a much larger regional variability (i.e. variability between catchments) than the w_Q variants. For the SSM and runoff variant, the median correlation increases from 0.29 to 0.52 with decreasing w_Q, and the variant using all three variables is similar. For the snow cover and runoff variant w_Q has little effect on soil moisture correlation and correlation is similar to the runoff only calibration (w_Q=1).

Similar patterns are observed for the snow cover efficiency. The SSM weighting has little effect on the snow cover simulations. The median O_{SC} is between 0.75 and 0.79 for w_Q larger than 0.0. The variants that use SSC show increasing performance with decreasing w_Q and the regional variability decreases. For w_Q less than 0.5, the median O_{SC} is between 0.84 to 0.91, which is 5 to 13% larger than the median for calibration to runoff only (O_{SC} =0.79). These results indicate that the simultaneous use of SSM and SSC in model calibration can improve

Die approbierte gedruckte Originalversion dieser Dissertation ist an der TU Wien Bibliothek verfügbar.
The approved original version of this doctoral thesis is available in print at TU Wien Bibliothek.
TU Bibliothek Your knowledge hub WIEN

simulations of soil moisture and snow cover in the calibration period, without any significant reduction in runoff model efficiency, particularly for w_Q between 0.3 and 0.4.

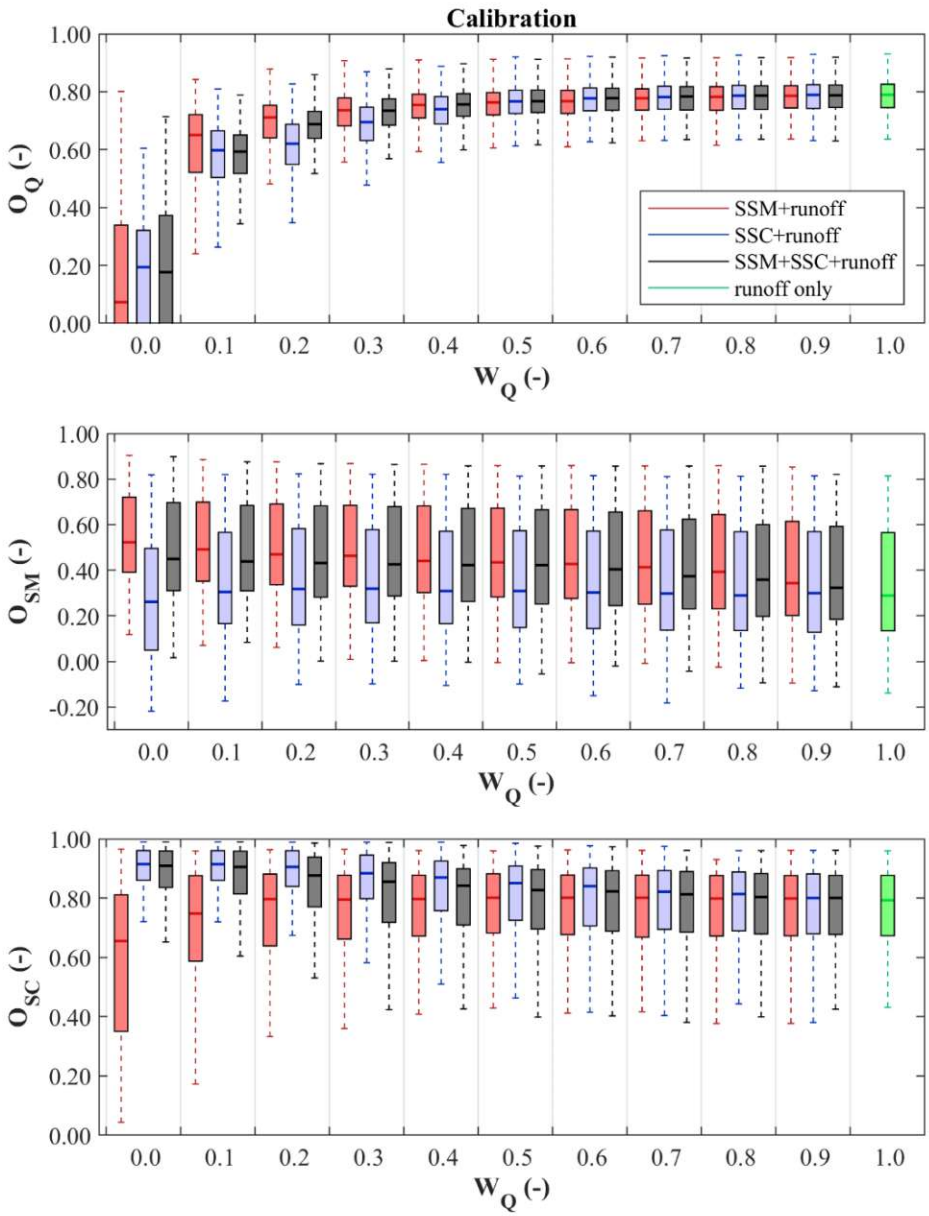

Figure 3.3 Hydrologic model performance for three multiple objective calibration variants: calibration to satellite soil moisture and runoff (red boxes), to satellite snow cover and runoff (blue boxes) and to satellite soil moisture, snow cover and runoff (grey boxes). Top, middle and bottom panels show runoff (Eq. 3.2), soil moisture (Eq. 3.5) and snow cover (Eq. 3.6) model efficiency for different weights of the runoff objective w_Q in the calibration period 2000-2010, respectively. w_Q =1 represents calibration to runoff only. Boxes represent the values from the different catchments and the size of the boxes represents the spatial variability across the 213 catchments.

Die approbierte gedruckte Originalversion dieser Dissertation ist an der TU Wien Bibliothek verfügbar.
The approved original version of this doctoral thesis is available in print at TU Wien Bibliothek.
TU Bibliothek Your knowledge hub WIEN

Table 3.4. Median of runoff (Eq. 3.2), soil moisture (Eq. 3.5) and snow cover (Eq. 3.6) model efficiency obtained from three multiple objective calibration variants: (1) to satellite soil moisture (ASCAT) and runoff (var1); (2) to satellite snow cover (MODIS) and runoff (var2); (3) to satellite soil moisture (ASCAT), satellite snow cover (MODIS) and runoff (var3) in 213 catchments in the calibration period 2000-2010.

Weight w_Q	Runoff model efficiency			Soil moisture efficiency			Snow cover efficiency		
	Var1	Var2	Var3	Var1	Var2	Var3	Var1	Var2	Var3
0.00	0.07	0.19	0.18	0.52	0.26	0.45	0.66	0.91	0.91
0.10	0.65	0.60	0.59	0.49	0.30	0.44	0.75	0.91	0.91
0.20	0.71	0.62	0.69	0.47	0.32	0.43	0.80	0.91	0.88
0.30	0.74	0.70	0.73	0.46	0.32	0.43	0.80	0.88	0.86
0.40	0.75	0.74	0.76	0.44	0.31	0.42	0.80	0.87	0.84
0.50	0.76	0.77	0.77	0.43	0.31	0.42	0.80	0.85	0.83
0.60	0.77	0.78	0.78	0.43	0.30	0.40	0.80	0.84	0.82
0.70	0.78	0.78	0.78	0.41	0.30	0.37	0.80	0.82	0.81
0.80	0.78	0.79	0.79	0.39	0.29	0.36	0.80	0.81	0.80
0.90	0.79	0.79	0.79	0.34	0.30	0.32	0.80	0.80	0.80
1.00	0.79	0.79	0.79	0.29	0.29	0.29	0.79	0.79	0.79

Table 3.5. Median of runoff (Eq. 3.2), soil moisture (Eq. 3.5) and snow cover (Eq. 3.6) model efficiency obtained from three multiple objective calibration variants: (1) to satellite soil moisture (ASCAT) and runoff (var1); (2) to satellite snow cover (MODIS) and runoff (var2); (3) to satellite soil moisture (ASCAT), satellite snow cover (MODIS) and runoff (var3) in 213 catchments in the validation period 2010-2014.

Weight w_Q	Runoff model efficiency			Soil moisture efficiency			Snow cover efficiency		
	Var1	Var2	Var3	Var1	Var2	Var3	Var1	Var2	Var3
0.00	0.06	0.11	0.17	0.54	0.35	0.48	0.69	0.93	0.93
0.10	0.60	0.57	0.57	0.49	0.43	0.48	0.75	0.93	0.92
0.20	0.67	0.59	0.66	0.51	0.43	0.49	0.81	0.92	0.91
0.30	0.69	0.65	0.70	0.49	0.43	0.49	0.82	0.91	0.88
0.40	0.71	0.70	0.72	0.48	0.42	0.49	0.81	0.89	0.86
0.50	0.72	0.72	0.72	0.48	0.41	0.48	0.82	0.87	0.85
0.60	0.72	0.73	0.73	0.48	0.41	0.47	0.82	0.86	0.84
0.70	0.72	0.73	0.73	0.46	0.40	0.45	0.82	0.84	0.83
0.80	0.73	0.73	0.73	0.45	0.41	0.43	0.82	0.83	0.83
0.90	0.73	0.73	0.73	0.43	0.40	0.42	0.82	0.82	0.82
1.00	0.73	0.73	0.73	0.40	0.40	0.40	0.81	0.81	0.81

Die approbierte gedruckte Originalversion dieser Dissertation ist an der TU Wien Bibliothek verfügbar.
The approved original version of this doctoral thesis is available in print at TU Wien Bibliothek.
TU Bibliothek Your knowledge hub WIEN

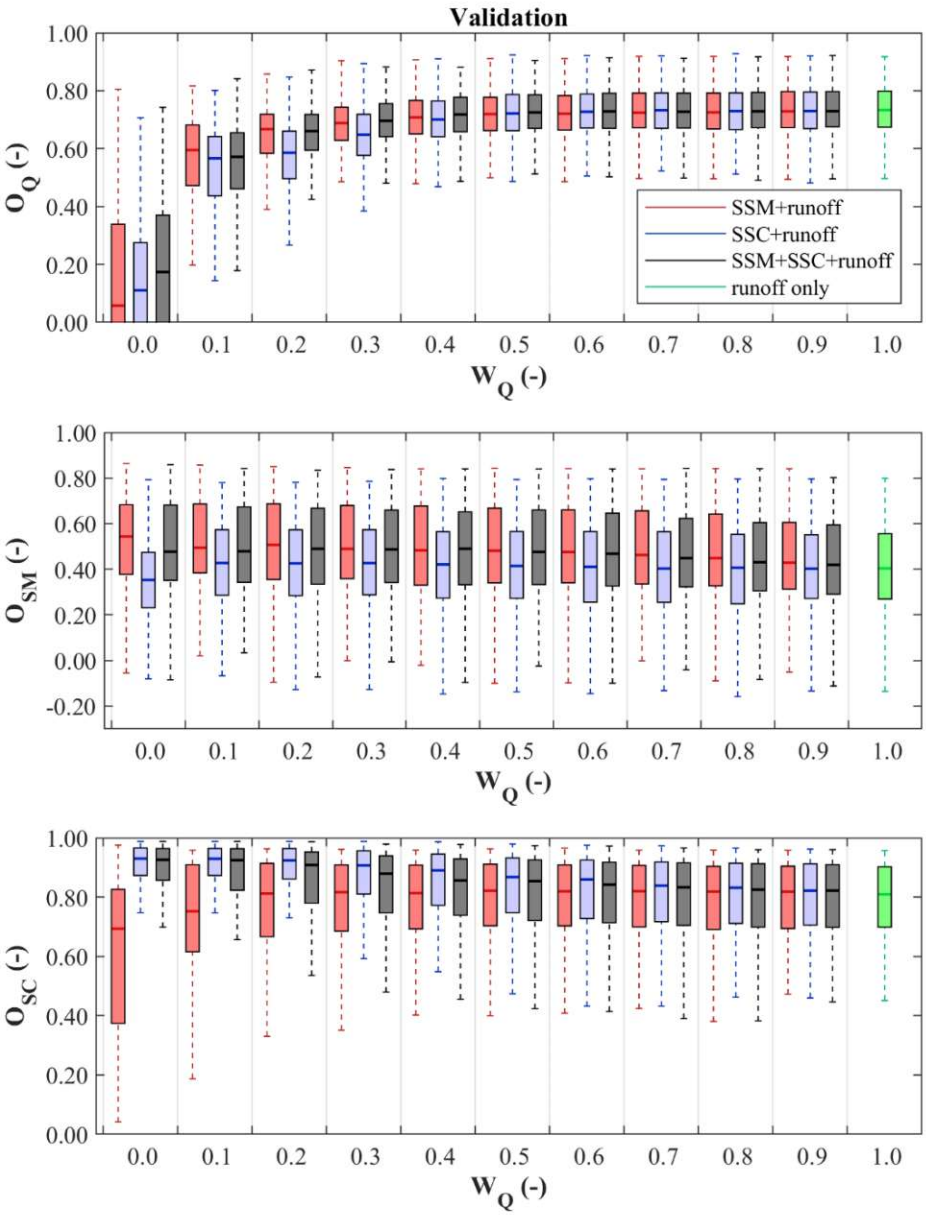

Figure 3.4 Hydrologic model performance for three multiple objective calibration variants: calibration to satellite soil moisture and runoff (red boxes), to satellite snow cover and runoff (blue boxes) and to satellite soil moisture, snow cover and runoff (grey boxes). Top, middle and bottom panels show runoff (Eq. 3.2), soil moisture (Eq. 3.5) and snow cover (Eq. 3.6) model efficiency for different weights of the runoff objective in the validation period 2010-2014, respectively. w_Q =1 represents calibration to runoff only. Boxes represent the values from the different catchments and the size of the boxes represents the spatial variability across the 213 catchments.

The model performance for the validation period (2010-2014) is presented in Fig. 3.4 and Table 3.5. The patterns of changing model efficiency with changing w_Q are very similar to those in the calibration period. The median of validation runoff model efficiency of the SSM and runoff calibration variant for w_Q >0.3 is between 0.71 and 0.73, which is similar or only somewhat

Die approbierte gedruckte Originalversion dieser Dissertation ist an der TU Wien Bibliothek verfügbar.
The approved original version of this doctoral thesis is available in print at TU Wien Bibliothek.
TU Bibliothek Your knowledge hub WIEN

smaller than that for calibration to runoff only (w_Q=1). The SSC and runoff calibration variant results show a slightly lower runoff model performance for weights w_Q< 0.3 compared to the other calibration variants. The calibration with all three variables gives practically identical validation efficiencies as the variant with SSM and runoff.

The median soil moisture correlation increases from 0.43 to 0.54 with decreasing w_Q for the SSM and runoff calibration variant and ranges from 0.42 to 0.49 for the variant that uses all variables. The smallest correlations are found for the SSC and runoff variant, where the median of correlation r varies between 0.35 and 0.43. The regional variability in r is however much larger for all variants than for the calibration period. The scatter (i.e. difference between 75- and 25- percentiles) in r is around 0.3 for all w_Q. For the variants that include SSM the 75-percentiles vary between 0.60 and 0.68.

The snow cover efficiency for w_Q larger than 0.5 is very similar for all three variants. For w_Q smaller than 0.5, O_{SC} tends to increase and the regional variability decreases for the variants involving SSC. The validation O_{SC} is about 2% larger than that obtained in the calibration period. Similar to the calibration period, the weighting of SSM and runoff has hardly any impact on O_{SC}. Adding SSC data to SSM and runoff improves the snow simulation, particularly for w_Q less than 0.4.

It is also interesting to compare the relative performances in the validation period to that in the calibration period. The runoff model performance always decreases when moving from the calibration to the validation period, although the decrease is relatively small, suggesting that there is no overfitting. The soil moisture model performance in contrast always increases when moving from the calibration to the validation period. This is likely because in the case of soil moisture the calibration period only consists of about four years. The snow model performance increases slightly, probably because the proportion of days with temperatures below 0 °C for the validation period is 0.21, which is lower than that for the calibration period (0.24), but the precipitation during the days with the air temperature below 0 °C does not show obvious changes (2.62 mm·day^{-1} for the calibration and 2.67 mm·day^{-1} for the validation periods).

The correlation (in terms of the Pearson correlation coefficient) between model performance and selected catchment attributes (Table 3.1) is evaluated in Fig. 3.5 and Fig. 3.6 in order to understand in which type of catchments SSM and SSC have the most relevant effect on model performance. The runoff model efficiency during the calibration period (Fig. 3.5, left panel) increases with the increasing mean number of days with negative air temperatures (MTL0, correlation over 0.57 for w_Q larger than 0.4) and mean catchment elevation (MELE, correlation over 0.55 for w_Q larger than 0.4) and tends to decrease with increasing catchment mean annual air temperature (MAT, absolute correlation over 0.57 for w_Q larger than 0.4). The larger runoff model efficiency in Alpine catchments than in the lowlands is likely related to the seasonality of snowmelt runoff which is easier to simulate than the individual, more erratic events in the lowlands (Merz and Blöschl, 2009). The correlation of runoff model efficiency and catchment attributes increases with increasing runoff weight w_Q and is not statistically significant or low (i.e. less 0.4) for w_Q<0.4 for most of the attributes. The correlations of the catchment attributes with soil moisture and snow efficiencies are not consistently related to runoff weight. Soil moisture efficiency increases with increasing fraction of agricultural land (AP) where the correlation varies between 0.75 and 0.79 for different w_Q. This trend may be explained by the fact that soil moisture can generally be monitored more accurately in relatively flat, agricultural landscape than in rugged mountainous terrain (Brocca et al. 2013; Parajka et al., 2006), which in Austria are furthermore dominantly covered by forests and other dense vegetation impenetrable to the radar and scatterometer signals. Accordingly, we find the soil moisture

Die approbierte gedruckte Originalversion dieser Dissertation ist an der TU Wien Bibliothek verfügbar.
The approved original version of this doctoral thesis is available in print at TU Wien Bibliothek.
TU Bibliothek Your knowledge hub WIEN

efficiency tends to decrease with increasing forest cover (FP, correlation varies between -0.35 and -0.49). The active rooting zones are much shallower in agricultural lands, whereas tree root much deeper. Hence the satellite soil moisture data used in this Chapter which monitored for the top 100 cm soil layer may fit the soil moisture for arable land better. Also snow model efficiency tends to increase with decreasing MELE and SL (correlation is between -0.52 to -0.89) but increases with increasing MAT (correlations exceed 0.8 for most of the w_Q). In the flatlands, snow is less important so the cumulative number of days with potential snow errors in the objective function is generally lower.

The correlations for the validation period (Fig. 3.6) have the same pattern as for the calibration period (Fig. 3.5). The attributes with the largest correlations with runoff efficiency are the same and correlation tends to increase with increasing w_Q as well. The correlation is generally only slightly lower than that estimated in the calibration period. The soil moisture efficiency in the validation period is positively correlated with AP (correlation = 0.76-0.79) and MAT (correlation = 0.55-0.68), but the correlation with AP is lower than in the calibration period. The largest negative correlation of soil moisture efficiency and attributions is found for calibration to runoff only (w_Q=1) in general and is larger than 0.7 for MELE, catchment elevation range (ER), and standard deviation of MAT and mean daily potential global radiation (SDGR). The snow model efficiency is clearly related to topography, as it increases with decreasing MELE and increasing MAT.

The relationship between model efficiencies and catchment attributes for the other two calibration variants are similar and are presented in Supplement, Fig. 3.7-3.10. The results show that including snow or soil moisture data in model calibration does not change the correlation between model efficiencies and catchment characteristics. It is obvious that for runoff weight w_Q>=0.4 for O_Q, w_Q>=0.0 for O_{SM}, and w_Q>=0.1 for O_{SC}, the correlations between model efficiency and catchment characteristics are similar to that for the runoff only calibration. The model efficiency is mainly related to topography and certain climate, land cover and soil attributes, which are, on the other hand, cross-correlated with topography (Fig. 3.7).

Die approbierte gedruckte Originalversion dieser Dissertation ist an der TU Wien Bibliothek verfügbar.
The approved original version of this doctoral thesis is available in print at TU Wien Bibliothek.
TU Bibliothek Your knowledge hub WIEN

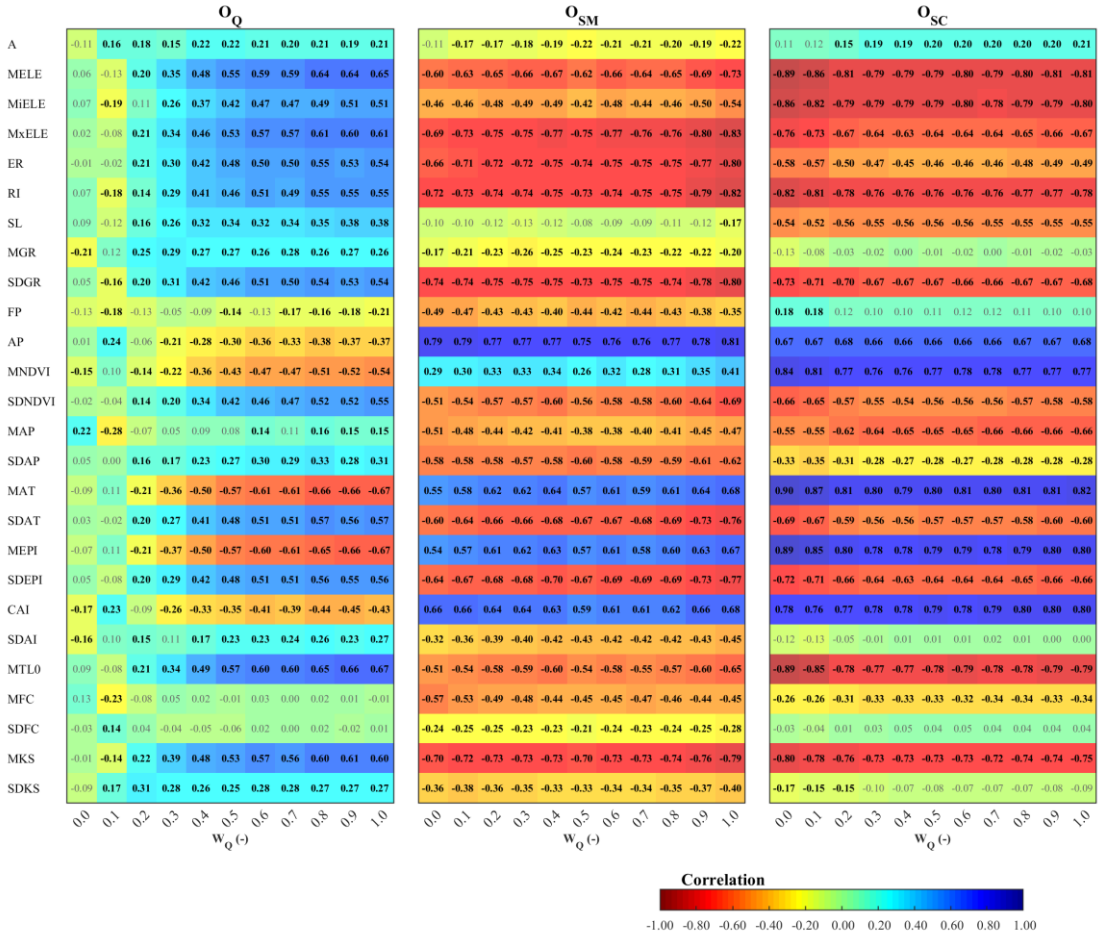

Figure 3.5 Correlation between catchment attributes (Table 3.1) and model performance, i.e. runoff (Eq. 3.2, left panel), soil moisture (Eq. 3.5, middle panel) and snow cover (Eq. 3.6, right panel), obtained from multiple objective calibration to satellite soil moisture (ASCAT), satellite snow cover (MODIS) and runoff (Var 3 of Table 3.4, SSM+SCM+runoff) in the calibration period 2000-2010. Cool and warm colors represent positive and negative correlations, respectively. Bold print indicates significance with p-value lower than 0.05.

Die approbierte gedruckte Originalversion dieser Dissertation ist an der TU Wien Bibliothek verfügbar.
The approved original version of this doctoral thesis is available in print at TU Wien Bibliothek.
TU Bibliothek Your knowledge hub WIEN

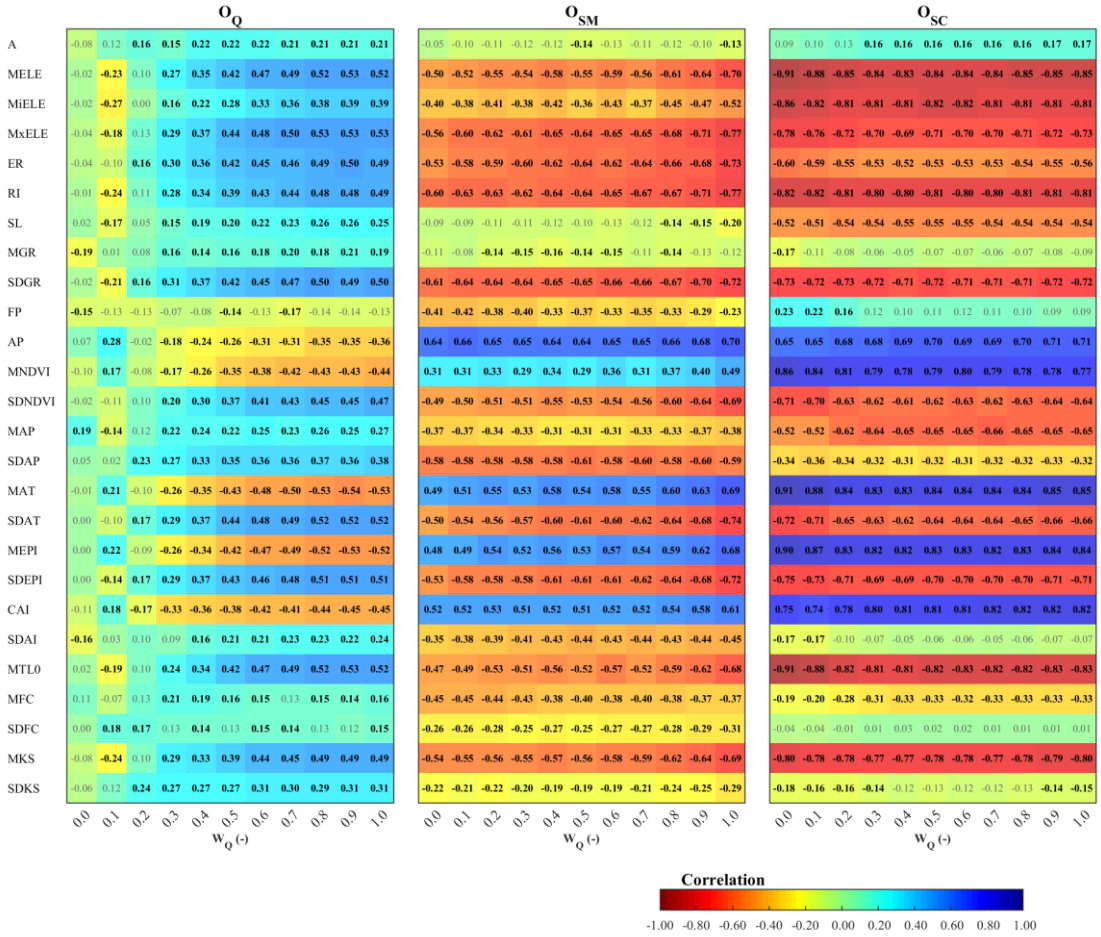

Figure 3.6 Correlation between catchment attributes (Table 3.1) and model performance, i.e. runoff (Eq. 3.2, left panel), soil moisture (Eq. 3.5, middle panel) and snow cover (Eq. 3.6, right panel), obtained from multiple objective calibration to satellite soil moisture (ASCAT), satellite snow cover (MODIS) and runoff (Var 3 of Table 3.5, SSM+SCM+runoff) in the validation period 2010-2014. Cool and warm colors represent positive and negative correlations, respectively. Bold print indicates significance with p-value lower than 0.05.

Die approbierte gedruckte Originalversion dieser Dissertation ist an der TU Wien Bibliothek verfügbar.
The approved original version of this doctoral thesis is available in print at TU Wien Bibliothek.
TU Bibliothek Your knowledge hub WIEN

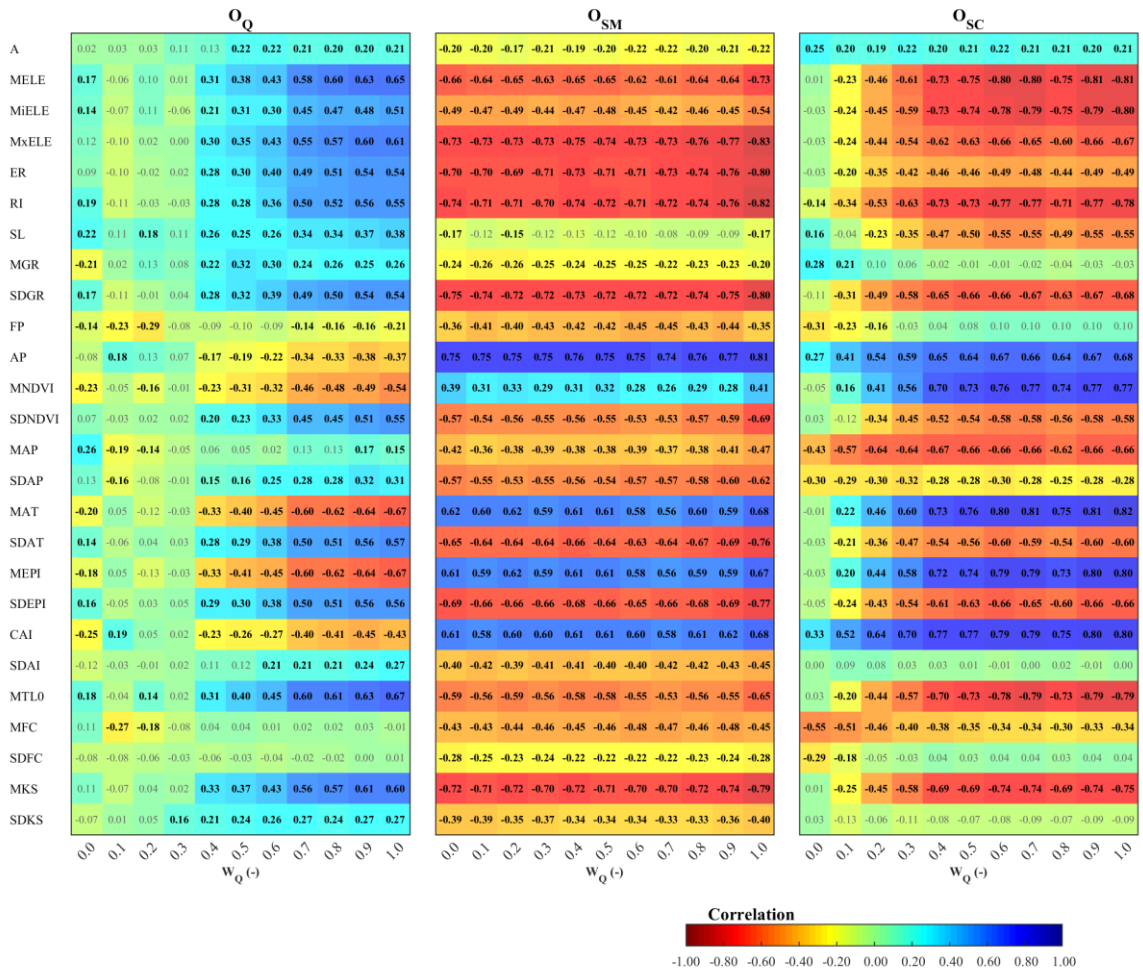

Figure 3.7 Correlation between catchment attributes (Table 2.1) and model performance, i.e. runoff (Eq. 3.2, left panel), soil moisture (Eq. 3.5, middle panel) and snow cover (Eq. 3.6, right panel), obtained from multiple objective calibration to satellite soil moisture (ASCAT) and runoff (Var 1 of Table 2.4, SSM+runoff) in the calibration period 2000-2010. Cool and warm colors represent positive and negative correlations, respectively. Bold print indicates significance with p-value lower than 0.05.

Die approbierte gedruckte Originalversion dieser Dissertation ist an der TU Wien Bibliothek verfügbar.
The approved original version of this doctoral thesis is available in print at TU Wien Bibliothek.
TU Bibliothek Your knowledge hub WIEN

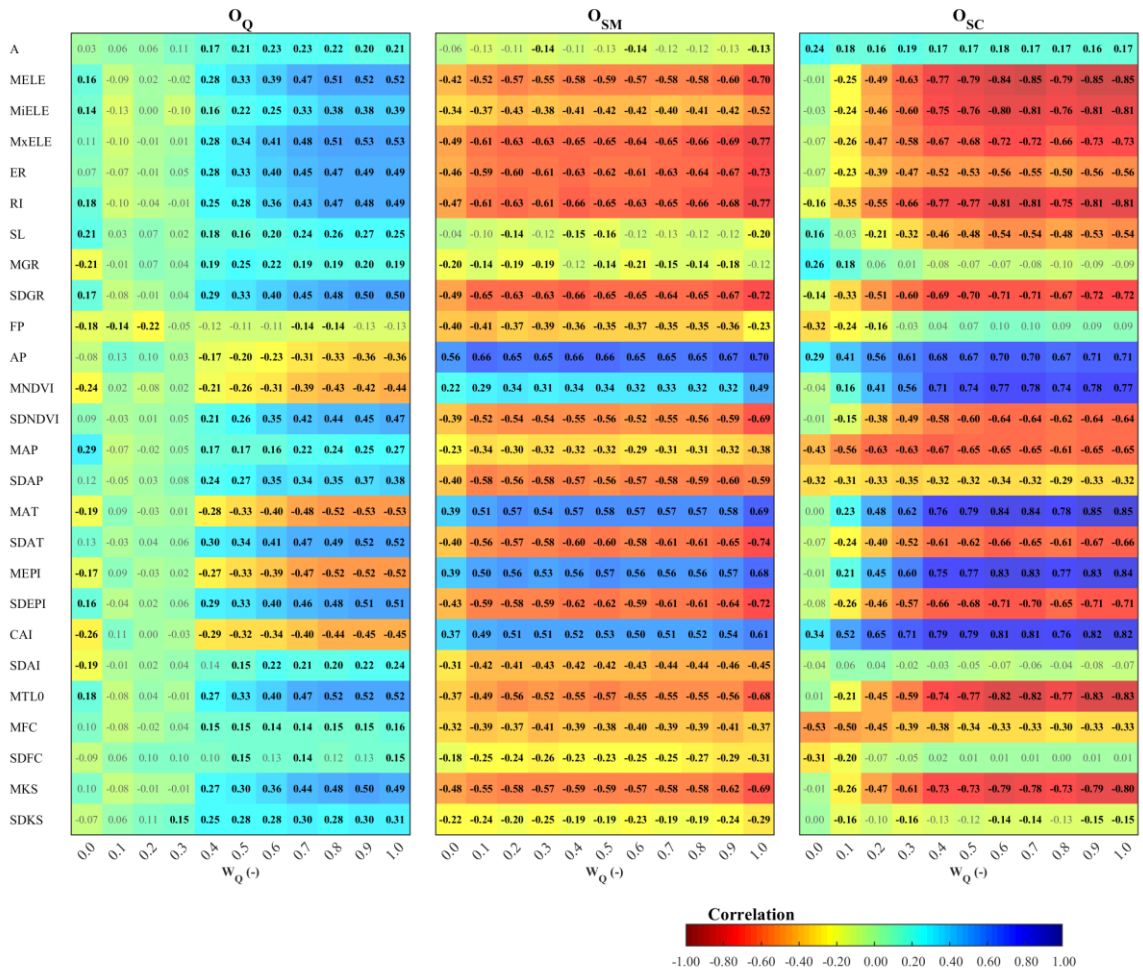

Figure 3.8 Correlation between catchment attributes (Table 2.1) and model performance, i.e. runoff (Eq. 3.2, left panel), soil moisture (Eq. 3.5, middle panel) and snow cover (Eq. 3.6, right panel), obtained from multiple objective calibration to satellite soil moisture (ASCAT) and runoff (Var 1 of Table 2.5, SSM+runoff) in the validation period 2010-2014. Cool and warm colors represent positive and negative correlations, respectively. Bold print indicates significance with p-value lower than 0.05.

Die approbierte gedruckte Originalversion dieser Dissertation ist an der TU Wien Bibliothek verfügbar.
The approved original version of this doctoral thesis is available in print at TU Wien Bibliothek.
TU Bibliothek Your knowledge hub WIEN

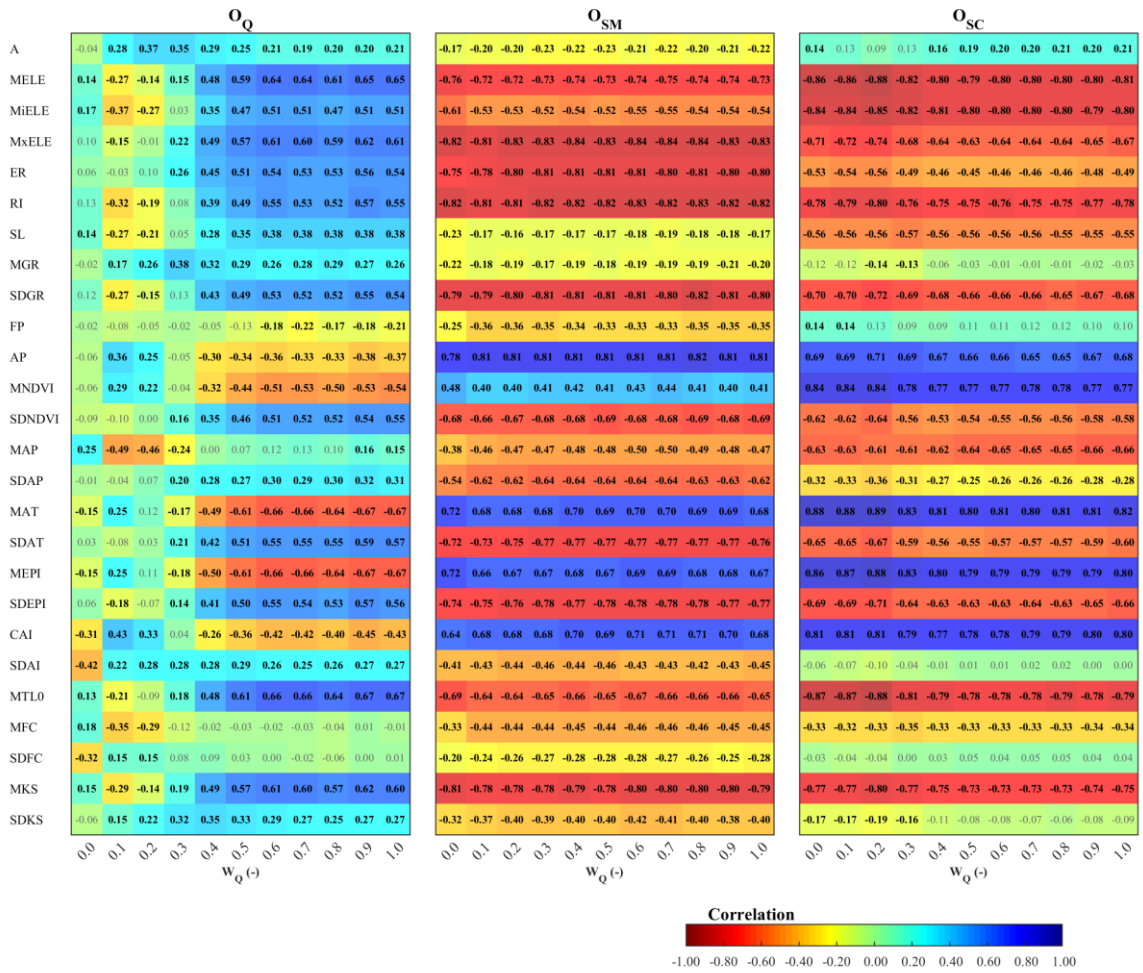

Figure 3.9 Correlation between catchment attributes (Table 2.1) and model performance, i.e. runoff (Eq. 3.2, left panel), soil moisture (Eq. 3.5, middle panel) and snow cover (Eq. 3.6, right panel), obtained from multiple objective calibration to satellite snow cover (MODIS) and runoff (Var 2 of Table 2.4, SCM+runoff) in the calibration period 2000-2010. Cool and warm colors represent positive and negative correlations, respectively. Bold print indicates significance with p-value lower than 0.05.

Die approbierte gedruckte Originalversion dieser Dissertation ist an der TU Wien Bibliothek verfügbar.
The approved original version of this doctoral thesis is available in print at TU Wien Bibliothek.
TU Bibliothek Your knowledge hub WIEN

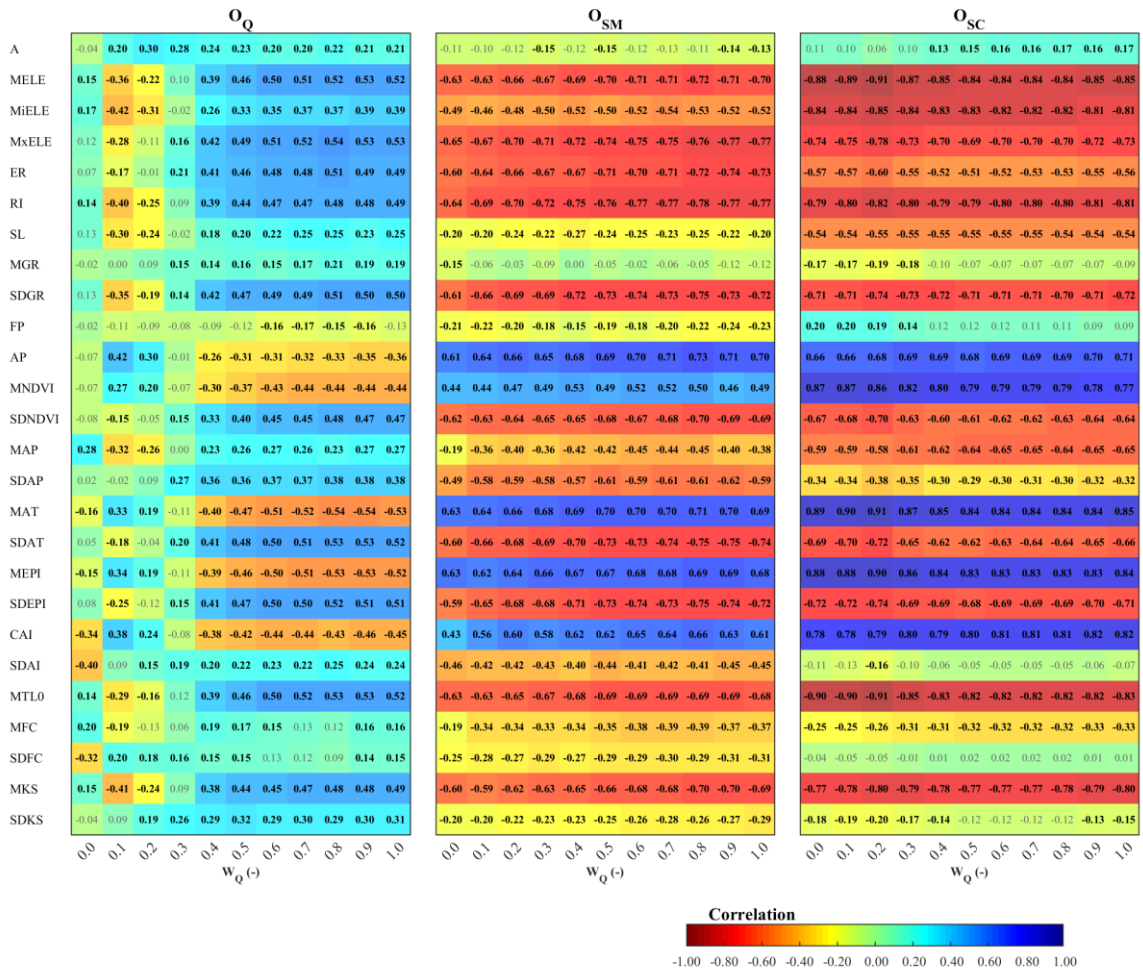

Figure 3.10 Correlation between catchment attributes (Table 2.1) and model performance, i.e. runoff (Eq. 3.2, left panel), soil moisture (Eq. 3.5, middle panel) and snow cover (Eq. 3.6, right panel), obtained from multiple objective calibration to satellite snow cover (MODIS) and runoff (Var 2 of Table 2.5, SSM+SCM+runoff) in the validation period 2010-2014. Cool and warm colors represent positive and negative correlations, respectively. Bold print indicates significance with p-value lower than 0.05.

3.4.2 Variability in calibrated model parameter values

Figure 3.7 compares the medians of the model parameters for all catchments obtained with the three multiple calibration variants, grouped by snow, soil, runoff generation and runoff routing parameters in the columns from left to right. The snow-related parameters (left column) are similar for the two calibration variants that use satellite snow cover. In contrast, the variant that uses soil moisture and runoff tends to have different values, particularly for the threshold temperature parameters (Tr, Ts, meltT). The medians of the snow correction (SCF) and melt (DDF) factors tend to be similar in all three variants if $w_Q > 0.4$.

The soil-related parameters (2nd column) show similar patterns. The variants that use satellite soil moisture in model calibration have more similar soil model parameter values than the one

Die approbierte gedruckte Originalversion dieser Dissertation ist an der TU Wien Bibliothek verfügbar.
The approved original version of this doctoral thesis is available in print at TU Wien Bibliothek.
TU Bibliothek Your knowledge hub WIEN

that uses only SSC and runoff. This suggests that adding soil moisture satellite data in model calibration affects the soil-related parameters strongly and adding snow and soil moisture satellite data is complementary for influencing both snow and soil moisture related parameters. The similarity of the variant using all three variables with those variants where alternatively SSC and SSM are left out suggests that SSC is more important for the snow-related parameters, and SSM is more important for the soil-related parameters, as would be expected. Increasing the runoff weight tends to decrease the difference between the calibration variants of the snow-related and the soil-related parameters. The runoff generation-related parameters (3rd column) tend to be more similar for the two variants that use SSC, and the runoff routing-related parameters (right column) are always rather similar.

In the next step the model parameters obtained by multiple objective calibration are compared with those obtained by traditional calibration to runoff only (Fig. 3.12). The figure shows that the similarity between model parameters decreases with decreasing w_Q.

Snow-related parameters calibrated using SSC (middle column, top five lines) deviate quickly from those using runoff only as $w_Q$decreases. Similarly, the soil-related parameters calibrated using SSM (left column, lines 6-8 from top) deviate quickly from their counterparts based only on runoff calibration. The difference in similarity/correlation between multiple objective calibration variants and runoff only calibration is smaller for runoff generation parameters. The runoff routing model parameters seem to be not very sensitive to selected model efficiencies and the correlation between model parameters is very small.

Die approbierte gedruckte Originalversion dieser Dissertation ist an der TU Wien Bibliothek verfügbar.
The approved original version of this doctoral thesis is available in print at TU Wien Bibliothek.
TU WIEN Bibliothek Your knowledge hub

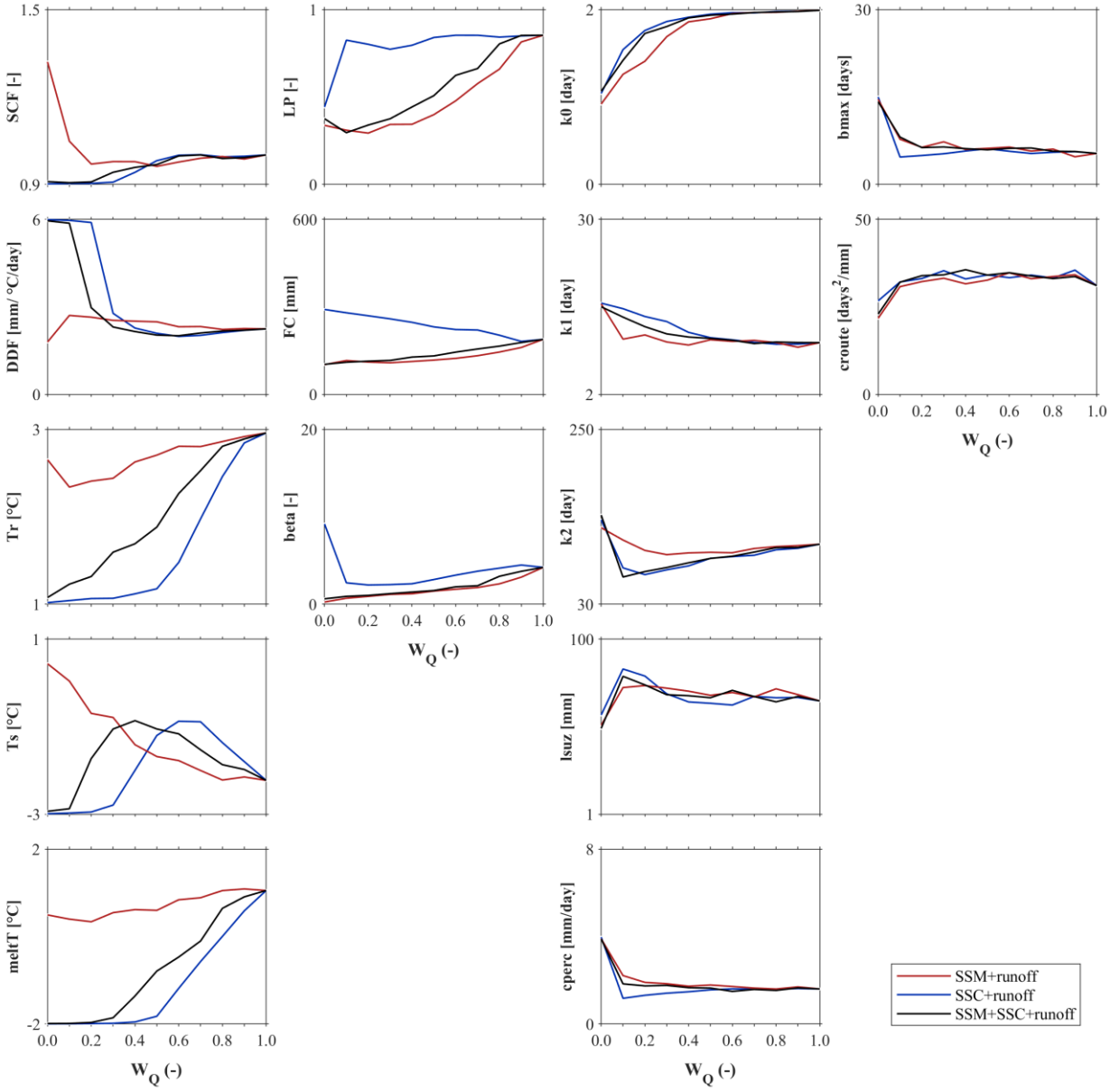

Figure 3.11 Medians of the parameter values from the three multiple objective calibration variants (lines) and different runoff weights w_Q (Table 3.3). Red, blue and grey lines represent the calibration variants using soil moisture and runoff, snow cover and runoff, and soil moisture, snow cover data and runoff, respectively. Lines represent the median of the 213 Austrian catchments.

Die approbierte gedruckte Originalversion dieser Dissertation ist an der TU Wien Bibliothek verfügbar.
The approved original version of this doctoral thesis is available in print at TU Wien Bibliothek.
TU Bibliothek Your knowledge hub WIEN

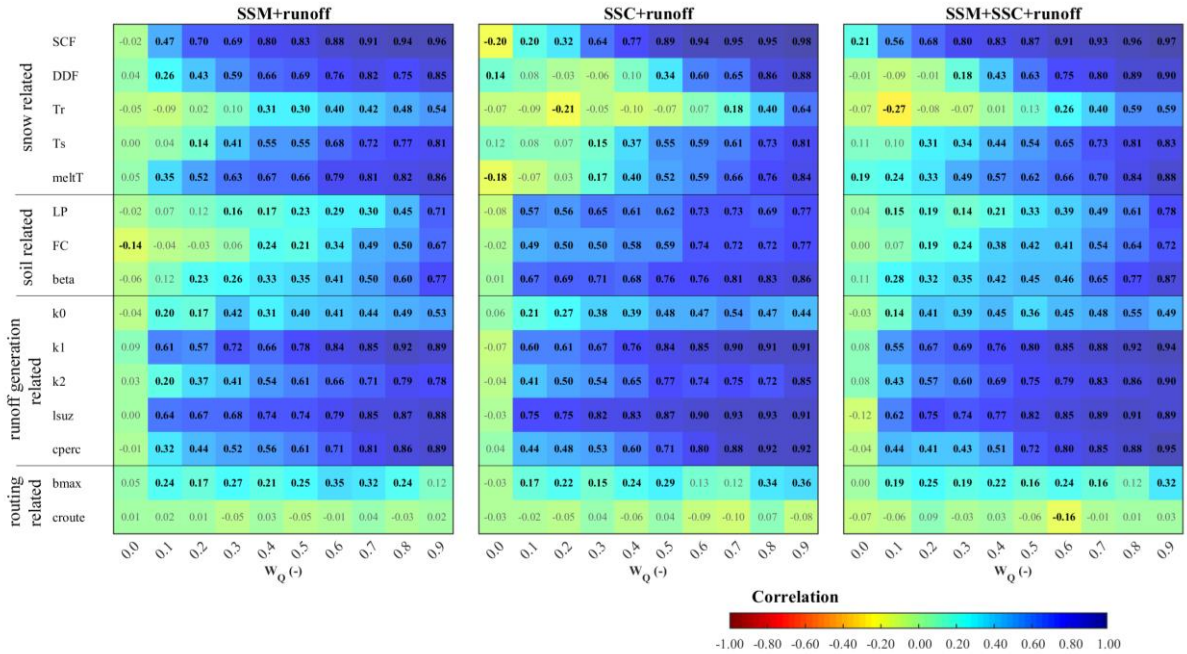

Figure 3.12 Correlation of parameter values from three multiple objective calibration variants (runoff weights w_Q = 0.0 to 0.9, Table 3.3) with those from traditional calibration to runoff only (w_Q=1.0). Left, middle and right panels represent calibration variants using soil moisture and runoff, snow cover and runoff and all three variables, respectively (Var 1, 2, 3 of Table 4 and 5). Cool and warm colors represent positive and negative correlations, respectively. Bold print indicates significance with p-value lower than 0.05.

3.4.3 Comparison of multiple objective and runoff only calibration efficiencies

The relative difference between the model efficiency of the three multi-objective variants and that based on calibration to runoff only is presented in Fig. 3.13. The runoff model efficiency of multiple objective calibration tends to be slightly lower than the traditional calibration to runoff only. The median of difference in runoff model efficiency of the two variants that use SSM in model calibration is less than 3.2% for w_Q larger than 0.3 in both calibration and validation periods. The multiple objective calibration to SSC and runoff has a somewhat larger median of difference for w_Q between 0.2 and 0.4, but for larger w_Q the median is almost identical with that of the other multiple objective variants. The integration of soil moisture in model calibration improves the correlation of satellite and simulated soil moisture. The median improvement for w_Q <0.6 is larger than 30% and 15% in the calibration and validation periods, respectively. The calibration to all variables has a median relative improvement about 3% to 35% lower than the calibration to SSM and runoff in the calibration period, but is very similar in the validation period. The calibration to SSM and runoff does not improve snow cover simulations, but the use of all variables improves the snow model efficiency. For w_Q less than 0.5 the median improvement is larger than 5% in both calibration and validation periods.

Given that the median runoff efficiency is not improved by the addition of soil moisture and snow data (Fig. 3.13) it is of interest to see how the changes are distributed in space. Figure 3.10 shows that in up to 40% of catchments the validation runoff efficiency is improved by using multiple objective calibration as compared to calibration to runoff alone. The number of catchments with runoff improvements increases with increasing runoff weight. The flipside, of course, is that in the remaining catchments the runoff model efficiency deteriorates. The

Die approbierte gedruckte Originalversion dieser Dissertation ist an der TU Wien Bibliothek verfügbar.
The approved original version of this doctoral thesis is available in print at TU Wien Bibliothek.
TU Bibliothek Your knowledge hub WIEN

calibration variants that use SSM data improve soil moisture simulations in more than 80% of the catchments for all weights, and the addition of snow data does not change the performance. The snow model efficiency is vastly improved by the inclusion of the SSC data, for w_Q<0.6 in almost all catchments, and the inclusion of soil moisture (in the variant that uses all variables) has still a very big improvement of snow simulations as compared to the case when only runoff is used in the calibration.

Overall, there are two important messages. The inclusion of soil moisture data in the calibration mainly improves the soil moisture simulations; the inclusion of snow data in the calibration mainly improves the snow simulations; and including both of them improves both soil moisture and snow simulations to a similar extent. Second, when comparing the panels of Fig. 3.10, one sees that the snow data are more efficient in improving snow simulations than the soil moisture data are in improving soil moisture simulations.

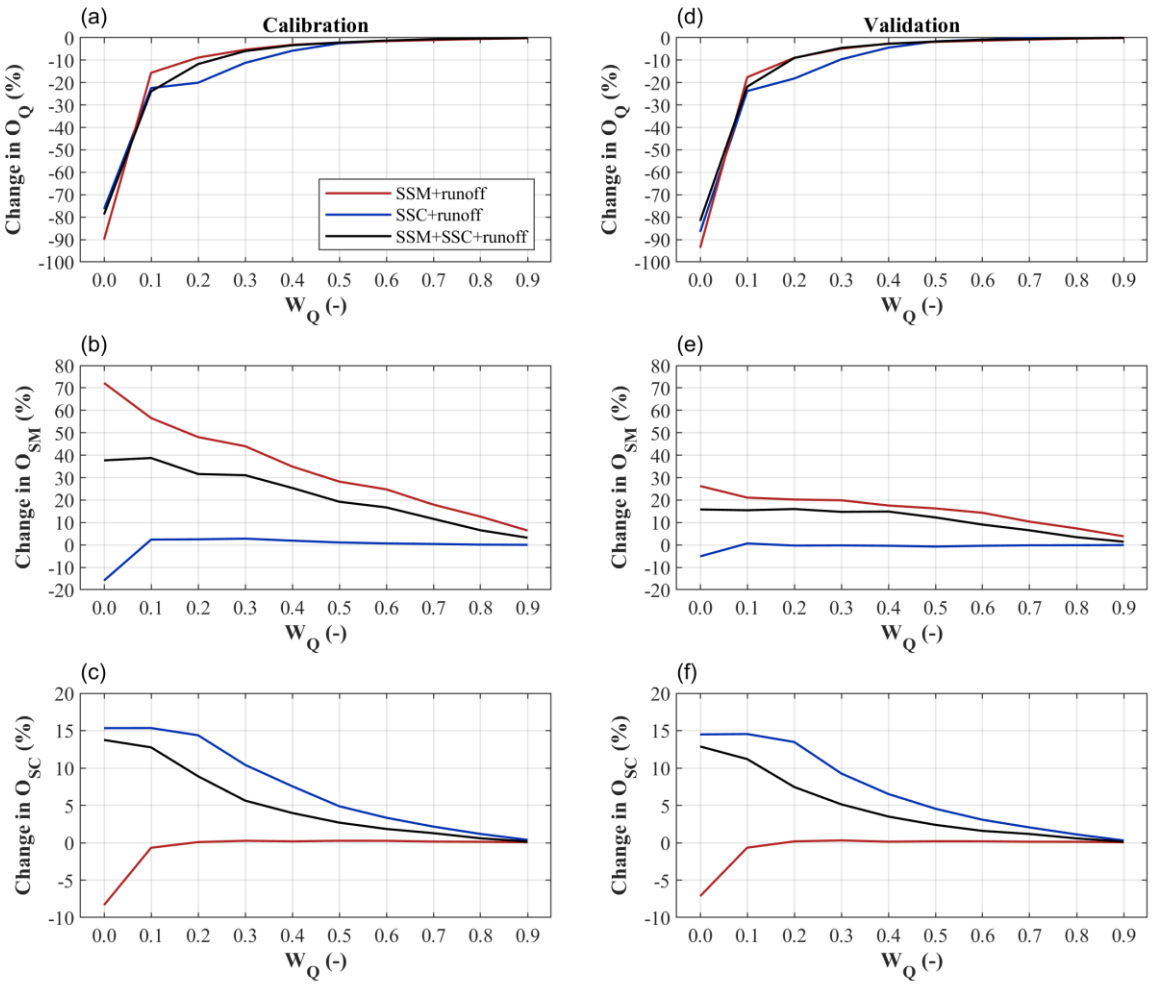

Figure 3.13 Relative difference in model efficiency (O_Q: runoff model efficiency; O_{SM}: soil moisture model efficiency; O_{SC}: snow model efficiency) of three multiple objective calibration variants (lines) using different runoff weights w_Q (Table 3.3) compared to traditional calibration to runoff only (w_Q=1). Red, blue and grey lines represent calibration variants using soil moisture and runoff, snow cover and runoff, and soil moisture, snow cover and runoff, respectively. Lines represent the median of the 213 Austrian catchments. Top (a,d), middle (b,e) and bottom (c,f) panels refer to runoff, soil moisture and snow cover efficiencies in the calibration (left panels, a-c) and validation (right panels,d-f) periods, respectively.

Die approbierte gedruckte Originalversion dieser Dissertation ist an der TU Wien Bibliothek verfügbar.
The approved original version of this doctoral thesis is available in print at TU Wien Bibliothek.
TU Bibliothek Your knowledge hub WIEN

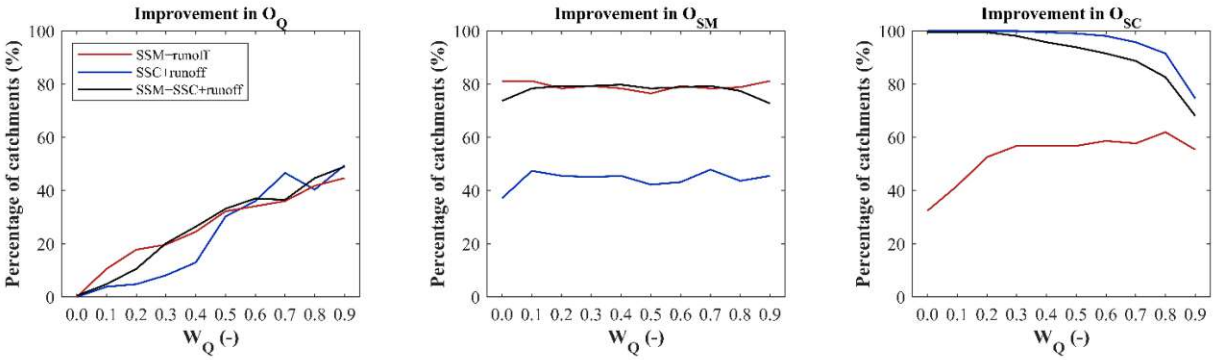

Figure 3.14 Relative number of catchments with improvement in runoff (left), soil moisture (centre) and snow cover (right) model efficiency in the validation period. Relative number relates to the 213 Austrian catchments used in this Chapter.

It is now of interest to see whether the catchments for which the runoff and soil moisture model efficiencies are improved by the inclusion of SSC and SSM data (Fig. 3.14) are different from those for which this is not the case. The distribution of the catchment attributes of these two catchment groups are therefore compared with the Kolmogorov-Smirnov two sample test (KS). Since the snow model efficiency is improved in almost all study catchments, it is not analysed here. Table 3.6 and 3.11 show the p–values of the KS for the runoff and soil moisture model efficiencies, respectively, indicating statistically significant differences between the catchment groups in many cases. For catchments with a large frequency of runoff improvements (e.g. for w_Q = 0.7 and 0.8) there are a number of differentiating factors including those related to topography (mean catchment elevation, mean catchment slope), proportion of agricultural land, mean annual air temperature, number of days with negative air temperature and mean saturated hydraulic conductivity. An example of differences between the groups in terms of mean catchment elevation (MELE) and percentage of arable land (AP) is presented in Fig. S.9. The results indicate that improvement in runoff is observed in catchments with lower mean catchment elevation and a larger proportion of agricultural land. The other catchment attributes with statistically significant differences are correlated with MELE, so have similar differences in the distributions as those presented in Fig. 3.15.

Since an improvement in soil moisture simulations is observed in 80% of the catchments (Fig. 3.14) their attributes are particularly interesting. The factors controlling the improvement include topographical (MELE, SL, ER, SDGR), land cover (FP, AP), climate (MAP, SDAP, MAT, CAI, MTLT0) and soil (MKS) attributes, similarly as for improvement in runoff. This is illustrated in Fig. 3.16 that indicates that improvement in soil moisture simulations occurs particularly in catchments with low mean catchment elevation and a large proportion of agricultural land. In contrast to the runoff improvements, the results for the improvement in soil moisture are not related to the runoff weight w_Q used in the model calibration.

Die approbierte gedruckte Originalversion dieser Dissertation ist an der TU Wien Bibliothek verfügbar.
The approved original version of this doctoral thesis is available in print at TU Wien Bibliothek.
TU Bibliothek Your knowledge hub WIEN

Table 3.6. Kolmogorov-Smirnov p-values testing the similarity of the distribution of catchment attributes across the 213 catchments between those catchments where the runoff model efficiency is improved in the validation period by the inclusion of the soil moisture and snow data in the calibration and those catchments where this is not the case. The null hypothesis that the two samples were drawn from the same distribution is rejected if the p-value is less than the significance level (bold print).

w_Q	**0**	**0.1**	**0.2**	**0.3**	**0.4**	**0.5**	**0.6**	**0.7**	**0.8**	**0.9**
A	0.70	0.34	0.22	0.32	0.15	0.93	**0.05**	0.26	0.46	0.96
MELE	0.23	**0.00**	**0.00**	**0.01**	**0.01**	**0.00**	0.17	**0.03**	0.05	0.25
MiELE	0.27	0.06	0.09	0.20	**0.03**	**0.01**	**0.03**	**0.01**	0.09	0.19
MxELE	0.60	**0.00**	**0.00**	**0.00**	**0.01**	**0.00**	0.23	**0.03**	**0.03**	0.35
ER	0.59	**0.00**	**0.00**	**0.00**	**0.00**	**0.00**	0.47	0.29	**0.02**	0.21
RI	0.49	**0.00**	**0.00**	**0.00**	**0.01**	**0.00**	0.14	**0.03**	**0.03**	0.05
SL	0.11	0.46	0.82	0.37	0.50	0.16	0.18	0.17	0.86	0.81
MGR	0.23	0.73	0.38	0.62	0.05	0.66	0.48	0.98	1.00	0.45
SDGR	0.44	**0.00**	**0.01**	**0.00**	**0.00**	**0.00**	0.11	0.07	**0.02**	0.06
FP	0.29	0.05	**0.05**	0.07	0.40	0.23	0.87	0.80	0.31	0.72
AP	0.20	**0.00**	**0.00**	**0.00**	**0.00**	**0.00**	0.08	**0.02**	**0.02**	0.17
MNDVI	0.71	**0.01**	0.10	**0.03**	**0.04**	**0.04**	**0.05**	**0.04**	0.15	0.21
SDNDVI	0.72	**0.00**	**0.04**	**0.00**	**0.00**	**0.01**	0.49	0.14	**0.01**	0.09
MAP	0.82	**0.00**	0.19	0.08	0.51	**0.01**	**0.03**	0.12	**0.01**	**0.05**
SDAP	0.34	**0.00**	0.05	**0.04**	0.15	0.38	0.93	0.92	**0.03**	0.39
MAT	0.20	**0.00**	**0.00**	**0.00**	**0.01**	**0.00**	0.11	**0.03**	0.10	0.42
SDAT	0.43	**0.00**	**0.01**	**0.01**	**0.00**	**0.01**	0.55	0.16	**0.02**	0.21
MEPI	0.15	**0.00**	**0.00**	**0.00**	**0.00**	**0.00**	0.07	**0.00**	0.13	0.26
SDEPI	0.36	**0.00**	**0.02**	**0.00**	**0.00**	**0.01**	0.63	0.18	**0.01**	0.06
CAI	0.56	**0.00**	**0.01**	**0.00**	0.05	**0.00**	0.20	**0.05**	**0.00**	**0.03**
SDAI	0.78	0.06	**0.03**	**0.04**	**0.01**	0.29	0.38	0.74	0.91	0.82
MTL0	0.20	**0.00**	**0.00**	**0.00**	**0.01**	**0.00**	0.19	**0.02**	0.11	0.31
MFC	0.67	0.14	**0.03**	0.30	0.38	0.08	0.10	0.16	**0.03**	0.10
SDFC	0.14	0.47	0.24	0.56	**0.04**	0.25	0.12	0.69	**0.01**	**0.01**
MKS	0.18	**0.00**	**0.00**	**0.00**	**0.00**	**0.00**	0.17	**0.01**	0.06	0.14
SDKS	0.40	0.19	0.38	0.98	0.07	**0.05**	0.47	0.55	0.11	0.27

Die approbierte gedruckte Originalversion dieser Dissertation ist an der TU Wien Bibliothek verfügbar.
The approved original version of this doctoral thesis is available in print at TU Wien Bibliothek.
TU Bibliothek Your knowledge hub WIEN

Table 3.7. Same as Table 3.6, but for the soil moisture model efficiency.

w_Q	**0**	**0.1**	**0.2**	**0.3**	**0.4**	**0.5**	**0.6**	**0.7**	**0.8**	**0.9**
A	0.53	0.31	0.18	0.61	0.23	0.26	0.45	0.98	0.98	0.26
MELE	**0.01**	**0.01**	**0.02**	0.07	0.09	**0.05**	0.05	0.70	0.14	0.94
MiELE	**0.01**	0.15	0.13	0.13	0.20	**0.04**	0.05	0.54	0.20	0.74
MxELE	**0.01**	**0.00**	**0.01**	**0.01**	**0.01**	**0.00**	**0.01**	0.13	**0.02**	0.31
ER	0.07	0.08	0.08	**0.03**	**0.04**	**0.02**	0.06	0.22	0.10	0.35
RI	**0.01**	**0.03**	**0.01**	**0.03**	**0.03**	**0.01**	**0.02**	0.38	0.05	0.34
SL	0.32	**0.02**	0.50	0.93	0.35	0.73	0.90	0.45	0.80	0.46
MGR	0.59	0.55	0.69	0.43	0.79	0.25	0.50	0.61	0.49	0.81
SDGR	**0.00**	**0.01**	**0.01**	**0.01**	**0.05**	**0.02**	**0.03**	0.14	0.07	0.17
FP	**0.00**	**0.00**	**0.00**	**0.00**	**0.01**	**0.02**	0.10	0.58	**0.05**	0.35
AP	**0.00**	**0.04**	**0.01**	**0.04**	**0.04**	**0.00**	**0.00**	0.41	0.12	0.32
MNDVI	0.23	**0.01**	0.25	0.89	0.97	0.58	0.36	0.89	0.62	0.67
SDNDVI	0.06	0.63	0.87	0.78	0.62	0.27	0.11	0.69	0.56	0.59
MAP	**0.00**	**0.02**	**0.01**	**0.00**	0.17	**0.01**	**0.03**	0.23	0.07	0.72
SDAP	**0.03**	0.14	0.07	**0.00**	**0.01**	**0.01**	**0.00**	**0.01**	**0.02**	0.07
MAT	**0.01**	**0.02**	**0.01**	**0.03**	**0.05**	**0.02**	**0.02**	0.40	0.12	1.00
SDAT	**0.04**	0.05	0.07	0.08	0.09	0.05	0.07	0.19	0.36	0.22
MEPI	**0.00**	**0.00**	**0.04**	**0.04**	0.06	**0.02**	**0.02**	0.32	0.18	1.00
SDEPI	**0.03**	0.06	**0.03**	**0.04**	**0.05**	**0.03**	**0.05**	0.34	0.17	0.32
CAI	**0.01**	0.05	**0.01**	**0.01**	**0.04**	**0.01**	**0.02**	0.39	0.07	0.82
SDAI	0.44	0.95	0.59	0.79	0.52	0.40	0.44	0.05	0.75	**0.04**
MTL0	**0.01**	**0.02**	**0.02**	0.06	0.07	**0.02**	**0.02**	0.49	0.26	0.83
MFC	**0.00**	**0.00**	**0.00**	**0.01**	**0.04**	**0.01**	**0.04**	0.36	0.09	0.47
SDFC	0.19	0.47	0.34	0.15	0.24	0.05	0.86	0.97	0.16	0.76
MKS	**0.03**	**0.00**	**0.05**	**0.05**	0.06	**0.02**	**0.04**	0.53	0.18	0.76
SDKS	**0.04**	0.19	0.16	**0.04**	0.30	0.08	0.22	0.26	0.42	0.58

Die approbierte gedruckte Originalversion dieser Dissertation ist an der TU Wien Bibliothek verfügbar.
The approved original version of this doctoral thesis is available in print at TU Wien Bibliothek.
TU Bibliothek Your knowledge hub WIEN

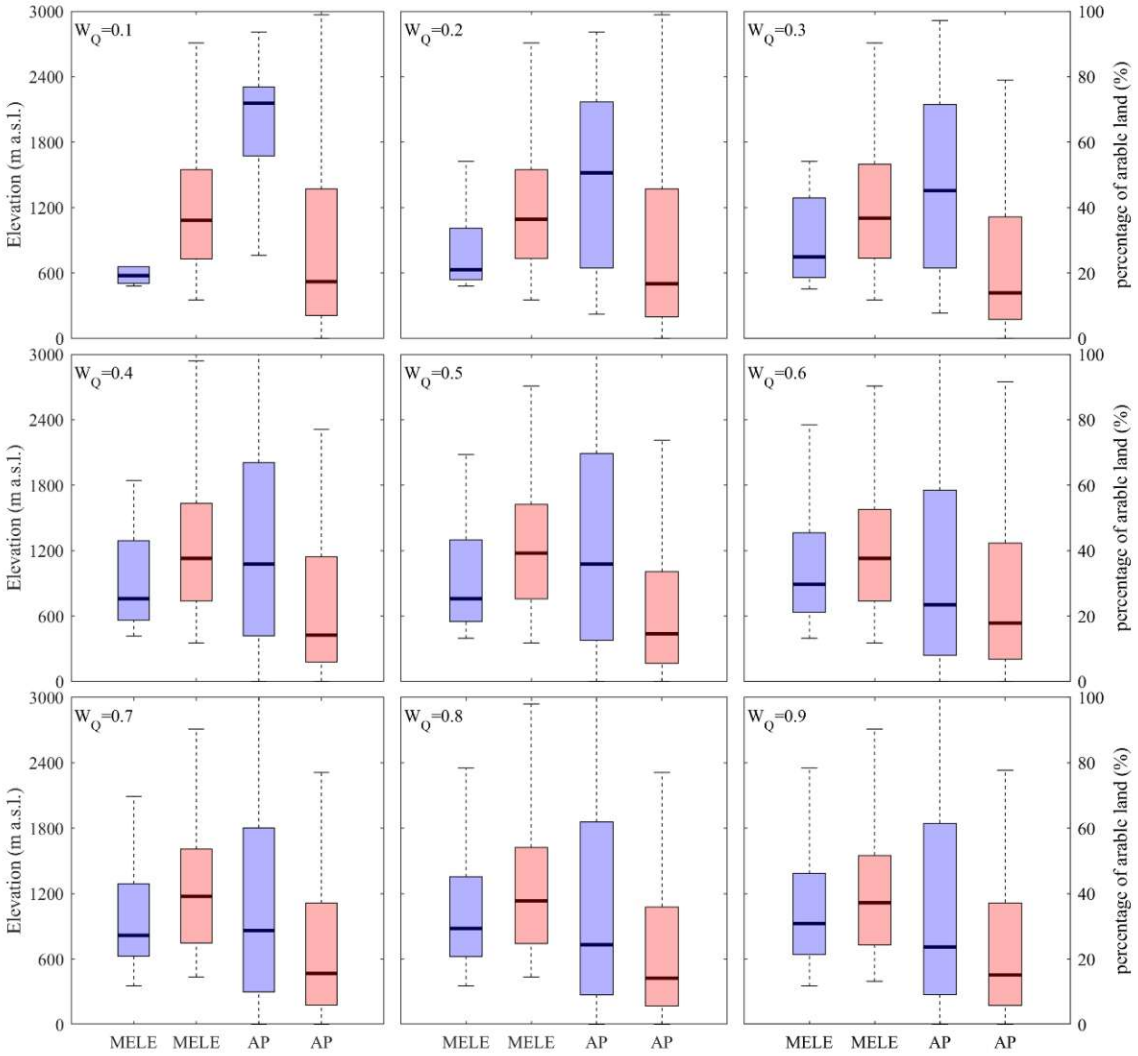

Figure 3.15 Distributions of mean catchment elevation (MELE) and percentage of arable land (AP) for the groups of catchments with (blue) and without (red) runoff model efficiency improvement in the validation period when including soil moisture and snow data in the calibration.

Die approbierte gedruckte Originalversion dieser Dissertation ist an der TU Wien Bibliothek verfügbar.
The approved original version of this doctoral thesis is available in print at TU Wien Bibliothek.
TU Bibliothek Your knowledge hub WIEN

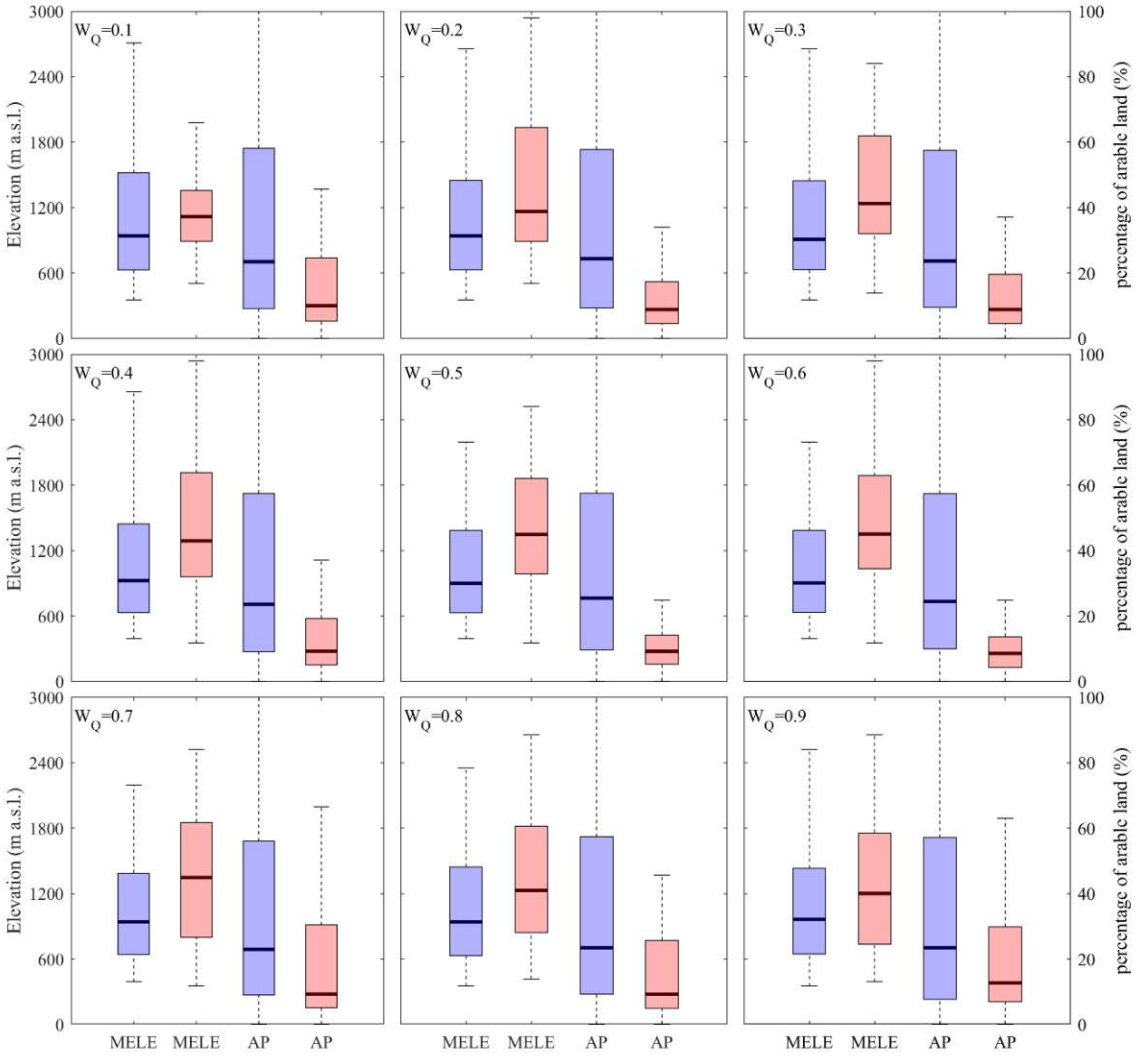

Figure 3.16 Distributions of mean catchment elevation (MELE) and percentage of arable land (AP) for the groups of catchments with (blue) and without (red) soil moisture model efficiency improvement in the validation period when including soil moisture and snow data in the calibration

3.5 Discussion

In this Chapter, we tested three multiple calibration variants using runoff data along with ASCAT SWI soil moisture and MODIS snow cover data. The calibration runoff model efficiency is similar to previous studies (Parajka et al., 2008, 2009; Sleziak et al., 2018) that used only runoff for model calibration. For example, the median of runoff model efficiency ranges between 0.77-0.79 (for runoff weights larger than 0.4) which is similar to the medians of 0.80 and 0.84 found in Parajka et al. (2008, 2009) for 148 Austrian catchments, and better than the median of 0.76 found for 320 Austrian catchments in Parajka et al., (2006) as well as

Die approbierte gedruckte Originalversion dieser Dissertation ist an der TU Wien Bibliothek verfügbar.
The approved original version of this doctoral thesis is available in print at TU Wien Bibliothek.
TU Bibliothek Your knowledge hub WIEN

the range 0.70-0.73 found for the same set of catchments as in this paper but using a lumped model (Sleziak et al., 2018).

Results show that the inclusion of satellite soil moisture data in the calibration mainly improves the soil moisture simulations. The median soil moisture correlation between hydrologic model outputs and ASCAT SWI is 0.4 to 0.52 (depending on the weight w_Q), which is significantly larger than the median of 0.26 found by using the coarser ERS scatterometer data in model calibration in Parajka et al. (2006). This reflects improvements both in the instrument specifications (better temporal and spatial sampling, higher radiometric accuracy, etc.) and the retrieval algorithm (Naeimi et al. 2009, Hahn et al. 2020).

The inclusion of satellite snow data mainly improves the snow simulations. Using MODIS snow cover data to constrain the model parameters shows strong ability in improving the accuracy of representing the snow accumulating and melting processes from the model. When giving weights w_Q<0.5 to snow, almost all the catchments showed improvements in snow cover simulations. In terms of the improvement in snow model efficiency, our results are better than the results from Parajka et al. (2008), in their study only 3 years MODIS snow cover data was used, the improvement of snow mapping even depended on the data availability.

The satellite snow data are more efficient in improving snow simulations than the satellite soil moisture data are in improving soil moisture simulations. Part of the reason may be related to problems in mapping soil moisture in the alpine region while MODIS snow cover is very accurate both in the lowlands and in the mountains. For example, Parajka and Blöschl (2006) and Tong et al. (2020) showed the classification accuracy of the MODIS snow cover range from 95% to over 97% in Austria. Furthermore, it is interesting that including both soil moisture and snow cover data improves both soil moisture and snow simulations to almost the same extent as if including them individually, without any significant deterioration in the other variable. This gives the possibility to consistently improve the simulations of snow and soil moisture in future model applications. Our validation results indicate that snow simulations are improved in almost all, soil moisture correlation in about 80% and runoff in up to 40% of the catchments. Overall, the runoff performance changes very little when including soil moisture and snow data in the calibration.

The calibrated snow-related parameters are strongly affected by including snow data, and to a lesser extent by soil moisture data, while the soil-related parameters are only affected by soil moisture data. This separation is a welcome property as it facilitates parameter calibration. The soil moisture data also have some effect on the snow-related parameters, this is in consistence with Nijzink et al (2018). As the melting changes the soil moisture directly, the soil moisture data provide additional constraints on the parameters controlling snowmelt. This can be helpful in understanding hydrological processes, especially for the variation of snow water equivalent.

3.6 Conclusions

Our results indicate that the runoff and soil moisture simulation improvement when including soil moisture data in the calibration is found mainly in catchments with lower mean catchment elevation and a larger proportion of agricultural land. While, overall, in 40% of the catchments the validation runoff efficiency is improved by the inclusion of soil moisture (Fig. 3.14, left panel), these are about 50% of the catchments if only those with elevation lower than the median (1011 m a.s.l) and agricultural area larger than its median (16.3%) are considered. Similarly, while, overall, in 80% of the catchments the validation soil moisture efficiency is improved by the inclusion of soil moisture (Fig. 3.14, middle panel), these are about 90% of the catchments if only those which low elevation and agricultural use are considered. The higher efficiency in improving the hydrologic model in the lowlands can be explained by the better quality of the

Die approbierte gedruckte Originalversion dieser Dissertation ist an der TU Wien Bibliothek verfügbar.
The approved original version of this doctoral thesis is available in print at TU Wien Bibliothek.
TU Bibliothek WIEN Your knowledge hub

ASCAT soil moisture retrievals (compared to the alpine regions), but is likely also due to the higher spatial consistency in soil texture and land cover type, and also lower slope and elevation variation. In contrast to a previous assessment of ERS assimilation into model calibration (Parajka et al., 2006), we found soil moisture improvement not only in lowland catchments with lower topographical variability, but also in catchments with smaller sizes (Fig. 3.5) which may be related to the higher spatial and temporal resolution of ASCAT as compared to ERS. Over flatlands, ASCAT retrievals have improved a lot compared to the ERS retrievals 15 years back, but in alpine regions, the rugged topography, dense alpine vegetation, and presence of snow and ice even during the summer, makes using the data still challenging, given the higher retrieval errors and invalid measurements when the ground is snow covered or frozen. Additionally, the large heterogeneity in temperature and snow cover in mountainous regions can lead to insufficient masking for frozen soil and snow cover. In the future studies, the use of soil moisture products with much finer spatial resolution may help reducing these errors and deficiencies for calibrating hydrological models (e.g. Bauer-Marschallinger et al., 2019; Long et al., 2019; Vergopolan et al., 2020; Abowarda et al., 2021).

This Chapter has evaluated the potential of assimilating the soil water index (representing root zone soil moisture) into hydrologic model calibration. It would be useful to extend this study to assimilate other variables, such as surface soil moisture estimates by using a dual soil moisture conceptual hydrologic model (Parajka et al., 2009) and also compare the role of the spatial resolution of soil moisture and snow data on their value in the assimilation.

Die approbierte gedruckte Originalversion dieser Dissertation ist an der TU Wien Bibliothek verfügbar.
The approved original version of this doctoral thesis is available in print at TU Wien Bibliothek.
TU Bibliothek Your knowledge hub WIEN

4. The value of satellite soil moisture and snow cover data for the transfer of hydrological model parameters to ungauged sites

The present chapter corresponds to the following scientific publication in its original form:

Tong, R., Parajka, J., Széles, B., Pfeil, I., Vreugdenhil, M., Komma, J., Valent, P., Blöschl, G. (2021). The value of satellite soil moisture and snow cover data for the transfer of hydrological model parameters to ungauged sites. Hydrol. Earth Syst. Sci. Discuss. [preprint], https://doi.org/10.5194/hess-2021-189, in review.

4.1 Prior knowledge of prediction in ungauged basins and the purpose of this chapter

Prediction of runoff hydrographs is one of the main scientific and practical hydrological applications. Understanding and representation of the processes and their interactions during runoff generation and their sensitivity to the controls are one of the unsolved problems in hydrology (Blöschl et al., 2019). It is also essential for many purposes of societal relevance, such as engineering design, for water resources management, hydropower operation or for risk assessment (Sachs and McArthur, 2005; Blöschl and Montanari, 2010; Kovacs et al., 2012; Parajka et al., 2013). However, in most places of interest, no runoff data are directly observed, so the runoff prediction needs to be based on additional information observed in the region or transferred from other gauged catchments.

Numerous studies have explored and evaluated methods for prediction of runoff in ungauged sites (He et al., 2011; Hrachowitz et al., 2013; Blöschl et al., 2013). The most frequently used method consists of applying a hydrological model driven by model parameters derived in catchments with runoff observations. The review and synthesis of studies and applications of hydrological models in ungauged sites presented in Parajka et al. (2013) and recently Guo et al. (2021) indicate that there is a variety of transfer approaches tested in different parts of the world, covering different climates, altitudes or landscape settings. These studies' main outcome is that the runoff predictions in ungauged catchments tend to be more accurate in humid than in arid regions and more accurate in large than in small catchments (Parajka et al, 2013). However, the selection and performance of methods differ between studies, and there is no general recommendation for the choice of the approach. There seems to be a consensus that the spatial proximity and similarity methods perform better in humid regions (Guo et al., 2021). In arid catchments similarity and parameter regression methods tend to be applied more frequently and perform slightly better (Parajka et al., 2013; Yang et al. 2018, 2020).

Recent studies have explored the role and impact of gauge density on the efficiency of the methods (Parajka et al., 2015; Lebecherel et al., 2016; Neri et al. 2020), as well as the advanced definition of similarity measures based on spatial patterns (Li and Zhang, 2017; Beck et al., 2020; Narbondo et al., 2020), or catchment response characteristics (Tegegne and Kim, 2018). Along with these investigations, one of the recent focuses in hydrological modelling evaluates the use of observations additional to runoff (Bouaziz et al., 2021). Multiple objective calibrations can help constrain hydrological models, reduce uncertainty, and improve hydrological predictions (Efstratiadis and Koutsoyiannis, 2010). Most of the previous studies investigated the potential of calibrating hydrological model parameters by using different runoff signatures or using some additional hydrological characteristics such as snow cover, cover, soil moisture, evaporation, groundwater level or their combinations (please see the review in Tong

Die approbierte gedruckte Originalversion dieser Dissertation ist an der TU Wien Bibliothek verfügbar.
The approved original version of this doctoral thesis is available in print at TU Wien Bibliothek.
TU Bibliothek Your knowledge hub WIEN

et al., 2021). However, only a few studies have investigated the application of multiple objective approaches for evaluating the transfer of model parameters to ungauged sites. Parajka et al. (2005 and 2006), examined the value of snow depth observation and scatterometer soil moisture measurements for improving hydrological simulations in ungauged catchments and showed that the use of scatterometer resulted in more consistent patterns of soil moisture estimates, but it did not improve the runoff model efficiencies in ungauged catchments. Zhang et al. (2020) recently used remotely sensed evapotranspiration to calibrate the hydrological model parameters without streamflow observations and found the streamflow-free calibration could be satisfactory for monthly and mean annual runoff simulation in the humid catchments. Huang et al. (2020) verified the effectiveness of this approach for the regionalization with spatial proximity method in ungagged basins. They reported that using the bias-corrected remotely sensed evapotranspiration has great potential in estimating daily and monthly runoff. However, the role and impact of using additional data for the prediction of daily hydrographs in ungauged sites are still not well understood. Such assessment is essential in particular for projecting impacts of changing climate or land use conditions on the hydrological cycle in general and specifically on runoff generation. The aim of this Chapter is to investigate the value of using model parameters obtained by multiple objective calibrations for daily hydrological predictions in ungauged sites. Specifically, we test the efficiency of different methods for transfer of such model parameters to ungauged sites and evaluate the model performance to observations of runoff and remotely sensed estimates of soil moisture and snow cover. We extend the results of Tong et al. (2021) who assessed the value of Metop ASCAT and MODIS satellites for calibration of conceptual hydrological models and to test to what extent it improves the performance of existing regionalization approaches. The analysis and comparison of model simulations of runoff, soil moisture and snow cover are performed for a large sample of catchments situated in different physiographic and climate zones of Austria, so allows evaluating the potential of the application of remotely sensed data at the regional scale.

4.2 Method

4.2.1 Hydrological model

The transfer of the model parameters is evaluated for a conceptual hydrological model (TUWmodel, Viglione and Parajka, 2020). The TUWmodel is a variant of the HBV model (Bergström 1992; Parajka et al., 2007) implemented in the R-environment (Astagneau et al., 2020). This study uses a semi-distributed version in which the inputs and outputs of the model are processed for elevation zones of 200 meters, but model parameters are assumed lumped in each catchment. We used a single soil layer version of TUWmodel. It simulates changes in snow, root zone and groundwater storages in each elevation zone. The model runs on a daily time step and combines three routines: snow routine, soil moisture routine, and river flow routing routine. The snow routine uses a degree-day concept to reflect snow accumulation and melt with a degree-day factor and a threshold melt temperature. The snowfall part of precipitation and snow accumulation is calculated by using snow and rain threshold temperatures. The soil moisture routine represents changes in the soil moisture state of the root zone due to evapotranspiration and runoff generation.

$$S_{SM,i} = S_{SM,i-1} + \left(PR + M - E_A\right) \cdot \Delta t \qquad (4.1)$$

where S_{SM} is the root zone soil moisture, which controls runoff generation and actual evaporation E_A, PR is rain, M is snowmelt, and Δt is the time step (one day). The contribution ΔS_{UZ} of rain and snowmelt to runoff is calculated by an explicit scheme as a function of the S_{SM} using a non-linear relationship controlled by two model parameters, maximum soil storage FC and nonlinearity parameter $BETA$ controlling characteristics of runoff generation

Die approbierte gedruckte Originalversion dieser Dissertation ist an der TU Wien Bibliothek verfügbar.
The approved original version of this doctoral thesis is available in print at TU Wien Bibliothek.
TU Bibliothek WIEN Your knowledge hub

$$\Delta S_{UZ} = (\theta)^{BETA} (PR + M) \cdot \Delta t \qquad (4.2)$$

$$\theta = \frac{S_{SM}}{FC} \qquad (4.3)$$

Actual evapotranspiration is estimated from potential evaporation (model input) and a model parameter representing the soil moisture state above which the actual equals potential evaporation. For a comparison with satellite soil moisture estimates, simulated root zone soil moisture is scaled by the maximum soil moisture storage *FC* model parameter and represents hence the relative root zone soil moisture θ .

The runoff routing module represents routing on the hillslopes and river flow routing in the stream. The runoff response function consists of two reservoirs, representing the upper and lower storage zones. The outflows from reservoirs in each elevation zone is summed up and routed by a triangular transfer function.

The model involves 15 model parameters. They are automatically calibrated using the multi-objective calibration strategy of Tong et al., (2021). The joint objective function O_F consists of weighting three individual parts related to runoff (O_Q), soil moisture (O_{SM}), and snow cover (O_{SC}).

$$O_F = w_Q \cdot O_Q + w_{SM} \cdot O_{SM} + w_{SC} \cdot O_{SC} \qquad (4.4)$$

where w_Q is the weight to the runoff objective function, w_{SM} and w_{SC} are the weights to the soil moisture and snow cover objectives, respectively. Multiple objective approaches for each regionalization method are examined for 11 runoff weights w_Q (ranging from 0.0 to 1.0 with a step of 0.1). The combinations of weights are taken from Tong et al. (2021), where the weights of soil moisture and snow are equal, and the total sum of all weights is 1.0. More details about the combinations of the objective functions are presented in Tong et al. (2021).

The runoff objective function O_Q emphasizes both high and low flows (Parajka and Blöschl, 2008b) and is described by a compound objective function combing two variants of Nash-Sutcliffe coefficients, i.e. it is estimated from observed and logarithmic-transformed river flow values (Nash and Sutcliffe, 1970):

$$O_Q = 0.5 \cdot NSE + 0.5 \cdot NSE_{log} \qquad (4.5)$$

$$NSE = 1 - \frac{\sum_{i=1}^{n} \left(Q_{obs,i} - Q_{sim,i}\right)^2}{\sum_{i=1}^{n} \left(Q_{obs,i} - \overline{Q_{obs}}\right)^2} \qquad (4.6)$$

$$NSE_{\log} = 1 - \frac{\sum_{i=1}^{n} \left(\log(Q_{obs,i}) - \log(Q_{sim,i})\right)^2}{\sum_{i=1}^{n} \left(\log(Q_{obs,i}) - \log(\overline{Q_{obs}})\right)^2} \qquad (4.7)$$

where $Q_{obs,i}$ and $Q_{sim,i}$ are the river flow observation and simulation of day i.

The measure of soil moisture agreement (O_{SM}) is determined by the Pearson correlation coefficient (O_{SM}) between the satellite soil water index (SWI) and simulated relative soil moisture in each elevation zone:

Die approbierte gedruckte Originalversion dieser Dissertation ist an der TU Wien Bibliothek verfügbar.
The approved original version of this doctoral thesis is available in print at TU Wien Bibliothek.
TU Bibliothek Your knowledge hub WIEN

$$O_{SM} = \frac{\sum_{i=1}^{N_{days}} \sum_{j=1}^{N_{zones}} \left((\theta_{sim,i,j} - \overline{\theta_{sim}})(\theta_{obs,i,j} - \overline{\theta_{obs}}) \right)}{\sqrt{\sum_{i=1}^{N_{days}} \sum_{j=1}^{N_{zones}} \left((\theta_{sim,i,j} - \overline{\theta_{sim}})^2 (\theta_{obs,i,j} - \overline{\theta_{obs}})^2 \right)}} \qquad (4.8)$$

where $\theta_{sim,i,j}$ is the simulated relative soil moisture from the hydrological model and $\theta_{obs,i,j}$ is the averaged value of the observed Soil Water Index (SWI) from ASCAT pixels for the day i and elevation zone j. $\overline{\theta_{sim}}$ and $\overline{\theta_{obs}}$ are the mean value of the simulations and observations for the days and elevation zones which are not masked in the ASCAT SWI product due to presence of snow or frozen ground. It assesses the correspondence of the satellite soil moisture (assumed as ground truth) and simulated time series. The use of O_{SM} has the advantage of not being sensitive to the units and it also allows comparison with the results of previous studies (e.g., Parajka et al., 2006; Gruber et al., 2020; Beck et al., 2021).

The snow cover objective function O_{SC} minimises the sum of snow overestimation S_O and underestimation S_U errors (Parajka and Blöschl, 2008b):

$$O_{SC} = 1 - (S_O + S_U) \qquad (4.9)$$

The snow overestimation error shows the percentage of the condition if the snow is simulated from the model, but the snow cover is not retrieved by the satellite (MODIS):

$$S_O = \frac{1}{\sum_{i=1}^{N_{days}} \sum_{j=1}^{N_{zones}} A_{i,j}} \sum_{i=1}^{N_{days}} \sum_{j=1}^{N_{zones}} A_{i,j} \cap (SWE_{i,j} > \xi_{SWE}) \cap (\mathrm{SCA}_{i,j} = 0) \qquad (4.10)$$

where $A_{i,j}$ is the area of zone j that is cloud-free according to MODIS observation on the day i. $SWE_{i,j}$ is the simulated snow water equivalent in elevation zone j greater than 10mm (Parajka and Blöschl, 2008b), $SCA_{i,j}$ is the MODIS snow covered area within this zone, and N_{days} is the number of days with cloud cover less than a threshold (ξ_C) 50%.

The snow underestimation error indicates the percentage of the condition if no snow is simulated, but snow cover retrieved by the MODIS is over a threshold (ξ_{SCA}) of 25% in the zone, i.e.:

$$S_U = \frac{1}{\sum_{i=1}^{N_{days}} \sum_{j=1}^{N_{zones}} A_{i,j}} \sum_{i=1}^{N_{days}} \sum_{j=1}^{N_{zones}} A_{i,j} \cap (SWE_{i,j} = 0) \cap (\mathrm{SCA}_{i,j} > \xi_{SCA}) \qquad (4.11)$$

4.2.2 Transfer of model parameters to ungauged sites

The hydrological predictions at the ungauged sites are, in this Chapter, based on model simulations driven by model parameters transferred from the gauged locations where the model has been calibrated, i.e. the sites with runoff observations. For the transfer (i.e. regionalization), four groups of methods are evaluated (Table 4.1). The first group estimates model parameters as the arithmetic mean of all calibrated values in the study region (termed "global mean") or, alternatively, as the arithmetic mean of model parameters within a radius of 50 km from the catchment of interest (termed "local mean"). This arithmetic mean regionalization approach

Die approbierte gedruckte Originalversion dieser Dissertation ist an der TU Wien Bibliothek verfügbar.
The approved original version of this doctoral thesis is available in print at TU Wien Bibliothek.
TU Bibliothek Your knowledge hub WIEN

assumes similarity of all catchments within a specified radius where differences in the parameter values are caused only by random factors.

In the second group, the model parameters for ungauged sites are independently estimated from linear regressions between calibrated model parameters and catchment attributes. Similarly, as in the first group, two approaches are tested. The global multiple linear regression uses attributes and model parameters from all gauged catchments. The local multiple linear regression is applied within a 50 km search radius from an ungauged site. In all cases, the regression coefficients are estimated by the ordinary least squares method. For consistency with previous studies, a set of three catchment attributes associated with the largest multiple correlation coefficient for each ungauged site and each model parameter is used. To avoid multicollinearity, the variance inflation factor (Hirsch et al., 1992) is examined. For the transfer of model parameters, such a regression model is used, which has the largest correlation coefficient for the inflation factor less than 10.

The third group of transfer methods is based on the spatial proximity (or spatial distance) between the ungauged and the gauged catchments. The spatial distance between the two catchments is characterized by the distance between the respective catchment centroids. We test two methods of this group: the inverse distance weighting and the ordinary kriging. In both methods, individual parameters from several donor catchments are independently interpolated to a centroid of the ungauged catchment and then combined and used in the hydrological model. The power parameter in inverse distance interpolation is set to two. The ordinary kriging method is based on a fixed exponential variogram with a nugget of 10% of the observed variance, a sill equal to the variance, and a range of 60 km. The test calculations in previous studies (Merz and Blöschl, 2004; Parajka et al., 2005) showed that this setting is consistent with the empirical variograms of most of the calibrated model parameters.

The fourth group of methods is based on the similarity between catchments with runoff observations and ungauged sites. The main idea of the similarity group of methods is to find for an ungauged site a donor catchment that is most similar in terms of certain catchment attributes. The entire collection of model parameters calibrated for a donor catchment is then transferred to the ungauged site. The similarity is defined by a similarity index Φ (Burn and Boorman, 1993; Merz and Blöschl, 2004),

$$\Phi = \sum_{i=1}^{k} \frac{|X_i^G - X_i^U|}{\Delta X_i} \qquad (4.12)$$

where X^G represents a vector of the normalized catchment attributes of the gauged (donor) catchments; X^U are the normalized attributes of the ungauged catchment; and ΔX is the normalized range of attributes. In previous studies (e.g. Parajka et al., 2005) a large number of catchment attributes and their combination have been tested in the study region. Based on the results and preliminary analyses (not shown here) for this study, we selected the approach with the best results. This variant is based on an *a priori* defined combination of the following catchment attributes: mean catchment elevation, stream network density, lake attenuation index and areal proportion of porous aquifers, land use, soils and geologic units. Similar to other approaches, also in this approach, we examine two variants. While the global similarity combination uses all study catchments for estimation of the similarity, the local similarity combination estimates the similarity only within 50 km radius around the ungauged site.

Die approbierte gedruckte Originalversion dieser Dissertation ist an der TU Wien Bibliothek verfügbar.
The approved original version of this doctoral thesis is available in print at TU Wien Bibliothek.
TU Bibliothek Your knowledge hub WIEN

Table 4.1 The list of model parameter transfer methods tested in the Chapter.

Group	Transfer method	Abbreviation
Arithmetic mean	Global mean	GM
	Local mean	LM
Regression	Global regression	GR
	Local regression	LR
Spatial proximity	Inverse distance weighting	ID
	Kriging	KR
Similarity	Global combination of physiographic attributes	GS
	Local combination of physiographic attributes	LS

4.2.3 Evaluation of the prediction accuracy

The performance and efficiency of parameter transfer methods are evaluated by leave-one-out cross validation. Each catchment with observed runoff is considered in turn as ungauged and the transfer methods are used to estimate the parameter sets from other gauged catchments. The hydrological model is applied to simulate daily runoff, soil moisture and snow cover in the ungauged catchment. These simulations are then compared with the observations. The accuracy is quantified by three objectives O_Q, O_{SM}, and O_{SC} in two periods, i.e. in the period used for model calibration (2000-2010, 2007-2010 for O_{SM}) and in an independent validation period (2010-2014). The efficiencies of the transferred model parameters are estimated for eleven different calibration variants (i.e. weight given to runoff) and compared to the efficiency obtained by a transfer of model parameters calibrated to runoff only.

4.3 Data

4.3.1 Study region

The study region is Austria which represents a wide range of physiographic conditions. The topography varies from flat land in the East and North to Alpine terrain in the West and South. Mean annual precipitation is less than 400 mm/year in the East and more than 2500 mm/year in the West. Land use is mainly agricultural in the lowlands and forest in the medium elevation ranges. Alpine vegetation and rocks prevail in the highest alpine regions.

The analysis is carried out for 213 catchments (Fig. 4.1). These catchments have been selected following previous studies (Viglione et al., 2013, Sleziak et al., 2020, Tong et al., 2021) and represent catchments with no significant anthropogenic effects on the water balance. The size of the catchments ranges from 13.7 to 6214 km^2 and the averaged slope varies from 1.74% to 43.91%. As previous studies have shown that the performance of regionalization methods differs between climatic zones (Parajka et al., 2013; Yang et al., 2020), separation of the effect of elevation and climate on the results was deemed important and the catchments were split into two groups representing drier lowland and hilly regions (catchments with mean elevation below 900 m a.s.l.) and wetter alpine conditions (catchments with mean elevation above 900 m a.s.l.). Out of the 213 catchments, 94 are classified as lowland catchments, and 119 as alpine catchments (Fig. 4.1). The threshold of 900 m is chosen as a compromise between balancing the number of catchments in the groups and representing different physiographic regions.

Die approbierte gedruckte Originalversion dieser Dissertation ist an der TU Wien Bibliothek verfügbar.
The approved original version of this doctoral thesis is available in print at TU Wien Bibliothek.
TU Bibliothek Your knowledge hub WIEN

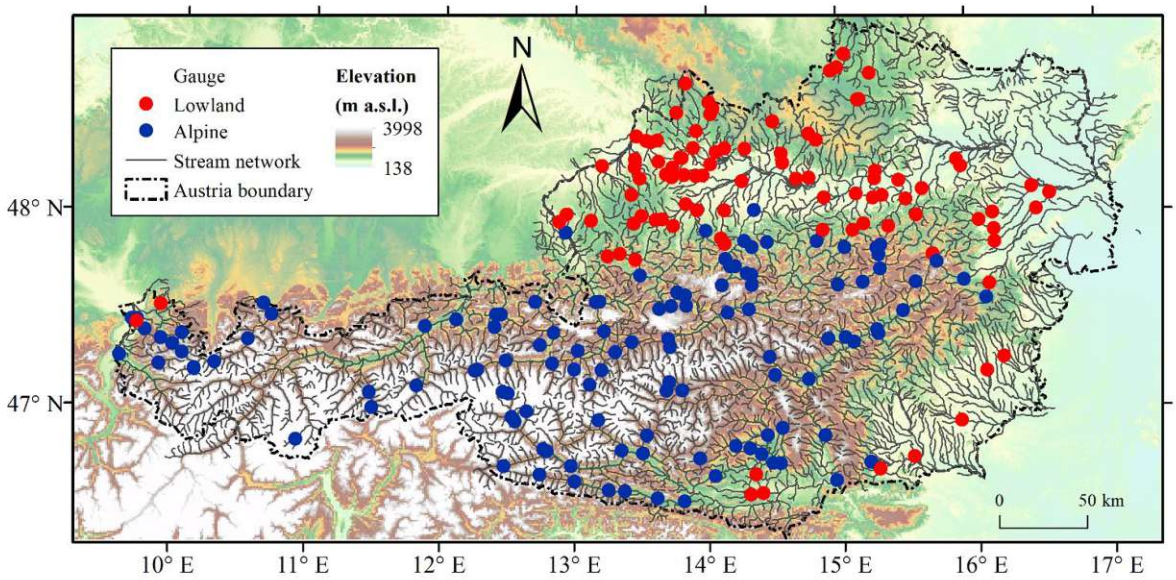

Figure 4.1 Location of 94 lowland (red symbols) and 119 alpine (blue symbols) study catchments.

4.3.2 Hydrologic and climate data

The runoff data have been obtained from Central Hydrographical Bureau (HZB, ehyd.gv.at). The analysis period is from Sep. 2000 to Aug. 2014, which is split into the calibration (September 2000-August 2010) and validation periods (September 2010- August 2014).

Model inputs (i.e. mean of daily climate characteristics for elevation zones) are derived from the SPARTACUS gridded dataset (Hiebl and Frei, 2016, 2018). This dataset includes grid maps of maximum and minimum daily air temperature and precipitation with a spatial resolution of 1km. Daily mean air temperature is estimated as the mean between minimum and maximum air temperature. Potential evaporation model input is estimated by the Blaney-Criddle approach (Parajka et al., 2003). This approach estimates potential evaporation from mean daily air temperature and a potential sunshine duration index, which is calculated from a 1 km digital elevation model of Austria.

4.3.3 MODIS snow cover

The snow cover maps used in model calibration and regionalization validation are based on the combination of the daily, 500m resolution, Terra (MOD10A1) and Aqua (MYD10A1) MODIS datasets (Hall and Riggs, 2016a, 2016b). We use the latest collection 6 snow cover products, which includes the Normalized Difference Snow Index (NDSI). Snow cover mapping from MODIS products is performed in two steps. In the first step, NDSI pixels are classified into snow and land cover classes based on seasonally varying NDSI thresholds (Tong et al., 2020). In the second step, resulting the snow cover maps from Aqua and Terra products are combined to reduce the impact of clouds (Parajka and Blöschl, 2008b). Finally, for each elevation zone of each catchment, the frequency of pixels classified as clouds, snow and land is calculated. This allows estimating the percent snow cover area of each catchment needed for the calculation of the snow cover model objective function.

Die approbierte gedruckte Originalversion dieser Dissertation ist an der TU Wien Bibliothek verfügbar.
The approved original version of this doctoral thesis is available in print at TU Wien Bibliothek.
TU Bibliothek Your knowledge hub WIEN

4.3.4 ASCAT soil moisture

The satellite soil moisture data used in this Chapter is the Soil Water Index (SWI) derived from an experimental version of the upcoming Disaggregated Metop ASCAT Surface Soil Moisture v2 product (H28) provided by the EUMETSAT Satellite Application Facility on Support to Operational Hydrology and Water Management (H SAF). The original ASCAT surface soil moisture dataset at 12.5 km (before disaggregation) is based on a new parameterization for the vegetation correction (Hahn et al., 2020), which has shown improved performance over Austria (Pfeil et al., 2018). The disaggregation process consists of a directional resampling method utilizing the connection between regional (12.5 km) and local (0.5 km) scale Sentinel-1 backscatter observations describing temporally stable soil moisture patterns also reflected in the radar backscatter measurements (Wagner et al. 2008). Surface and root zone soil moisture are available, where the root zone soil moisture is represented by the Soil Water Index (SWI), which is determined by an exponential filter introduced by Wagner et al. (1999a,b) and Albergel et al. (2008) with a characteristic time lag (T). The T-value represents the smoothing of soil moisture dynamics by infiltration, with higher T-values corresponding to a higher degree of smoothing. In order not to lose information on short-term soil moisture dynamics still present in deeper soil layers, T should be carefully chosen. Paulik et al (2014) compared the ASCAT SWI dataset to in situ soil moisture and found that the SWI agrees better with in situ soil moisture from deeper layers than the original surface soil moisture dataset. Moreover, they related the T-value with soil depth layers and found that the T-values 10 and 20 led to the highest correlations in the shallow subsurface (around 0-20 cm). To prevent the loss of short-term soil moisture dynamics, T-value=10 days was selected in this study. Besides, to exclude invalid ASCAT measurements affected by snow and frozen ground, soil moisture is masked using soil temperature and snow cover from the ECMWF Copernicus Climate Service (C3S) ERA5-Land, when soil temperatures at a soil depth of 0-7 cm are below 1°C or snow cover exceeds 30 % of the pixel.

4.4 Results

4.4.1 Efficiency of transfer methods to simulate runoff

Figure 4.2 shows the median of runoff leave-one-out cross-validation efficiency for eight parameter transfer methods (panels) and 11 calibration variants (i.e. different runoff weight w_Q used in model calibration) in the calibration (blue symbols) and validation (red symbols) period. Panels on the left and right show the results for the lowland and alpine group of catchments, respectively. The results for the runoff weight w_Q =1.0 represent the case when the model is calibrated to runoff only. The case w_Q=0.0 represents the case when the model is calibrated to satellite soil moisture and snow cover without using observed runoff.

The results show that the differences between the transfer methods are smaller than those between the different calibration variants, i.e. the different methods of calibrating the model in gauged catchments, for weights below 0.4. The impact of the choice of calibration variant (weight on runoff w_Q) is smaller if the w_Q is larger than 0.4. In this case, the differences between the transfer methods are larger, and the choice of transfer method is more important than that of the calibration variant. The worst parameter transfer (i.e. regionalisation) methods are the global mean and the local regression approach. The median of runoff efficiency is particularly low, i.e. between 0.24 and 0.41, for calibration variants using w_Q <0.3 in the calibration period. If w_Q is larger than 0.7, the median of runoff efficiency of global mean and local regression is between 0.42 and 0.5 for the lowland and between 0.61-0.63 for the alpine catchments. The best transfer methods are global and local similarity and kriging interpolation.

Die approbierte gedruckte Originalversion dieser Dissertation ist an der TU Wien Bibliothek verfügbar.
The approved original version of this doctoral thesis is available in print at TU Wien Bibliothek.
TU Bibliothek Your knowledge hub WIEN

If the w_Q is larger than 0.4, the median efficiency is between 0.67 and 0.69 in the lowland and between 0.71 and 0.74 in the alpine region. The efficiency of the transfer of model parameters calibrated by multiple objective approaches (for w_Q>0.4) for the similarity and kriging methods is the same as that for the transfer of model parameters obtained by calibration to runoff only (w_Q=1). The reason for the similar runoff efficiency of the regionalization methods between w_Q=0.4 to 1.0 is that the runoff model efficiencies of the donor catchments do not change obviously when the satellite soil moisture and snow cover were both included in the calibration with this w_Q range (Tong et al., 2021). In the validation period, the median of multiple objective calibrations (w_Q=0.8) of kriging in the lowland and similarity in the alpine catchments is even larger than the runoff efficiency obtained by a transfer (kriging or similarity) based on parameters calibrated to runoff only (variant w_Q=1). Additionally, Table 4.2 also shows that the regional variability (runoff model efficiency between catchments) is small for kriging while large for local regression methods. A comparison of local and global variants of the transfer methods indicates that the local methods are only slightly better than the global methods in terms of runoff efficiency. The largest difference occurs for the mean approach, but the runoff efficiency of the local mean is noticeably lower than for the spatial proximity or similarity approaches. An exception is the regression of model parameters, which has a larger runoff efficiency for the global than the local approach. The results also show that the performance of transfer methods is better in the alpine than in the lowland catchments. In both groups, however, similarity and kriging are the best approaches for predicting daily runoff.

Die approbierte gedruckte Originalversion dieser Dissertation ist an der TU Wien Bibliothek verfügbar.
The approved original version of this doctoral thesis is available in print at TU Wien Bibliothek.
TU Bibliothek Your knowledge hub WIEN

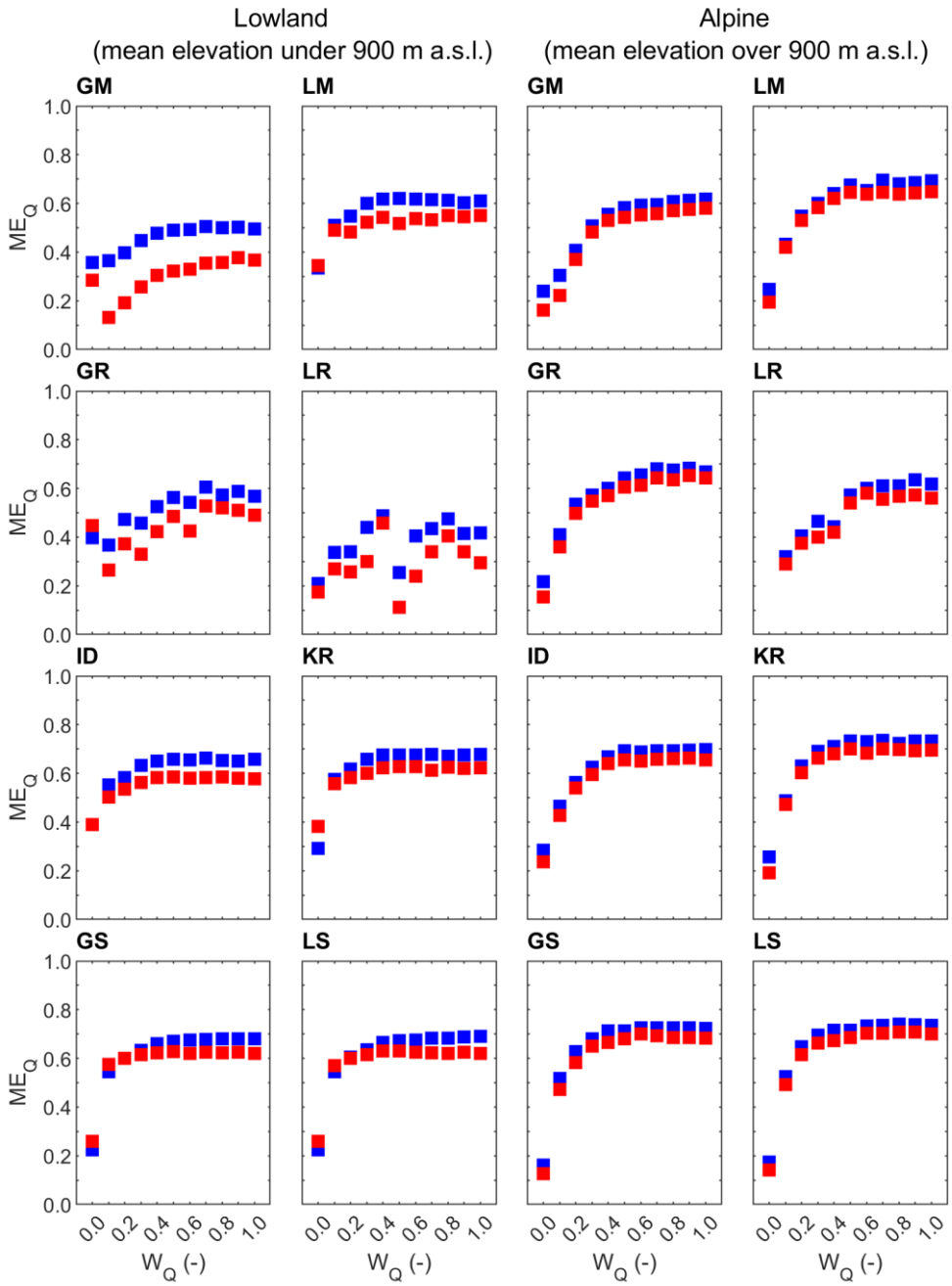

Figure 4.2 Median of leave-one-out runoff model efficiency (Eq. 4.5) obtained by eight groups of parameter transfer methods and eleven calibration weights for lowland (94) and alpine (119) catchments in the calibration (2000-2010, blue symbols) and validation (2010-2014, red symbols) periods.

Die approbierte gedruckte Originalversion dieser Dissertation ist an der TU Wien Bibliothek verfügbar.
The approved original version of this doctoral thesis is available in print at TU Wien Bibliothek.
TU WIEN Bibliothek Your knowledge hub

Table 4.2 Scatter (difference of 75% and 25% quantiles of model efficiency) of leave-one-out runoff model efficiency (Eq. 4.5) obtained by eight groups of parameter transfer methods and eleven calibration weights for lowland (94) and alpine (119) catchments in the calibration (2000-2010, first value) and validation (2010-2014, second value) periods.

	w_Q	0.0	0.1	0.2	0.3	0.4	0.5	0.6	0.7	0.8	0.9	1.0
Lowlands	GM	0.17/ 0.32	0.22/ 0.56	0.25/ 0.47	0.23/ 0.39	0.22/ 0.34	0.21/ 0.34	0.22/ 0.35	0.21/ 0.32	0.21/ 0.31	0.20/ 0.30	0.21/ 0.31
	LM	0.32/ 0.29	0.15/ 0.27	0.15/ 0.22	0.14/ 0.24	0.15/ 0.23	0.15/ 0.19	0.19/ 0.21	0.17/ 0.22	0.16/ 0.25	0.17/ 0.25	0.18/ 0.27
	GR	0.26/ 0.28	0.27/ 0.66	0.18/ 0.37	0.25/ 0.37	0.22/ 0.33	0.20/ 0.31	0.24/ 0.38	0.18/ 0.24	0.17/ 0.21	0.15/ 0.26	0.17/ 0.32
	LR	0.94/ 1.82	0.51/ 0.85	0.88/ 1.45	0.56/ 0.72	0.56/ 0.55	1.10/ 1.61	0.63/ 1.05	0.68/ 1.15	0.58/ 0.86	0.61/ 0.84	0.61/ 0.84
	ID	0.23/ 0.30	0.13/ 0.29	0.13/ 0.25	0.14/ 0.22	0.14/ 0.20	0.15/ 0.23	0.15/ 0.23	0.15/ 0.21	0.15/ 0.23	0.15/ 0.22	0.16/ 0.23
	KR	0.45/ 0.47	0.13/ 0.19	0.12/ 0.16	0.13/ 0.16	0.13/ 0.15	0.15/ 0.19	0.14/ 0.18	0.12/ 0.17	0.12/ 0.18	0.13/ 0.18	0.13/ 0.21
	GS	0.50/ 0.57	0.12/ 0.15	0.12/ 0.13	0.14/ 0.15	0.15/ 0.12	0.15/ 0.13	0.16/ 0.12	0.17/ 0.11	0.17/ 0.11	0.17/ 0.11	0.17/ 0.13
	LS	0.53/ 0.57	0.12/ 0.15	0.12/ 0.14	0.14/ 0.16	0.15/ 0.14	0.15/ 0.13	0.16/ 0.12	0.16/ 0.11	0.17/ 0.12	0.17/ 0.11	0.17/ 0.12
Alpine	GM	0.22/ 0.29	0.21/ 0.26	0.18/ 0.24	0.20/ 0.26	0.18/ 0.23	0.19/ 0.24	0.18/ 0.25	0.19/ 0.24	0.19/ 0.23	0.19/ 0.22	0.18/ 0.22
	LM	0.29/ 0.35	0.23/ 0.24	0.19/ 0.19	0.18/ 0.19	0.14/ 0.17	0.15/ 0.18	0.15/ 0.18	0.15/ 0.19	0.15/ 0.20	0.15/ 0.19	0.15/ 0.19
	GR	0.29/ 0.35	0.26/ 0.25	0.20/ 0.24	0.18/ 0.24	0.19/ 0.21	0.18/ 0.18	0.19/ 0.17	0.19/ 0.17	0.20/ 0.19	0.16/ 0.16	0.17/ 0.18
	LR	0.96/ 0.99	0.51/ 0.59	0.61/ 0.61	0.58/ 0.61	0.45/ 0.46	0.35/ 0.37	0.38/ 0.51	0.37/ 0.43	0.57/ 0.71	0.38/ 0.45	0.48/ 0.53
	ID	0.24/ 0.34	0.25/ 0.25	0.21/ 0.21	0.19/ 0.19	0.16/ 0.19	0.16/ 0.17	0.16/ 0.18	0.15/ 0.17	0.17/ 0.17	0.16/ 0.18	0.15/ 0.17
	KR	0.33/ 0.46	0.21/ 0.23	0.18/ 0.20	0.15/ 0.18	0.13/ 0.16	0.12/ 0.16	0.11/ 0.15	0.11/ 0.17	0.11/ 0.15	0.11/ 0.15	0.11/ 0.14
	GS	0.48/ 0.59	0.24/ 0.22	0.21/ 0.22	0.17/ 0.20	0.14/ 0.17	0.16/ 0.19	0.17/ 0.21	0.16/ 0.22	0.17/ 0.20	0.17/ 0.21	0.18/ 0.23
	LS	0.50/ 0.53	0.23/ 0.20	0.22/ 0.22	0.17/ 0.18	0.13/ 0.16	0.16/ 0.17	0.15/ 0.20	0.16/ 0.18	0.16/ 0.19	0.14/ 0.19	0.16/ 0.21

4.4.2 Efficiency of transfer methods to simulate soil moisture

The evaluation of eight parameter transfer methods to simulate root zone soil moisture is presented in Fig. 4.3. The results show the median correlation between the satellite root zone soil moisture index and simulated relative root zone soil moisture in lowland (left two panels) and alpine (right two panels) catchments. The comparison of different transfer methods and calibration variants indicates that the difference between the transfer methods is similar as that found for the prediction of daily runoff. The best transfer methods are kriging and similarity (local and global) approaches. In the lowland catchments, the median of soil moisture

Die approbierte gedruckte Originalversion dieser Dissertation ist an der TU Wien Bibliothek verfügbar.
The approved original version of this doctoral thesis is available in print at TU Wien Bibliothek.
TU Bibliothek Your knowledge hub WIEN

correlation ranges between 0.62 and 0.70 for these methods. The impact of the calibration variants is, for each transfer method, smaller than found for runoff. Generally, the correlation increases with decreasing w_Q and the soil moisture agreement tends to be larger if the w_Q is smaller than 0.4. A much smaller agreement (correlation) between soil moisture estimates is found in the alpine catchments, this may likely be due to the heterogeneity in temperature and snow cover in mountainous regions when the soil moisture is retrieved from the satellite (Tong et al., 2021). Also here, the best transfer methods are local and global similarity and kriging, but the median correlation varies only between 0.14 and 0.22. From Table 4.3, the regional variability of soil moisture correlation is similar for each method and larger in the lowlands than that in the alpine regions. The comparison between the correlations of the calibration and validation periods shows a similar pattern. Interestingly, in the alpine catchments, the validation period correlations are slightly higher than those found for the transfer in the calibration period. This is likely related to the warmer validation period. Warming decreases snow cover area particularly in the alpine regions and hence decreases the frequency of pixels which need to be masked in the soil moisture dataset.

Die approbierte gedruckte Originalversion dieser Dissertation ist an der TU Wien Bibliothek verfügbar.
The approved original version of this doctoral thesis is available in print at TU Wien Bibliothek.
TU Bibliothek Your knowledge hub WIEN

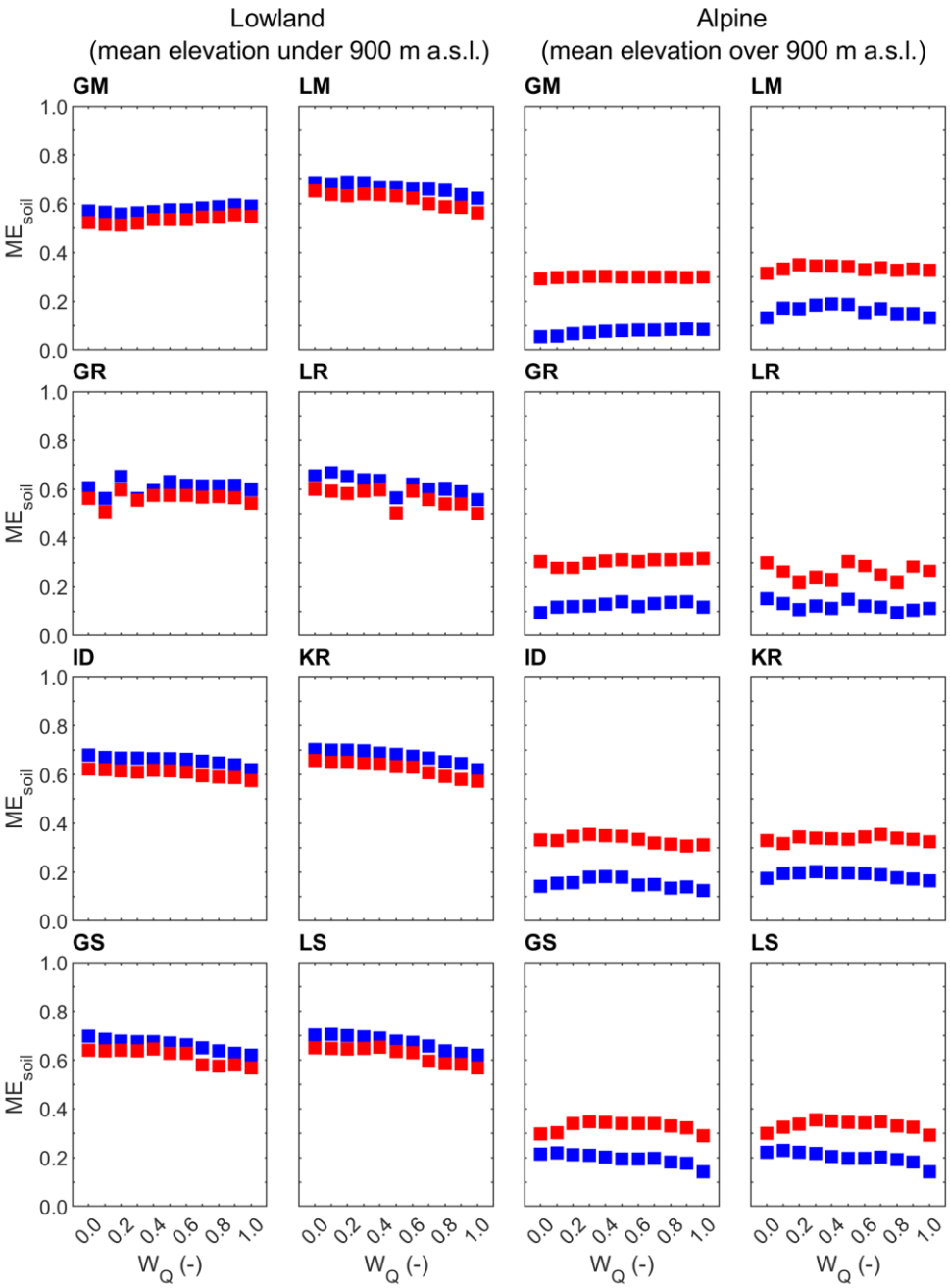

Figure 4.3 Median of leave-one-out soil moisture correlation (Eq. 4.8) obtained by eight groups of parameter transfer methods and eleven calibration weights for lowland (94) and alpine (119) catchments in the calibration (2007-2010, blue symbols) and validation (2010-2014, red symbols) periods.

Die approbierte gedruckte Originalversion dieser Dissertation ist an der TU Wien Bibliothek verfügbar.
The approved original version of this doctoral thesis is available in print at TU Wien Bibliothek.
TU Bibliothek Your knowledge hub WIEN

Table 4.3 Scatter (difference of 75% and 25% quantiles of model efficiency) of leave-one-out soil moisture correlation (Eq. 4.8) obtained by eight groups of parameter transfer methods and eleven calibration weights for lowland (94) and alpine (119) catchments in the calibration (2007-2010, first value) and validation (2010-2014, second value) periods.

	w_Q	0.0	0.1	0.2	0.3	0.4	0.5	0.6	0.7	0.8	0.9	1.0
Lowlands	GM	0.24/ 0.22	0.24/ 0.22	0.25/ 0.22	0.25/ 0.23	0.26/ 0.24	0.26/ 0.23	0.27/ 0.24	0.28/ 0.24	0.28/ 0.24	0.29/ 0.24	0.28/ 0.24
	LM	0.30/ 0.31	0.31/ 0.28	0.32/ 0.28	0.32/ 0.29	0.32/ 0.29	0.32/ 0.28	0.32/ 0.28	0.31/ 0.26	0.31/ 0.26	0.31/ 0.25	0.30/ 0.25
	GR	0.29/ 0.24	0.23/ 0.26	0.29/ 0.26	0.29/ 0.31	0.27/ 0.27	0.30/ 0.23	0.30/ 0.27	0.30/ 0.25	0.30/ 0.25	0.30/ 0.24	0.28/ 0.24
	LR	0.28/ 0.26	0.27/ 0.24	0.27/ 0.22	0.30/ 0.25	0.31/ 0.29	0.34/ 0.34	0.33/ 0.31	0.27/ 0.25	0.27/ 0.25	0.30/ 0.29	0.30/ 0.29
	ID	0.29/ 0.27	0.28/ 0.27	0.28/ 0.27	0.29/ 0.28	0.30/ 0.28	0.30/ 0.28	0.29/ 0.28	0.29/ 0.25	0.31/ 0.24	0.30/ 0.24	0.29/ 0.24
	KR	0.29/ 0.26	0.29/ 0.26	0.29/ 0.27	0.29/ 0.26	0.29/ 0.27	0.29/ 0.28	0.29/ 0.29	0.28/ 0.25	0.31/ 0.25	0.29/ 0.25	0.30/ 0.26
	GS	0.29/ 0.26	0.30/ 0.28	0.30/ 0.27	0.30/ 0.26	0.30/ 0.26	0.30/ 0.27	0.31/ 0.28	0.30/ 0.27	0.30/ 0.26	0.30/ 0.24	0.27/ 0.25
	LS	0.29/ 0.26	0.31/ 0.28	0.31/ 0.27	0.30/ 0.27	0.31/ 0.26	0.30/ 0.27	0.31/ 0.28	0.31/ 0.27	0.33/ 0.27	0.31/ 0.26	0.31/ 0.27
Alpine	GM	0.23/ 0.19	0.23/ 0.18	0.23/ 0.19	0.24/ 0.19	0.24/ 0.19	0.23/ 0.20	0.23/ 0.20	0.23/ 0.19	0.23/ 0.19	0.23/ 0.19	0.22/ 0.19
	LM	0.26/ 0.25	0.20/ 0.25	0.18/ 0.25	0.17/ 0.26	0.17/ 0.26	0.21/ 0.26	0.19/ 0.26	0.20/ 0.26	0.21/ 0.24	0.21/ 0.24	0.22/ 0.23
	GR	0.22/ 0.21	0.16/ 0.25	0.14/ 0.39	0.15/ 0.37	0.17/ 0.26	0.18/ 0.28	0.20/ 0.24	0.16/ 0.25	0.20/ 0.28	0.20/ 0.22	0.19/ 0.24
	LR	0.27/ 0.32	0.22/ 0.30	0.17/ 0.37	0.19/ 0.37	0.16/ 0.34	0.20/ 0.30	0.22/ 0.30	0.21/ 0.39	0.16/ 0.37	0.16/ 0.35	0.15/ 0.34
	ID	0.25/ 0.24	0.24/ 0.25	0.21/ 0.26	0.20/ 0.25	0.17/ 0.24	0.21/ 0.27	0.23/ 0.28	0.22/ 0.28	0.21/ 0.25	0.20/ 0.23	0.21/ 0.22
	KR	0.23/ 0.29	0.20/ 0.29	0.21/ 0.28	0.21/ 0.29	0.19/ 0.27	0.21/ 0.30	0.22/ 0.28	0.19/ 0.28	0.21/ 0.26	0.20/ 0.25	0.21/ 0.23
	GS	0.24/ 0.29	0.20/ 0.28	0.23/ 0.25	0.18/ 0.25	0.16/ 0.24	0.17/ 0.23	0.18/ 0.23	0.18/ 0.24	0.18/ 0.21	0.17/ 0.20	0.17/ 0.19
	LS	0.22/ 0.31	0.20/ 0.28	0.24/ 0.26	0.20/ 0.25	0.18/ 0.24	0.19/ 0.25	0.20/ 0.24	0.20/ 0.24	0.20/ 0.21	0.19/ 0.21	0.16/ 0.19

4.4.3 Efficiency of transfer methods to simulate snow cover

The efficiency of eight transfer methods to simulate snow cover is evaluated in Fig. 4.4. The results indicate the smallest difference in snow efficiency between the transferred methods. A much larger difference and impact on snow efficiency is linked to the weight used in model calibration. The difference in snow efficiency between transfer methods for the same w_Q is mostly between 1 and 3%, but the snow efficiency for different w_Q (and the same transfer method) ranges between 8 and 17%. The snow efficiency decreases with increasing w_Q, and it

Die approbierte gedruckte Originalversion dieser Dissertation ist an der TU Wien Bibliothek verfügbar.
The approved original version of this doctoral thesis is available in print at TU Wien Bibliothek.
TU Bibliothek Your knowledge hub WIEN

is generally larger in the lowland than in the alpine catchments. It is related to the different frequencies of snow cover conditions in these two regions, generally the snow free condition is with less error for the simulation. Interestingly, in the alpine catchments, the similarity-based approaches and kriging have the smallest efficiency, and the most accurate results are obtained by the global mean and global regression methods. At the same time, the regional variability of the snow model efficiencies (Table 4.4) has a small difference between different w_Q. Also indicated in the table 4.4, the local regression method performed relatively unstable for simulating snow, and in the Alpine regions the regional variability of snow model efficiency is larger than that in the lowlands. The impact of the calibration variant is, however, much more important than the selection of transfer method. The comparison between calibration and validation periods indicates an overall larger snow efficiency in the validation period. This is likely linked with a warmer validation period and generally fewer days with snow cover associated with an increase in air temperature in the last decades (Duethmann and Blöschl, 2018).

Die approbierte gedruckte Originalversion dieser Dissertation ist an der TU Wien Bibliothek verfügbar.
The approved original version of this doctoral thesis is available in print at TU Wien Bibliothek.
TU Bibliothek Your knowledge hub WIEN

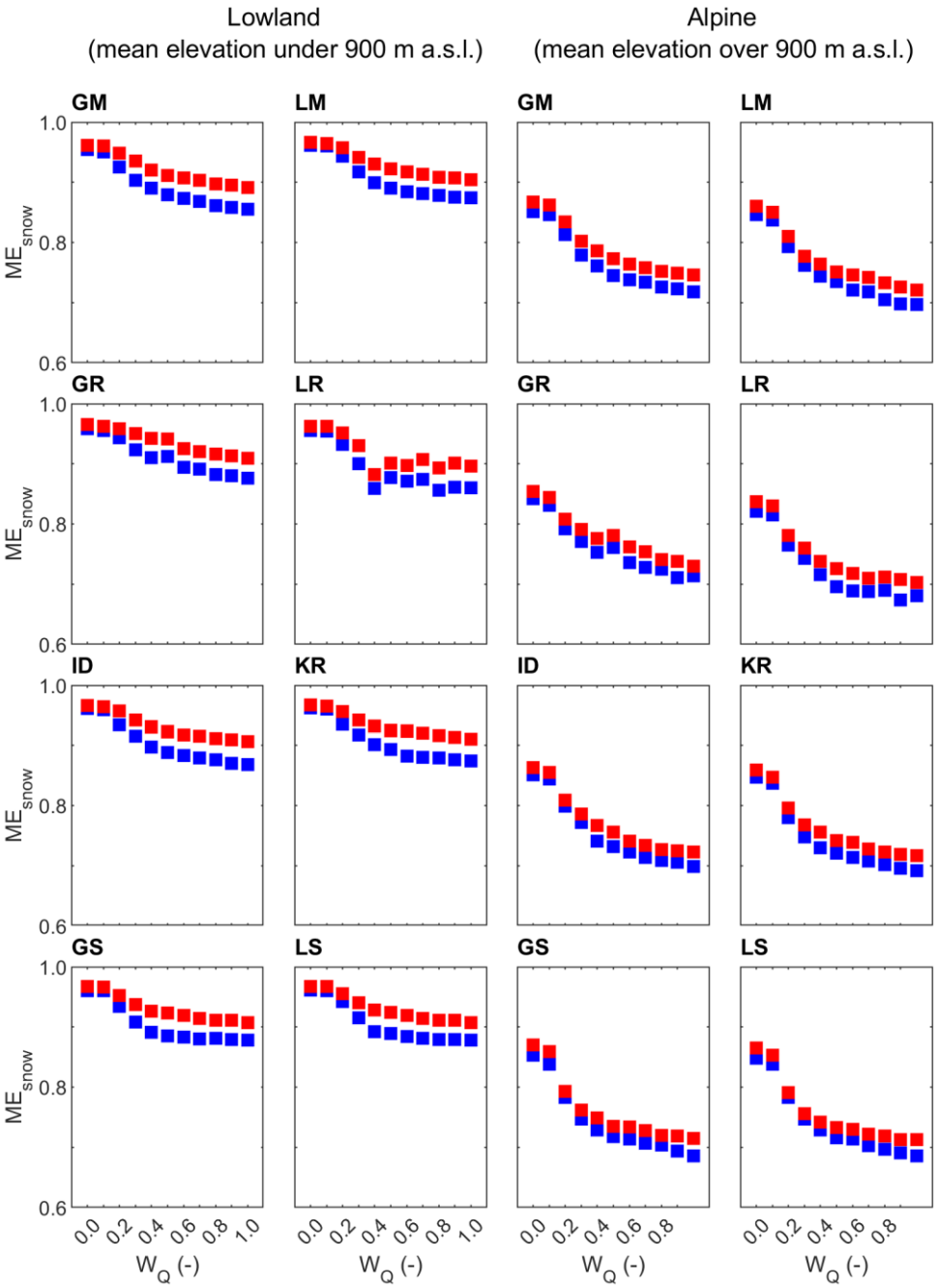

Figure 4.4 Median of leave-one-out snow model efficiency (Eq. 4.9) obtained by eight groups of parameter transfer methods and eleven calibration weights for lowland (94) and alpine (119) catchments in the calibration (2000-2010, blue symbols) and validation (2010-2014, red symbols) periods.

Die approbierte gedruckte Originalversion dieser Dissertation ist an der TU Wien Bibliothek verfügbar.
The approved original version of this doctoral thesis is available in print at TU Wien Bibliothek.
TU Bibliothek Your knowledge hub WIEN

Table 4.4 Scatter (difference of 75% and 25% quantiles of model efficiency) of leave-one-out snow model efficiency (Eq. 4.9) obtained by eight groups of parameter transfer methods and eleven calibration weights for lowland (94) and alpine (119) catchments in the calibration (2000-2010, first value) and validation (2010-2014, second value) periods.

	w_Q	0.0	0.1	0.2	0.3	0.4	0.5	0.6	0.7	0.8	0.9	1.0
Lowlands	GM	0.05/ 0.02	0.05/ 0.03	0.06/ 0.04	0.06/ 0.05	0.06/ 0.05	0.06/ 0.06	0.06/ 0.06	0.06/ 0.06	0.06/ 0.06	0.06/ 0.06	0.06/ 0.06
	LM	0.04/ 0.03	0.04/ 0.02	0.06/ 0.04	0.07/ 0.05	0.08/ 0.07	0.08/ 0.07	0.08/ 0.07	0.08/ 0.07	0.08/ 0.06	0.07/ 0.07	0.06/ 0.07
	GR	0.05/ 0.03	0.05/ 0.02	0.06/ 0.04	0.07/ 0.06	0.06/ 0.06	0.06/ 0.06	0.07/ 0.07	0.06/ 0.06	0.07/ 0.06	0.07/ 0.06	0.07/ 0.07
	LR	0.04/ 0.03	0.05/ 0.03	0.07/ 0.05	0.10/ 0.07	0.13/ 0.12	0.10/ 0.09	0.09/ 0.07	0.08/ 0.09	0.10/ 0.09	0.09/ 0.08	0.09/ 0.08
	ID	0.04/ 0.03	0.04/ 0.02	0.06/ 0.04	0.06/ 0.05	0.06/ 0.05	0.06/ 0.05	0.06/ 0.05	0.07/ 0.06	0.07/ 0.06	0.07/ 0.06	0.07/ 0.06
	KR	0.04/ 0.02	0.04/ 0.02	0.06/ 0.04	0.06/ 0.05	0.06/ 0.05	0.06/ 0.05	0.06/ 0.05	0.07/ 0.05	0.07/ 0.05	0.07/ 0.05	0.07/ 0.06
	GS	0.04/ 0.03	0.04/ 0.03	0.07/ 0.04	0.07/ 0.05	0.06/ 0.05	0.07/ 0.05	0.07/ 0.05	0.06/ 0.05	0.07/ 0.05	0.07/ 0.05	0.07/ 0.06
	LS	0.04/ 0.03	0.04/ 0.03	0.07/ 0.04	0.07/ 0.05	0.06/ 0.05	0.06/ 0.05	0.07/ 0.05	0.07/ 0.06	0.07/ 0.06	0.08/ 0.06	0.07/ 0.06
Alpine	GM	0.09/ 0.08	0.09/ 0.08	0.10/ 0.09	0.12/ 0.10	0.12/ 0.11	0.13/ 0.11	0.13/ 0.12	0.13/ 0.12	0.13/ 0.12	0.13/ 0.12	0.14/ 0.12
	LM	0.10/ 0.10	0.12/ 0.11	0.13/ 0.12	0.15/ 0.12	0.15/ 0.13	0.16/ 0.14	0.17/ 0.14	0.17/ 0.14	0.17/ 0.14	0.16/ 0.14	0.16/ 0.14
	GR	0.11/ 0.11	0.11/ 0.11	0.14/ 0.12	0.14/ 0.12	0.15/ 0.12	0.15/ 0.13	0.16/ 0.15	0.17/ 0.15	0.16/ 0.15	0.16/ 0.14	0.15/ 0.14
	LR	0.14/ 0.12	0.17/ 0.14	0.20/ 0.19	0.17/ 0.14	0.18/ 0.17	0.18/ 0.18	0.19/ 0.18	0.20/ 0.18	0.16/ 0.16	0.17/ 0.15	0.18/ 0.17
	ID	0.10/ 0.11	0.13/ 0.12	0.15/ 0.14	0.16/ 0.13	0.16/ 0.14	0.16/ 0.14	0.16/ 0.14	0.16/ 0.14	0.16/ 0.14	0.16/ 0.14	0.16/ 0.14
	KR	0.11/ 0.11	0.14/ 0.14	0.17/ 0.15	0.17/ 0.14	0.16/ 0.15	0.16/ 0.16	0.16/ 0.15	0.15/ 0.14	0.16/ 0.15	0.17/ 0.15	0.16/ 0.14
	GS	0.11/ 0.10	0.15/ 0.14	0.16/ 0.16	0.18/ 0.15	0.17/ 0.14	0.16/ 0.14	0.16/ 0.14	0.17/ 0.14	0.14/ 0.13	0.16/ 0.13	0.16/ 0.14
	LS	0.11/ 0.10	0.14/ 0.13	0.16/ 0.15	0.18/ 0.16	0.18/ 0.14	0.17/ 0.14	0.17/ 0.15	0.17/ 0.14	0.16/ 0.13	0.16/ 0.13	0.15/ 0.13

4.4.4 Improvement of multi objective regionalization vs runoff only regionalization

This section analyses the impact of calibration and runoff weight on the efficiency of different transfer methods to simulate runoff, soil moisture and snow cover. We compared the efficiencies between predictions obtained by transferring model parameters obtained by multiple-objective calibration (i.e. w_Q<1) and by parameters calibrated to runoff only (w_Q=1). Positive efficieny values thus mean an improvement when using a multiple-objective calibration compared to a runoff-only calibration. The results are shown in Fig. 4.5 for the

Die approbierte gedruckte Originalversion dieser Dissertation ist an der TU Wien Bibliothek verfügbar.
The approved original version of this doctoral thesis is available in print at TU Wien Bibliothek.
TU Bibliothek Your knowledge hub WIEN

calibration period and in Fig. 4.6 for the validation period. Figure 4.5 and 4.6 show the relative improvement in snow cover (x-axis), soil moisture (y-axis) and runoff (colour of symbol) efficiencies for eight transfer methods (panels) and ten calibration weights (symbol size) in the lowland (left) and alpine (right) catchments. The results show that the runoff predictions are very similar (i.e. within 1% range) if the runoff weight is larger than 0.5. The largest impact of the multiple objective calibration is found for the soil moisture prediction, where the improvement is larger than for snow cover. In the lowland catchments, the soil moisture improvement is about 1 to 7% for w_Q larger than 0.4. In the case of snow cover, the improvement is within 5% when w_Q larger than 0.4. The patterns of improvement for the best transfer methods (kriging and similarity approaches) are very similar. The improvement increases with decreasing runoff weight but at the expense of decreasing runoff efficiency. The largest improvement of soil moisture (i.e. over 25%) is found for the similarity approaches in the alpine catchments, but the overall soil moisture efficiency is rather low. The patterns of improvement are very consistent with those obtained for the transfer of model parameters in the validation period (Fig 4.6). The improvement in soil moisture and snow cover increases with decreasing of runoff weight and the improvement is larger in the alpine than the lowland catchments.

Die approbierte gedruckte Originalversion dieser Dissertation ist an der TU Wien Bibliothek verfügbar.
The approved original version of this doctoral thesis is available in print at TU Wien Bibliothek.
TU WIEN Bibliothek Your knowledge hub

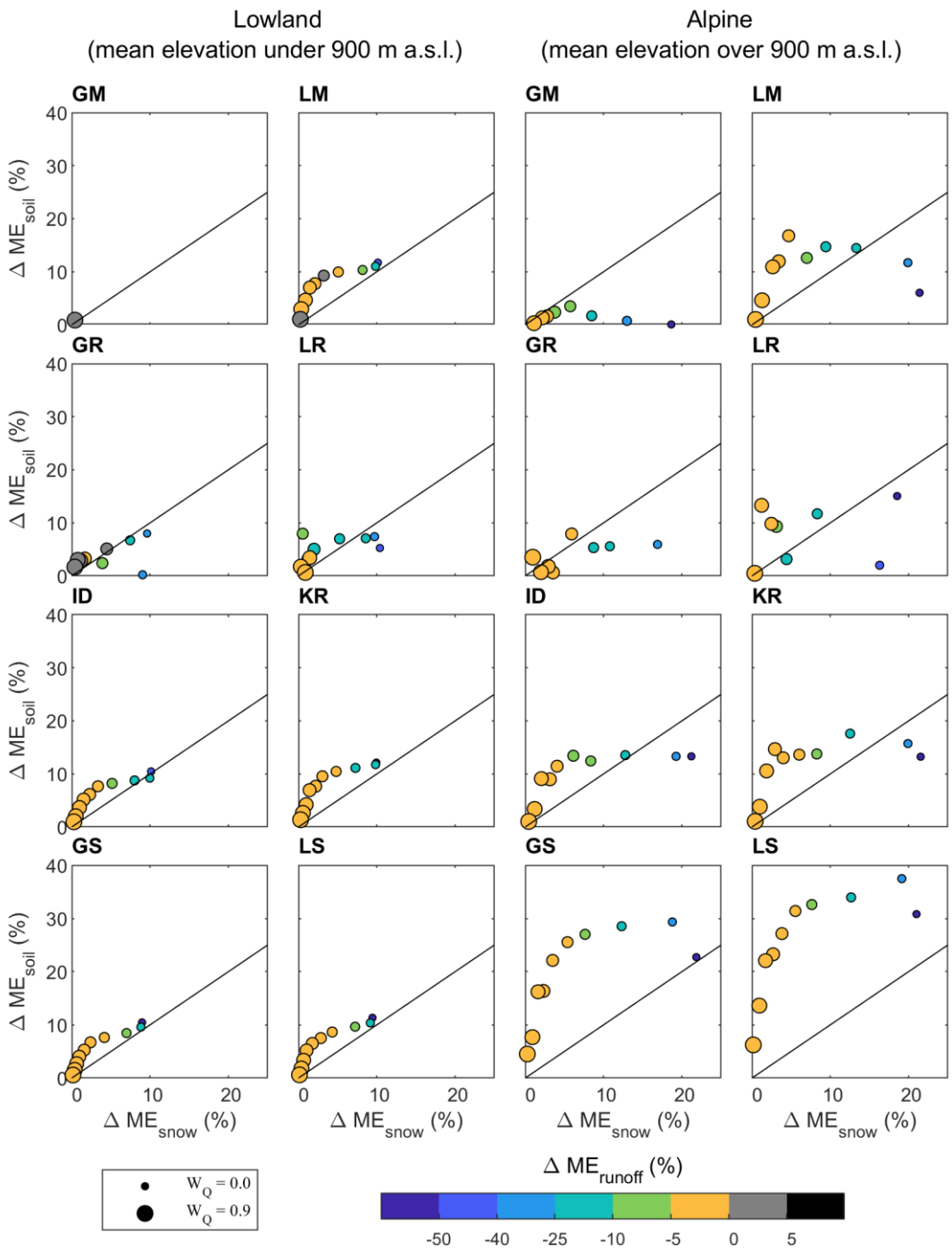

Figure 4.5 The relative difference (%) in the median of snow cover (horizontal axis), soil moisture (vertical axis) and runoff (colour of symbols) efficiency between model simulations obtained by transferring model parameters calibrated by multiple-objective calibration and calibration to runoff only. The relative difference is estimated for eight model transfer methods (panels) applied in the lowland (left panels) and alpine (right panels) catchments in the calibration period 2000-2010 (soil moisture: 2007-2010).

Die approbierte gedruckte Originalversion dieser Dissertation ist an der TU Wien Bibliothek verfügbar.
The approved original version of this doctoral thesis is available in print at TU Wien Bibliothek.
TU Bibliothek Your knowledge hub WIEN

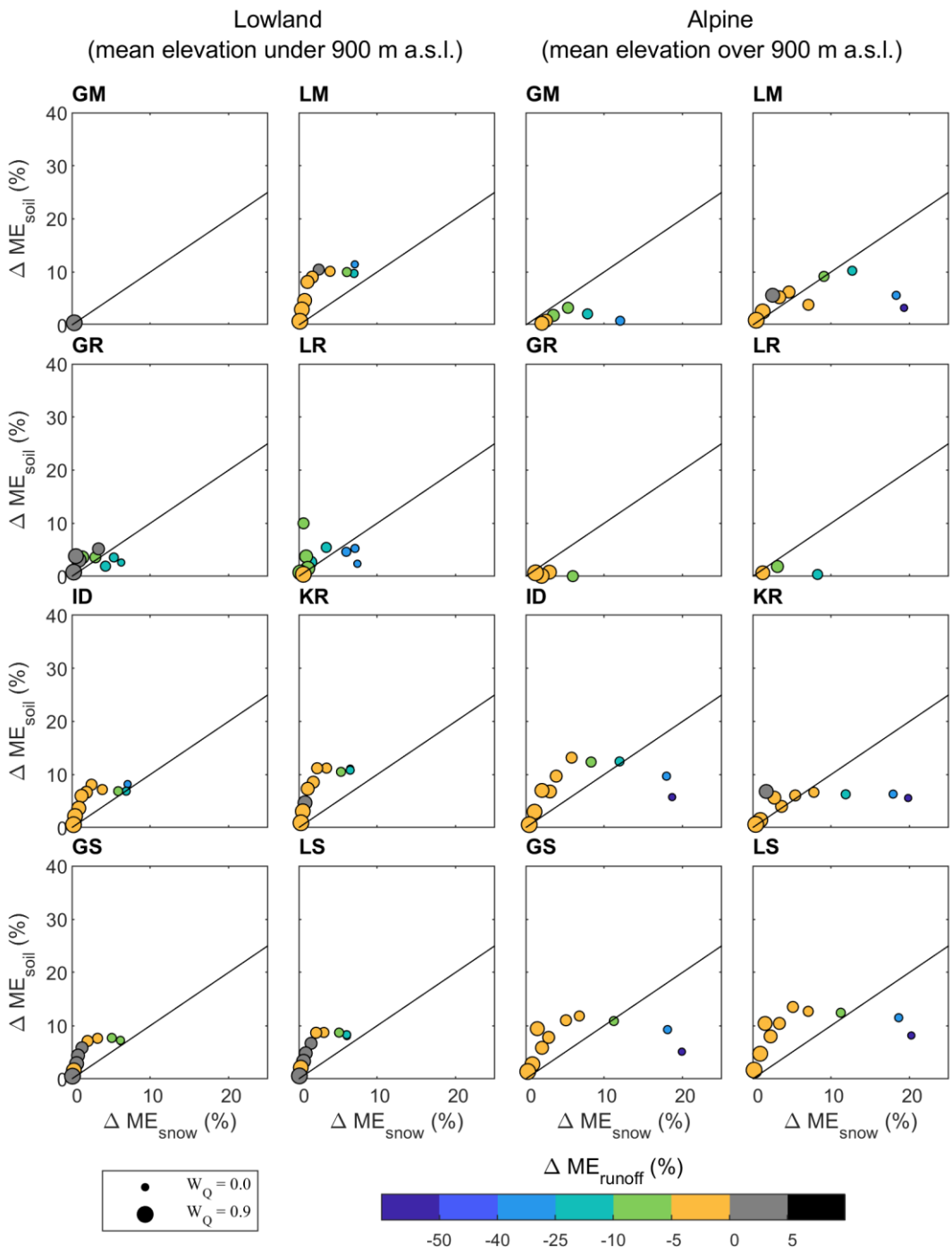

Figure 4.6 Same as Fig. 4.5, but for the validation period (2010-2014)

4.5 Discussion

The main aim of the Chapter was to test to what extent satellite data can improve the prediction of daily runoff in ungauged catchments. Tong et al. (2021) showed that ASCAT and MODIS satellites in hydrological model calibration improve simulations of a conceptual hydrological model, and that the improvements of runoff and soil moisture simulations were larger in low elevation and agricultural catchments. Here, we tested different methods for transferring model parameters from gauged to ungauged sites in the study region (Merz and Blöschl, 2004, Parajka et al., 2005). We examined which method and to what extent transferring model parameters

Die approbierte gedruckte Originalversion dieser Dissertation ist an der TU Wien Bibliothek verfügbar.
The approved original version of this doctoral thesis is available in print at TU Wien Bibliothek.
TU Bibliothek Your knowledge hub WIEN

calibrated to different objectives improves the prediction of runoff, soil moisture and snow cover at ungauged sites. The results showed that the improvement is largest in the simulation of soil moisture and snow cover without a significant impact on runoff prediction accuracy. The assessment of the efficiencies of the different transfer methods indicates that the similarity approach and kriging of model parameters are the best in the study region. This finding is in line with that of Yang et al. (2020) who concluded that the spatial proximity and similarity approaches are relatively better than the parameter average or regression method in Norwegian catchments. This finding is also entirely consistent with the results of Parajka et al. (2005), who calibrated the model parameters in a larger number of catchments but using only runoff and interpolated snow depth (but not soil moisture). While in this Chapter we examined all 30 transfer approaches of Parajka et al. (2005), for clarity, we present only the results for the main transfer approaches. The results and efficiency of other similarity combinations tested in Parajka et al. (2005) are slightly lower or very similar in terms of runoff, soil moisture and snow cover efficiency. The efficiency of global and local regression and arithmetic mean methods are very similar, even though here we use 107 catchments (33%) fewer than tested in Parajka et al. (2005). Overall, the lower prediction accuracy of global mean or local regression is also consistent with the global assessment of the accuracy of the transfer methods presented in Parajka et al. (2013).

The results of Tong et al. (2021) show that using only satellite soil moisture and snow cover data is not sufficient for calibrating a conceptual hydrological model in ungauged catchments. The lower runoff accuracy of the calibration variants with no or only small weight to runoff is also reflected in the performance of the transfer methods. Satellite soil moisture and snow cover data are very useful for constraining model parameters related to the simulation of snow cover and soil moisture (Nijzink et al., 2018, Tong et al., 2021). However, the use of runoff is still essential for the accurate prediction of the complete runoff hydrographs. This finding agrees with the previous assessment of using soil moisture estimates from ERS scatterometer observations to improve hydrological simulations in gauged and ungauged catchments (Parajka et al., 2006). The scatterometer data assimilation did not improve the prediction in ungauged sites but provided more consistent patterns of soil moisture estimates. The use of the experimental disaggregated ASCAT dataset showed that the detailed spatial and temporal resolution of satellite soil moisture improves the application and agreement of soil moisture estimates in smaller lowland catchments. Similarly, as found in Széles et al. (2020) for a small Austrian catchment, the use of soil moisture data has a larger impact on the overall consistency of the model simulations compared to snow cover observations.

4.6 Conclusions

The findings of this chapter indicate that the method used to calibrate the model in a gauged catchment has a greater effect on runoff prediction accuracy in ungauged catchments than the parameter transfer method implemented. The global and local similarity and the kriging approaches to spatially transferring parameters perform better than the other methods tested. The performance of the approaches also differs between lowland and alpine catchments; the soil moisture and snow cover prediction efficiencies are higher in lowland catchments, but the runoff prediction efficiency is higher in alpine catchments. The prediction efficiencies of soil moisture and snow cover are improved when the multiple objective calibration with satellite soil moisture and snow cover were added for the gauged sites. The simulation of runoff has similar results, and the accuracy is largely determined by the weight given to the runoff objective in the multiple objective calibrations.

This Chapter suggests that the future evaluation of the transfer of model parameters to ungauged sites will benefit from examining what type of information will improve the calibration and

Die approbierte gedruckte Originalversion dieser Dissertation ist an der TU Wien Bibliothek verfügbar.
The approved original version of this doctoral thesis is available in print at TU Wien Bibliothek.
TU Bibliothek Your knowledge hub WIEN

transfer of model parameters related to the runoff generation and routing. It will also be interesting to examine the role of nested catchments in parameter transfer and the impact of stream gauge density on the results. A suitable choice of a combination of estimated runoff signatures and satellite observations is also one of the possible future research directions. The results of this Chapter show that the recent advances in remote sensing of water balance components may indeed contribute to improving the predictions of daily hydrographs in ungauged catchments.

Die approbierte gedruckte Originalversion dieser Dissertation ist an der TU Wien Bibliothek verfügbar.
The approved original version of this doctoral thesis is available in print at TU Wien Bibliothek.
TU WIEN Bibliothek Your knowledge hub

5. Overall conclusions and outlook

Hydrological modelling is an essential tool for the estimation and prediction of runoff and other water balance components. Estimates of hydrologic characteristics are needed for numerous water resource management purposes, such as the allocation of water to industry, irrigation or water supply, engineering design, or environmental management. However, the application of hydrological models is often challenging due to limited observations of hydrological variables and large spatial variability of the environment.

This thesis focuses on the potential of using recent satellite datasets of soil moisture and snow cover for improving hydrological simulations at the regional scale. In line with technological advances, remote sensing products of soil moisture and snow cover are constantly improving, including decreasing spatial and temporal resolutions, novel retrieval and classification methods, and an increasing length of observations. The question is to what extent these recent advances in remote sensing will actually improve the estimation of water balance components, including runoff at ungauged sites.

The thesis addresses three specific research questions. Chapter 2 examines the ways to improve snow cover mapping based on MODIS datasets. The evaluation of the sensitivity and accuracy of different Normalized Difference Snow Index (NDSI) thresholds shows that using spatiotemporally variable thresholds improves the regional snow cover mapping in forested regions above 900m a.s.l. in January to March. Compared to previous studies, which evaluated earlier MODIS versions based on a fixed threshold, the accuracy in Austria increased in the range of 3-10%. The increased accuracy has numerous implications for operational and scientific applications. Snow cover is a fundamental factor of the terrestrial system and an indicator of changing climate (Dong, 2018). Increasing air temperature will lead to changes in snow melting. Snowmelt floods in the alpine region may thus change and occur earlier, more frequently and/or can have a larger magnitude. Accurate monitoring and mapping of snow cover may therefore assist in predicting and reducing the risk of snowmelt floods and avalanches. Changes in melt water rates from the snowpack may also change the seasonal runoff, especially in spring, which will affect the availability and management of water supply. Snow also plays an important role in winter tourism which is of high economic relevance. Long-term records of snow cover characteristics provide an essential database for the selection, development and promotion of ski resorts in many regions of the world.

Chapter 3 examines the value of the new MODIS snow classification along with a new ASCAT soil moisture product for calibration and validation of a conceptual hydrologic model. The study is carried out in 213 catchments situated in different physiographic and climate zones of Austria. The results show that including soil moisture data in the calibration primarily improves soil moisture simulations; including snow data primarily improves snow simulations, including both improves soil moisture and snow simulations to a similar extent. The combined calibration of runoff, satellite soil moisture, and snow cover data notably improves soil moisture simulations (in 80% of the catchments) and snow (in nearly all catchments) compared to traditional calibration to runoff only. The results show that the combined use of soil moisture and snow cover datasets can also improve simulations of runoff, which was not the case in most of the previous studies. The improvements of the runoff and soil moisture model efficiencies are larger in low elevation and agricultural catchments. The multiple objective calibrations have a substantial effect on constraining the model parameters. Obviously, snow-related parameters

Die approbierte gedruckte Originalversion dieser Dissertation ist an der TU Wien Bibliothek verfügbar.
The approved original version of this doctoral thesis is available in print at TU Wien Bibliothek.
TU Bibliothek WIEN Your knowledge hub

are strongly affected by including snow data in model calibration and, to a lesser extent, by soil moisture data and vice versa. Using both satellite datasets allows a robust constraining of the snow and soil moisture modules of the conceptual hydrologic model. Improved model efficiency and reduction of parameter uncertainty have important implications for operational forecasting for agricultural and water resource management purposes, in addition to projections of impacts of climate change on water balance components. The results show how important additional information in hydrological modelling is and how large the uncertainties are if only runoff is used for model calibration.

One of the applications of the use of hydrological models constrained by multiple-objective satellite observations is investigated in Chapter 4. This chapter evaluates the efficiency of different methods for spatially transferring model parameters obtained by multiple objective calibrations to ungauged sites. The predictive accuracy is evaluated by leave-one-out cross-validation. The results show that the method used for model calibration in the gauged catchment has a larger impact on runoff prediction accuracy in the ungauged catchments than the choice of the parameter transfer method. A comparison of model transfer methods based on parameters calibrated to runoff, snow cover, and soil moisture with those based on parameters calibrated to runoff only indicates that the former outperforms the latter in terms of simulating soil moisture and snow cover. The performance of simulating runoff is similar, and the accuracy depends mainly on the weight given to the runoff objective in the multiple objective calibrations. For the runoff simulations, the results are in line with previous studies (for example Parajka et al., 2013, Yang et al., 2020) in that the spatial proximity and similarity approaches are the best among the regionalization methods. The results of Chapter 4 show that the spatial proximity and similarity methods perform best also in terms of soil moisture simulations. For the snow cover simulation, the performance of the different methods does not vary much, and it is more sensitive to the weight given to snow when the parameters are calibrated in gauged catchments.

The accurate estimation of water balance components at the regional scale is important for many issues. Simulations of snow cover can assist in filling observational gaps due to cloud cover of snow cover maps from optical satellites, and therefore contribute to more reliable applications of snow cover. The accurate prediction of soil moisture can be of benefit for the operation of irrigation reservoirs, the forecasting of crop production and the prediction of food prices. Soil moisture is also a key indicator of agriculture drought in many sensitive regions. Similarly, the soil moisture prior to a storm is very relevant for flood prediction.

The prediction of hydrographs in ungauged basins could strengthen our knowledge in these regions where it is difficult to set up a hydrological station or where the capacity of water resources management is relatively low. A better understanding of water balance components in ungauged areas is advantageous to many potential developments, such as dam design, for which accurate re-constructions of streamflow time series are needed. With model parameters informed by satellite data, the related model predictions may be closer to reality. The simulation of hydrological variables is also relevant for understanding the impact of climate change on the water cycle. At the time this thesis is written, most countries around the world are setting themselves ambitious climate mitigation and adaptation goals. Most countries hope to achieve carbon neutrality by the mid-21st century. Among other strategies, further developing hydropower may help reduce CO_2 emissions. It is hoped that the methods and results presented in this thesis can make some, if very small, contribution to achieving these goals through more accurate hydrological predictions in ungauged basins.

The findings of this thesis suggest that future applications of hydrological models should consider information beyond runoff signatures in the model calibration. The improvement of the simulations of water balance components at the regional scale using this additional

Die approbierte gedruckte Originalversion dieser Dissertation ist an der TU Wien Bibliothek verfügbar.
The approved original version of this doctoral thesis is available in print at TU Wien Bibliothek.
TU Bibliothek Your knowledge hub WIEN

information is practicable. Multiple objective approaches are, therefore, to be recommended for the prediction of water balance components in ungauged basins for water management purposes. In future studies, it will be interesting to examine other satellite products and alternative methods of combining relevant information for hydrological modelling, e.g. related to the timing of runoff events. The test of more accurate satellite data with increased resolution, and more generally, the use of advanced technologies and measurements for hydrological modelling, will likely remain an attractive topic for hydrologists in the years to come.

Die approbierte gedruckte Originalversion dieser Dissertation ist an der TU Wien Bibliothek verfügbar.
The approved original version of this doctoral thesis is available in print at TU Wien Bibliothek.
TU WIEN Bibliothek Your knowledge hub

References

Abowarda, A. S., Bai, L., Zhang, C., Long, D., Li, X., Huang, Q., & Sun, Z. (2021). Generating surface soil moisture at 30 m spatial resolution using both data fusion and machine learning toward better water resources management at the field scale. Remote Sensing of Environment, 255, 112301. doi:https://doi.org/10.1016/j.rse.2021.112301

Albergel, C., Rüdiger, C., Pellarin, T., Calvet, J. C., Fritz, N., Froissard, F., . . . Martin, E. (2008). From near-surface to root-zone soil moisture using an exponential filter: an assessment of the method based on in-situ observations and model simulations. Hydrol. Earth Syst. Sci., 12(6), 1323-1337. doi:https://doi.org/10.5194/hess-12-1323-2008

Arsenault, K. R., Houser, P. R., & De Lannoy, G. J. (2014). Evaluation of the MODIS snow cover fraction product. Hydrological Processes, 28(3), 980-998.

Astagneau, P. C., Thirel, G., Delaigue, O., Guillaume, J. H. A., Parajka, J., Brauer, C. C., . . . Beven, K. J. (2020). Hydrology modelling R packages: a unified analysis of models and practicalities from a user perspective. Hydrol. Earth Syst. Sci. Discuss., 2020, 1-48. doi:10.5194/hess-2020-498

Ault, T. W., Czajkowski, K. P., Benko, T., Coss, J., Struble, J., Spongberg, A., . . . Gross, C. (2006). Validation of the MODIS snow product and cloud mask using student and NWS cooperative station observations in the Lower Great Lakes Region. Remote Sensing of Environment, 105(4), 341-353. doi:10.1016/j.rse.2006.07.004

Babaeian, E., Sadeghi, M., Jones, S. B., Montzka, C., Vereecken, H., & Tuller, M. (2019). Ground, Proximal, and Satellite Remote Sensing of Soil Moisture. Reviews of Geophysics, 57(2), 530-616. doi:https://doi.org/10.1029/2018rg000618

Bai, P., Liu, X., & Liu, C. (2018). Improving hydrological simulations by incorporating GRACE data for model calibration. Journal of Hydrology, 557, 291-304. doi:https://doi.org/10.1016/j.jhydrol.2017.12.025

Bauer-Marschallinger, B., Freeman, V., Cao, S., Paulik, C., Schaufler, S., Stachl, T., . . . Wagner, W. (2019). Toward Global Soil Moisture Monitoring With Sentinel-1: Harnessing Assets and Overcoming Obstacles. IEEE Transactions on Geoscience and Remote Sensing, 57(1), 520-539. doi:10.1109/TGRS.2018.2858004

Beck, H. E., Pan, M., Lin, P., Seibert, J., van Dijk, A. I. J. M., & Wood, E. F. (2020). Global Fully Distributed Parameter Regionalization Based on Observed Streamflow From 4,229 Headwater Catchments. Journal of Geophysical Research: Atmospheres, 125(17), e2019JD031485. doi:https://doi.org/10.1029/2019JD031485

Die approbierte gedruckte Originalversion dieser Dissertation ist an der TU Wien Bibliothek verfügbar.
The approved original version of this doctoral thesis is available in print at TU Wien Bibliothek.
TU Bibliothek Your knowledge hub WIEN

Beck, H. E., Pan, M., Miralles, D. G., Reichle, R. H., Dorigo, W. A., Hahn, S., . . . Wood, E. F. (2021). Evaluation of 18 satellite- and model-based soil moisture products using in situ measurements from 826 sensors. Hydrol. Earth Syst. Sci., 25(1), 17-40. doi:10.5194/hess-25-17-2021

Bergström, S. (1992). The HBV model – its structure and applications, SMHI Reports RH 4, Swedish Meteorological and Hydrological Institute (SMHI), Norrköping, Sweden.

Bitner, D., Carroll, T., Cline, D., & Romanov, P. (2002). An assessment of the differences between three satellite snow cover mapping techniques. Hydrological Processes, 16(18), 3723-3733. doi:10.1002/hyp.1231

Blöschl, G., Bierkens, M. F. P., Chambel, A., Cudennec, C., Destouni, G., Fiori, A., . . . Zhang, Y. (2019). Twenty-three unsolved problems in hydrology (UPH) – a community perspective. Hydrological Sciences Journal, 64(10), 1141-1158. doi:https://doi.org/10.1080/02626667.2019.1620507

Blöschl, G., & Montanari, A. (2010). Climate change impacts—throwing the dice? Hydrological Processes, 24(3), 374-381. doi:https://doi.org/10.1002/hyp.7574

Blöschl, G., Sivapalan, M., Wagener, T., Viglione, A., & Savenije, H. H. G. (Eds.). (2013). Runoff Prediction in Ungauged Basins – Synthesis across Processes, Places and Scales, Cambridge University Press, Cambridge, UK, 465 pp.

BMLRT: ehyd – Hydrographic data and analyses, available at: https://ehyd.gv.at/

Bouaziz, L. J. E., Fenicia, F., Thirel, G., de Boer-Euser, T., Buitink, J., Brauer, C. C., . . . Hrachowitz, M. (2021). Behind the scenes of streamflow model performance. Hydrol. Earth Syst. Sci., 25(2), 1069-1095. doi:10.5194/hess-25-1069-2021

Brocca, L., Crow, W. T., Ciabatta, L., Massari, C., Rosnay, P. d., Enenkel, M., . . . Wagner, W. (2017). A Review of the Applications of ASCAT Soil Moisture Products. IEEE journal of selected topics in applied earth observations and remote sensing, 10(5), 2285-2306. doi:https://doi.org/10.1109/JSTARS.2017.2651140

Brocca, L., Tarpanelli, A., Moramarco, T., Melone, F., Ratto, S. M., Cauduro, M., . . . Melzer, T. (2013). Soil Moisture Estimation in Alpine Catchments through Modeling and Satellite Observations. Vadose Zone Journal, 12(3), vzj2012.0102. doi:https://doi.org/10.2136/vzj2012.0102

Burn, D. H., & Boorman, D. B. (1993). Estimation of hydrological parameters at ungauged catchments. Journal of Hydrology, 143(3), 429-454. doi:https://doi.org/10.1016/0022-1694(93)90203-L

Bussieres, N., de Seve, D., & Walker, A. E. (2002). Evaluation of MODIS snow cover products over Canadian regions. Paper presented at the Geoscience and Remote Sensing Symposium, 2002. IGARSS'02. 2002 IEEE International.

Chen, F., Crow, W. T., Bindlish, R., Colliander, A., Burgin, M. S., Asanuma, J., & Aida, K. (2018). Global-scale evaluation of SMAP, SMOS and ASCAT soil moisture products using triple collocation. Remote Sensing of Environment, 214, 1-13. doi:https://doi.org/10.1016/j.rse.2018.05.008

Die approbierte gedruckte Originalversion dieser Dissertation ist an der TU Wien Bibliothek verfügbar.
The approved original version of this doctoral thesis is available in print at TU Wien Bibliothek.
TU Bibliothek Your knowledge hub WIEN

Chu, W., Gao, X., & Sorooshian, S. (2011). A new evolutionary search strategy for global optimization of high-dimensional problems. Information Sciences, 181(22), 4909-4927. doi:https://doi.org/10.1016/j.ins.2011.06.024

Clark, M. P., Schaefli, B., Schymanski, S. J., Samaniego, L., Luce, C. H., Jackson, B. M., . . . Ceola, S. (2016). Improving the theoretical underpinnings of process-based hydrologic models. Water Resources Research, 52(3), 2350-2365. doi:https://doi.org/10.1002/2015WR017910

Coll, J., & Li, X. (2018). Comprehensive accuracy assessment of MODIS daily snow cover products and gap filling methods. ISPRS journal of photogrammetry and remote sensing, 144, 435-452.

Crane, R., & Anderson, M. (1984). Satellite discrimination of snow/cloud surfaces. International Journal of Remote Sensing, 5(1), 213-223.

Da Ronco, P., Avanzi, F., De Michele, C., Notarnicola, C., & Schaefli, B. (2020). Comparing MODIS snow products Collection 5 with Collection 6 over Italian Central Apennines. International Journal of Remote Sensing, 41(11), 4174-4205.

Demirel, M. C., Özen, A., Orta, S., Toker, E., Demir, H. K., Ekmekcioğlu, Ö., . . . Sarı, Ö. (2019). Additional value of using satellite-based soil moisture and two sources of groundwater data for hydrological model calibration. Water, 11(10), 2083. doi:https://doi.org/10.3390/w11102083

Didan, K. (2015). MOD13A3 MODIS/Terra vegetation Indices Monthly L3 Global 1 km SIN Grid V006 [September 2002 to August 2014], NASA EOSDIS Land Processes DAAC, https://doi.org/10.5067/MODIS/MOD13A3.006

Dong, C. (2018). Remote sensing, hydrological modeling and in situ observations in snow cover research: A review. Journal of Hydrology, 561, 573-583.

Dong, J., & Peters-Lidard, C. (2010). On the relationship between temperature and MODIS snow cover retrieval errors in the Western US. IEEE journal of selected topics in applied earth observations and remote sensing, 3(1), 132-140.

Dorigo, W., Wagner, W., Albergel, C., Albrecht, F., Balsamo, G., Brocca, L., . . . Lecomte, P. (2017). ESA CCI Soil Moisture for improved Earth system understanding: State-of-the art and future directions. Remote Sensing of Environment, 203, 185-215. doi:https://doi.org/10.1016/j.rse.2017.07.001

Dozier, J. (1989). Spectral signature of alpine snow cover from the landsat thematic mapper. Remote Sensing of Environment, 28, 9-22. doi:10.1016/0034-4257(89)90101-6

Duethmann, D., Peters, J., Blume, T., Vorogushyn, S., & Güntner, A. (2014). The value of satellite - derived snow cover images for calibrating a hydrological model in snow - dominated catchments in Central Asia. Water Resources Research, 50(3), 2002-2021. doi:https://doi.org/10.1002/2013WR014382

Duethmann, D., & Blöschl, G. (2018). Why has catchment evaporation increased in the past 40 years? A data-based study in Austria. Hydrol. Earth Syst. Sci., 22(10), 5143-5158. doi:10.5194/hess-22-5143-2018

Die approbierte gedruckte Originalversion dieser Dissertation ist an der TU Wien Bibliothek verfügbar.
The approved original version of this doctoral thesis is available in print at TU Wien Bibliothek.
TU Bibliothek WIEN Your knowledge hub

Duethmann, D., Blöschl, G., & Parajka, J. (2020). Why does a conceptual hydrological model fail to correctly predict discharge changes in response to climate change? Hydrol. Earth Syst. Sci., 24(7), 3493-3511. doi:https://doi.org/10.5194/hess-24-3493-2020

Dwyer, J., & Schmidt, G. (2006). The MODIS reprojection tool Earth science satellite remote sensing (pp. 162-177): Springer.

Efstratiadis, A., & Koutsoyiannis, D. (2010). One decade of multi-objective calibration approaches in hydrological modelling: a review. Hydrological Sciences Journal, 55(1), 58-78. doi:https://doi.org/10.1080/02626660903526292

El Hajj, M., Baghdadi, N., Zribi, M., Rodríguez-Fernández, N., Wigneron, J. P., Al-Yaari, A., . . . Calvet, J.-C. (2018). Evaluation of SMOS, SMAP, ASCAT and Sentinel-1 soil moisture products at sites in Southwestern France. Remote Sensing, 10(4), 569. doi:https://doi.org/10.3390/rs10040569

Finger, D., Vis, M., Huss, M., & Seibert, J. (2015). The value of multiple data set calibration versus model complexity for improving the performance of hydrological models in mountain catchments. Water Resources Research, 51(4), 1939-1958. doi:https://doi.org/10.1002/2014wr015712

Franz, K. J., & Karsten, L. R. (2013). Calibration of a distributed snow model using MODIS snow covered area data. Journal of Hydrology, 494, 160-175. doi:https://doi.org/10.1016/j.jhydrol.2013.04.026

Gao, Y., Xie, H., Yao, T., & Xue, C. (2010). Integrated assessment on multi-temporal and multi-sensor combinations for reducing cloud obscuration of MODIS snow cover products of the Pacific Northwest USA. Remote Sensing of Environment, 114(8), 1662-1675.

Gladkova, I., Grossberg, M. D., Shahriar, F., Bonev, G., & Romanov, P. (2012). Quantitative restoration for MODIS band 6 on Aqua. IEEE Transactions on Geoscience and Remote Sensing, 50(6), 2409-2416.

Grayson, R., & Blöschl, G. (2001). Spatial patterns in catchment hydrology: observations and modelling: CUP Archive.

Gruber, A., De Lannoy, G., Albergel, C., Al-Yaari, A., Brocca, L., Calvet, J. C., . . . Wagner, W. (2020). Validation practices for satellite soil moisture retrievals: What are (the) errors? Remote Sensing of Environment, 244, 111806. doi:https://doi.org/10.1016/j.rse.2020.111806

Guo, Y., Zhang, Y., Zhang, L., & Wang, Z. (2021). Regionalization of hydrological modeling for predicting streamflow in ungauged catchments: A comprehensive review. WIREs Water, 8(1), e1487. doi:https://doi.org/10.1002/wat2.1487

Hahn, S., Wagner, W., Steele-Dunne, S. C., Vreugdenhil, M., & Melzer, T. (2020). Improving ASCAT Soil Moisture Retrievals With an Enhanced Spatially Variable Vegetation Parameterization. IEEE Transactions on Geoscience and Remote Sensing, 1-16. doi:10.1109/TGRS.2020.3041340

Hall, D. K., Kelly, R. E., Riggs, G. A., Chang, A. T., & Foster, J. L. (2002). Assessment of the relative accuracy of hemispheric-scale snow-cover maps. Annals of Glaciology, 34, 24-30.

Hall, D. K., & Riggs, G. A. (2007). Accuracy assessment of the MODIS snow products. Hydrological Processes: An International Journal, 21(12), 1534-1547.

Die approbierte gedruckte Originalversion dieser Dissertation ist an der TU Wien Bibliothek verfügbar.
The approved original version of this doctoral thesis is available in print at TU Wien Bibliothek.
TU Bibliothek Your knowledge hub WIEN

Hall, D. K., & Riggs, G. A. (2011). Normalized-Difference Snow Index (NDSI). In V. P. Singh, P. Singh, & U. K. Haritashya (Eds.), Encyclopedia of Snow, Ice and Glaciers (pp. 779-780). Dordrecht: Springer Netherlands.

Hall, D. K., & Riggs, G. A. (2016a). MODIS/Aqua Snow Cover Daily L3 Global 500m Grid, Version 6. [September 2002 to August 2014]. Boulder, Colorado USA. NASA National Snow and Ice Data Center Distributed Active Archive Center. https://doi.org/10.5067/MODIS/MYD10A1.006

Hall, D. K., & Riggs, G. A. (2016b). MODIS/Terra Snow Cover Daily L3 Global 500m Grid, Version 6. [September 2002 to August 2014]. Boulder, Colorado USA. NASA National Snow and Ice Data Center Distributed Active Archive Center. https://doi.org/10.5067/MODIS/MOD10A1.006

Hall, D. K., Riggs, G. A., DiGirolamo, N. E., & Román, M. O. (2019). Evaluation of MODIS and VIIRS cloud-gap-filled snow-cover products for production of an Earth science data record. Hydrol. Earth Syst. Sci., 23(12), 5227-5241. doi:10.5194/hess-23-5227-2019

Hall, D. K., Riggs, G. A., Salomonson, V. V., & Scharfen, G. R. (2000). Early results from the Moderate resolution Imaging Spectroradiometer (MODIS) global snow and ice cover products. Paper presented at the Geoscience and Remote Sensing Symposium, 2000. Proceedings. IGARSS 2000. IEEE 2000 International.

Han, P., Long, D., Han, Z., Du, M., Dai, L., & Hao, X. (2019). Improved understanding of snowmelt runoff from the headwaters of China's Yangtze River using remotely sensed snow products and hydrological modeling. Remote Sensing of Environment, 224, 44-59. doi:https://doi.org/10.1016/j.rse.2019.01.041

Härer, S., Bernhardt, M., Siebers, M., & Schulz, K. (2018). On the need for a time-and location-dependent estimation of the NDSI threshold value for reducing existing uncertainties in snow cover maps at different scales. The Cryosphere, 12(5), 1629-1642.

He, Y., Bárdossy, A., & Zehe, E. (2011). A review of regionalisation for continuous streamflow simulation. Hydrol. Earth Syst. Sci., 15(11), 3539-3553. doi:10.5194/hess-15-3539-2011

Hiebl, J., & Frei, C. (2016). Daily temperature grids for Austria since 1961—concept, creation and applicability. Theoretical and applied climatology, 124(1-2), 161-178. doi:https://doi.org/10.1007/s00704-015-1411-4

Hiebl, J., & Frei, C. (2018). Daily precipitation grids for Austria since 1961—Development and evaluation of a spatial dataset for hydroclimatic monitoring and modelling. Theoretical and applied climatology, 132(1-2), 327-345. doi:https://doi.org/10.1007/s00704-017-2093-x

Hirsch, R. M., Helsel, D. R., Cohn, T. A., & Gilroy, E. J. (1992). Statistical analysis of hydrological data, in: Handbook of Hydrology, edited by: Maidment, R., McGraw-Hill, New York, 17.1–17.55.

Hrachowitz, M., Savenije, H. H. G., Blöschl, G., McDonnell, J. J., Sivapalan, M., Pomeroy, J. W., . . . Cudennec, C. (2013). A decade of Predictions in Ungauged Basins (PUB)—a review. Hydrological Sciences Journal, 58(6), 1198-1255. doi:https://doi.org/10.1080/02626667.2013.803183

Huang, Q., Qin, G., Zhang, Y., Tang, Q., Liu, C., Xia, J., . . . Post, D. (2020). Using Remote Sensing Data-Based Hydrological Model Calibrations for Predicting Runoff in Ungauged or Poorly Gauged Catchments. Water Resources Research, 56(8), e2020WR028205. doi:https://doi.org/10.1029/2020WR028205

Die approbierte gedruckte Originalversion dieser Dissertation ist an der TU Wien Bibliothek verfügbar.
The approved original version of this doctoral thesis is available in print at TU Wien Bibliothek.
TU Bibliothek WIEN Your knowledge hub

HZB (1992). Anleitung zur Beobachtung und Messung von meteorologischen Parametern zur Erfassung des Wasserkreislaufes im Rahmen des Hydrographischen Dienstes in Österreich, (Guidelines of the Hydrographic Service in Austria for observing and measuring meteorological parameters for assessing the water cycle), Federal Ministry of Agriculture and Forestry, Vienna.

Immerzeel, W., & Droogers, P. (2008). Calibration of a distributed hydrological model based on satellite evapotranspiration. Journal of Hydrology, 349(3-4), 411-424. doi:https://doi.org/10.1016/j.jhydrol.2007.11.017

Kavetski, D., Kuczera, G., & Franks, S. W. (2006). Bayesian analysis of input uncertainty in hydrological modeling: 1. Theory. Water Resources Research, 42(3). doi:https://doi.org/10.1029/2005WR004368

Kim, H., Wigneron, J.-P., Kumar, S., Dong, J., Wagner, W., Cosh, M. H., . . . Lakshmi, V. (2020). Global scale error assessments of soil moisture estimates from microwave-based active and passive satellites and land surface models over forest and mixed irrigated/dryland agriculture regions. Remote Sensing of Environment, 251, 112052. doi:https://doi.org/10.1016/j.rse.2020.112052

Klein, A. G., & Barnett, A. C. (2003). Validation of daily MODIS snow cover maps of the Upper Rio Grande River Basin for the 2000–2001 snow year. Remote Sensing of Environment, 86(2), 162-176.

Kosugi, K. i. (1994). Three-parameter lognormal distribution model for soil water retention. Water Resources Research, 30(4), 891-901. doi:https://doi.org/10.1029/93wr02931

Kosugi, K. i. (1996). Lognormal Distribution Model for Unsaturated Soil Hydraulic Properties. Water Resources Research, 32(9), 2697-2703. doi:https://doi.org/10.1029/96wr01776

Kovacs, A., Honti, M., Zessner, M., Eder, A., Clement, A., & Blöschl, G. (2012). Identification of phosphorus emission hotspots in agricultural catchments. Science of the Total Environment, 433, 74-88. doi:https://doi.org/10.1016/j.scitotenv.2012.06.024

Kraatz, S., Khanbilvardi, R., & Romanov, P. (2017). A comparison of MODIS/VIIRS cloud masks over ice-bearing river: on achieving consistent cloud masking and improved river ice mapping. Remote Sensing, 9(3), 229.

Krajčí, P., Holko, L., Perdigão, R. A., & Parajka, J. (2014). Estimation of regional snowline elevation (RSLE) from MODIS images for seasonally snow covered mountain basins. Journal of Hydrology, 519, 1769-1778.

Kundu, D., Vervoort, R. W., & van Ogtrop, F. F. (2017). The value of remotely sensed surface soil moisture for model calibration using SWAT. Hydrological Processes, 31(15), 2764-2780. doi:https://doi.org/10.1002/hyp.11219

Kunnath-Poovakka, A., Ryu, D., Renzullo, L., & George, B. (2016). The efficacy of calibrating hydrologic model using remotely sensed evapotranspiration and soil moisture for streamflow prediction. Journal of Hydrology, 535, 509-524. doi:https://doi.org/10.1016/j.jhydrol.2016.02.018

Lebecherel, L., Andréassian, V., & Perrin, C. (2016). On evaluating the robustness of spatial-proximity-based regionalization methods. Journal of Hydrology, 539, 196-203. doi:https://doi.org/10.1016/j.jhydrol.2016.05.031

Die approbierte gedruckte Originalversion dieser Dissertation ist an der TU Wien Bibliothek verfügbar.
The approved original version of this doctoral thesis is available in print at TU Wien Bibliothek.
TU Bibliothek Your knowledge hub WIEN

Li, H., & Zhang, Y. (2017). Regionalising rainfall-runoff modelling for predicting daily runoff: Comparing gridded spatial proximity and gridded integrated similarity approaches against their lumped counterparts. Journal of Hydrology, 550, 279-293. doi:https://doi.org/10.1016/j.jhydrol.2017.05.015

Li, Y., Grimaldi, S., Pauwels, V. R., & Walker, J. P. (2018). Hydrologic model calibration using remotely sensed soil moisture and discharge measurements: The impact on predictions at gauged and ungauged locations. Journal of Hydrology, 557, 897-909. doi:https://doi.org/10.1016/j.jhydrol.2018.01.013

Liang, T., Huang, X., Wu, C., Liu, X., Li, W., Guo, Z., & Ren, J. (2008). An application of MODIS data to snow cover monitoring in a pastoral area: A case study in Northern Xinjiang, China. Remote Sensing of Environment, 112(4), 1514-1526. doi:10.1016/j.rse.2007.06.001

Lo, M. H., Famiglietti, J. S., Yeh, P. F., & Syed, T. (2010). Improving parameter estimation and water table depth simulation in a land surface model using GRACE water storage and estimated base flow data. Water Resources Research, 46(5). doi:https://doi.org/10.1029/2009WR007855

Long, D., Bai, L., Yan, L., Zhang, C., Yang, W., Lei, H., . . . Shi, C. (2019). Generation of spatially complete and daily continuous surface soil moisture of high spatial resolution. Remote Sensing of Environment, 233, 111364. doi:https://doi.org/10.1016/j.rse.2019.111364

López, P. L., Sutanudjaja, E. H., Schellekens, J., Sterk, G., & Bierkens, M. F. (2017). Calibration of a large-scale hydrological model using satellite-based soil moisture and evapotranspiration products. Hydrology and Earth System Sciences, 21(6), 3125-3144. doi:https://doi.org/10.5194/hess-21-3125-2017

Lyapustin, A., Wang, Y., Xiong, X., Meister, G., Platnick, S., Levy, R., . . . Angal, A. (2014). Scientific impact of MODIS C5 calibration degradation and C6+ improvements. Atmospheric Measurement Techniques, 7(12), 4353-4365. doi:10.5194/amt-7-4353-2014

Marchane, A., Jarlan, L., Hanich, L., Boudhar, A., Gascoin, S., Tavernier, A., . . . Berjamy, B. (2015). Assessment of daily MODIS snow cover products to monitor snow cover dynamics over the Moroccan Atlas mountain range. Remote Sensing of Environment, 160, 72-86. doi:10.1016/j.rse.2015.01.002

Merz, R., & Blöschl, G. (2004). Regionalisation of catchment model parameters. Journal of Hydrology, 287(1), 95-123. doi:https://doi.org/10.1016/j.jhydrol.2003.09.028

Merz, R., & Blöschl, G. (2009). A regional analysis of event runoff coefficients with respect to climate and catchment characteristics in Austria. Water Resources Research, 45(1). doi:https://doi.org/10.1029/2008wr007163

Merz, R., Parajka, J., & Blöschl, G. (2011). Time stability of catchment model parameters: Implications for climate impact analyses. Water Resources Research, 47(2). doi:https://doi.org/10.1029/2010wr009505

Milzow, C., Krogh, P. E., & Bauer-Gottwein, P. (2011). Combining satellite radar altimetry, SAR surface soil moisture and GRACE total storage changes for hydrological model calibration in a large poorly gauged catchment. Hydrol. Earth Syst. Sci., 15(6), 1729-1743. doi:https://doi.org/10.5194/hess-15-1729-2011

Die approbierte gedruckte Originalversion dieser Dissertation ist an der TU Wien Bibliothek verfügbar.
The approved original version of this doctoral thesis is available in print at TU Wien Bibliothek.
TU WIEN Bibliothek Your knowledge hub

Mishra, V., Negi, H., Rawat, A., Chaturvedi, A., & Singh, R. P. (2009). Retrieval of sub-pixel snow cover information in the Himalayan region using medium and coarse resolution remote sensing data. International Journal of Remote Sensing, 30(18), 4707-4731.

Mousa, B. G., & Shu, H. (2020). Spatial Evaluation and Assimilation of SMAP, SMOS, and ASCAT Satellite Soil Moisture Products Over Africa Using Statistical Techniques. Earth and Space Science, 7(1), e2019EA000841. doi:https://doi.org/10.1029/2019ea000841

Naeimi, V., Scipal, K., Bartalis, Z., Hasenauer, S., & Wagner, W. (2009). An Improved Soil Moisture Retrieval Algorithm for ERS and METOP Scatterometer Observations. IEEE Transactions on Geoscience and Remote Sensing, 47(7), 1999-2013. doi:https://doi.org/10.1109/TGRS.2008.2011617

Naeini, M. R., Yang, T., Sadegh, M., AghaKouchak, A., Hsu, K.-l., Sorooshian, S., . . . Lei, X. (2018). Shuffled complex-self adaptive hybrid evolution (SC-SAHEL) optimization framework. Environmental Modelling & Software, 104, 215-235. doi:https://doi.org/10.1016/j.envsoft.2018.03.019

Narbondo, S., Gorgoglione, A., Crisci, M., & Chreties, C. (2020). Enhancing Physical Similarity Approach to Predict Runoff in Ungauged Watersheds in Sub-Tropical Regions. Water, 12(2), 528. doi:https://doi.org/10.3390/w12020528

Nash, J. E., & Sutcliffe, J. V. (1970). River flow forecasting through conceptual models part I—A discussion of principles. Journal of Hydrology, 10(3), 282-290. doi:https://doi.org/10.1016/0022-1694(70)90255-6

Neri, M., Parajka, J., & Toth, E. (2020). Importance of the informative content in the study area when regionalising rainfall-runoff model parameters: the role of nested catchments and gauging station density. Hydrol. Earth Syst. Sci., 24(11), 5149-5171. doi:10.5194/hess-24-5149-2020

Nijzink, R. C., Almeida, S., Pechlivanidis, I. G., Capell, R., Gustafssons, D., Arheimer, B., . . . Hrachowitz, M. (2018). Constraining Conceptual Hydrological Models With Multiple Information Sources. Water Resources Research, 54(10), 8332-8362. doi:https://doi.org/10.1029/2017wr021895

Parajka, J., Merz, R., and Blöschl, G. (2003) Estimation of daily potential evapotranspiration for regional water balance modeling in Austria, in: 11th International Poster Day and Institute of Hydrology Open Day “Transport ofWater, Chemicals and Energy in the Soil – Crop Canopy – Atmosphere System”, Slovak Academy of Sciences, 20 November 2003, Bratislava, 299–306.

Parajka, J., Merz, R., & Blöschl, G. (2005). A comparison of regionalisation methods for catchment model parameters. Hydrol. Earth Syst. Sci., 9(3), 157-171. doi:10.5194/hess-9-157-2005

Parajka, J., & Blöschl, G. (2006). Validation of MODIS snow cover images over Austria. Hydrol. Earth Syst. Sci., 10(5), 679-689. doi:10.5194/hess-10-679-2006

Parajka, J., Naeimi, V., Blöschl, G., Wagner, W., Merz, R., & Scipal, K. (2006). Assimilating scatterometer soil moisture data into conceptual hydrologic models at the regional scale. Hydrol. Earth Syst. Sci., 10(3), 353-368. doi:https://doi.org/10.5194/hess-10-353-2006

Parajka, J., Merz, R., & Blöschl, G. (2007). Uncertainty and multiple objective calibration in regional water balance modelling: case study in 320 Austrian catchments. Hydrological Processes, 21(4), 435-446. doi:https://doi.org/10.1002/hyp.6253

Die approbierte gedruckte Originalversion dieser Dissertation ist an der TU Wien Bibliothek verfügbar.
The approved original version of this doctoral thesis is available in print at TU Wien Bibliothek.
TU Bibliothek Your knowledge hub WIEN

Parajka, J., & Blöschl, G. (2008a). Spatio - temporal combination of MODIS images - potential for snow cover mapping. Water Resources Research, 44(3).

Parajka, J., & Blöschl, G. (2008b). The value of MODIS snow cover data in validating and calibrating conceptual hydrologic models. Journal of Hydrology, 358(3-4), 240-258. doi:https://doi.org/10.1016/j.jhydrol.2008.06.006

Parajka, J., Naeimi, V., Blöschl, G., & Komma, J. (2009). Matching ERS scatterometer based soil moisture patterns with simulations of a conceptual dual layer hydrologic model over Austria. Hydrol. Earth Syst. Sci., 13(2), 259-271. doi:https://doi.org/10.5194/hess-13-259-2009

Parajka, J., Kohnová, S., Merz, R., Szolgay, J., Hlavčová, K., & Blöschl, G. (2009). Comparative analysis of the seasonality of hydrological characteristics in Slovakia and Austria/Analyse comparative de la saisonnalité de caractéristiques hydrologiques en Slovaquie et en Autriche. Hydrological Sciences Journal, 54(3), 456-473.

Parajka, J., Holko, L., Kostka, Z., & Blöschl, G. (2012). MODIS snow cover mapping accuracy in a small mountain catchment–comparison between open and forest sites. Hydrology and Earth System Sciences, 16(7), 2365-2377.

Parajka, J., Viglione, A., Rogger, M., Salinas, J. L., Sivapalan, M., & Blöschl, G. (2013). Comparative assessment of predictions in ungauged basins – Part 1: Runoff-hydrograph studies. Hydrol. Earth Syst. Sci., 17(5), 1783-1795. doi:https://doi.org/10.5194/hess-17-1783-2013

Parajka, J., Merz, R., Skøien, J. O., & Viglione, A. (2015). The role of station density for predicting daily runoff by top-kriging interpolation in Austria. Journal of Hydrology and Hydromechanics, 63(3), 228-234. doi:https://doi.org/10.1515/johh-2015-0024

Paulik, C., Dorigo, W., Wagner, W., & Kidd, R. (2014). Validation of the ASCAT Soil Water Index using in situ data from the International Soil Moisture Network. International Journal of Applied Earth Observation and Geoinformation, 30, 1-8. doi:https://doi.org/10.1016/j.jag.2014.01.007

Pfeil, I., Vreugdenhil, M., Hahn, S., Wagner, W., Strauss, P., & Blöschl, G. (2018). Improving the seasonal representation of ASCAT soil moisture and vegetation dynamics in a temperate climate. Remote Sensing, 10(11), 1788. doi:https://doi.org/10.3390/rs10111788

Pu, Z., Xu, L., & Salomonson, V. V. (2007). MODIS/Terra observed seasonal variations of snow cover over the Tibetan Plateau. Geophysical Research Letters, 34(6). doi:10.1029/2007gl029262

Rajib, M. A., Merwade, V., & Yu, Z. (2016). Multi-objective calibration of a hydrologic model using spatially distributed remotely sensed/in-situ soil moisture. Journal of Hydrology, 536, 192-207. doi:https://doi.org/10.1016/j.jhydrol.2016.02.037

Rakovec, O., Kumar, R., Attinger, S., & Samaniego, L. (2016). Improving the realism of hydrologic model functioning through multivariate parameter estimation. Water Resources Research, 52(10), 7779-7792. doi:https://doi.org/10.1002/2016WR019430

Riggs, G.A., Hall, D.K., & Román, M.O. (2016). MODIS snow products user guide for Collection 6. https://nsidc.org/sites/nsidc.org/files/files/MODIS-snow-user-guide-C6.pdf.

Die approbierte gedruckte Originalversion dieser Dissertation ist an der TU Wien Bibliothek verfügbar.
The approved original version of this doctoral thesis is available in print at TU Wien Bibliothek.
TU Bibliothek Your knowledge hub WIEN

Riggs, G. A., Hall, D. K., & Román, M. O. (2017). Overview of NASA's MODIS and Visible Infrared Imaging Radiometer Suite (VIIRS) snow-cover Earth System Data Records. Earth System Science Data, 9(2), 765-777.

Rittger, K., Painter, T. H., & Dozier, J. (2013). Assessment of methods for mapping snow cover from MODIS. Advances in Water Resources, 51, 367-380. doi:10.1016/j.advwatres.2012.03.002

Sachs, J. D., & McArthur, J. W. (2005). The Millennium Project: a plan for meeting the Millennium Development Goals. The Lancet, 365(9456), 347-353. doi:https://doi.org/10.1016/S0140-6736(05)17791-5

Seibert, J. (2000). Multi-criteria calibration of a conceptual runoff model using a genetic algorithm. Hydrol. Earth Syst. Sci., 4(2), 215-224. doi:https://doi.org/10.5194/hess-4-215-2000

Simic, A., Fernandes, R., Brown, R., Romanov, P., & Park, W. (2004). Validation of VEGETATION, MODIS, and GOES+ SSM/I snow-cover products over Canada based on surface snow depth observations. Hydrological Processes, 18(6), 1089-1104. doi:10.1002/hyp.5509

Sleziak, P., Szolgay, J., Hlavčová, K., Duethmann, D., Parajka, J., & Danko, M. (2018). Factors controlling alterations in the performance of a runoff model in changing climate conditions. Journal of Hydrology and Hydromechanics, 66(4), 381. doi:https://doi.org/10.2478/johh-2018-0031

Sleziak, P., Szolgay, J., Hlavčová, K., Danko, M., & Parajka, J. (2020). The effect of the snow weighting on the temporal stability of hydrologic model efficiency and parameters. Journal of Hydrology, 583, 124639. doi:https://doi.org/10.1016/j.jhydrol.2020.124639

Stillinger, T., Roberts, D. A., Collar, N. M., & Dozier, J. (2019). Cloud masking for Landsat 8 and MODIS Terra over snow‐covered terrain: Error analysis and spectral similarity between snow and cloud. Water Resources Research, 55(7), 6169-6184.

Sutanudjaja, E. H., van Beek, L. P. H., de Jong, S. M., van Geer, F. C., & Bierkens, M. F. P. (2014). Calibrating a large-extent high-resolution coupled groundwater-land surface model using soil moisture and discharge data. Water Resources Research, 50(1), 687-705. doi:https://doi.org/10.1002/2013wr013807

Széles, B., Parajka, J., Hogan, P., Silasari, R., Pavlin, L., Strauss, P., & Blöschl, G. (2020). The Added Value of Different Data Types for Calibrating and Testing a Hydrologic Model in a Small Catchment. Water Resources Research, 56(10), e2019WR026153. doi:https://doi.org/10.1029/2019WR026153

Széles, B., Parajka, J., Hogan, P., Silasari, R., Pavlin, L., Strauss, P., & Blöschl, G. (2021). Stepwise prediction of runoff using proxy data in a small agricultural catchment. Journal of Hydrology and Hydromechanics, 69(1), 65-75. doi: https://doi.org/10.2478/johh-2020-0029

Tang, Q., & Lettenmaier, D. P. (2010). Use of satellite snow-cover data for streamflow prediction in the Feather River Basin, California. International Journal of Remote Sensing, 31(14), 3745-3762. doi:10.1080/01431161.2010.483493

Tegegne, G., & Kim, Y.-O. (2018). Modelling ungauged catchments using the catchment runoff response similarity. Journal of Hydrology, 564, 452-466. doi:https://doi.org/10.1016/j.jhydrol.2018.07.042

Die approbierte gedruckte Originalversion dieser Dissertation ist an der TU Wien Bibliothek verfügbar.
The approved original version of this doctoral thesis is available in print at TU Wien Bibliothek.
TU Bibliothek Your knowledge hub WIEN

Tong, R., Parajka, J., Komma, J., & Blöschl, G. (2020). Mapping snow cover from daily Collection 6 MODIS products over Austria. Journal of Hydrology, 590, 125548. doi:https://doi.org/10.1016/j.jhydrol.2020.125548

Tong, R., Parajka, J., Salentinig, A., Pfeil, I., Komma, J., Széles, B., . . . Blöschl, G. (2021). The value of ASCAT soil moisture and MODIS snow cover data for calibrating a conceptual hydrologic model. Hydrol. Earth Syst. Sci., 25(3), 1389-1410. doi:10.5194/hess-25-1389-2021

Trautmann, T., Koirala, S., Carvalhais, N., Eicker, A., Fink, M., Niemann, C., & Jung, M. (2018). Understanding terrestrial water storage variations in northern latitudes across scales. Hydrol. Earth Syst. Sci., 22(7), 4061-4082. doi:https://doi.org/10.5194/hess-22-4061-2018

Udnæs, H.-C., Alfnes, E., & Andreassen, L. M. (2007). Improving runoff modelling using satellite-derived snow covered area? Hydrology Research, 38(1), 21-32. doi:https://doi.org/10.2166/nh.2007.032

Vergopolan, N., Chaney, N. W., Beck, H. E., Pan, M., Sheffield, J., Chan, S., & Wood, E. F. (2020). Combining hyper-resolution land surface modeling with SMAP brightness temperatures to obtain 30-m soil moisture estimates. Remote Sensing of Environment, 242, 111740. doi:https://doi.org/10.1016/j.rse.2020.111740

Viglione, A., Parajka, J., Rogger, M., Salinas, J., Laaha, G., Sivapalan, M., & Blöschl, G. (2013). Comparative assessment of predictions in ungauged basins-Part 3: Runoff signatures in Austria. Hydrology and Earth System Sciences, 17(6), 2263. doi:https://doi.org/10.5194/hess-17-2263-2013

Viglione, A. & Parajka, J. (2020) TUWmodel: Lumped/Semi-Distributed Hydrological Model for Education Purposes. R package version 1.1-1. https://CRAN.R-project.org/package=TUWmodel.

Wagener, T., & Montanari, A. (2011). Convergence of approaches toward reducing uncertainty in predictions in ungauged basins. Water Resources Research, 47(6). doi:https://doi.org/10.1029/2010WR009469

Wagner, W., Brocca, L., Naeimi, V., Reichle, R., Draper, C., Jeu, R. d., . . . Paulik, C. (2014). Clarifications on the "Comparison Between SMOS, VUA, ASCAT, and ECMWF Soil Moisture Products Over Four Watersheds in U.S.". IEEE Transactions on Geoscience and Remote Sensing, 52(3), 1901-1906. doi:https://doi.org/10.1109/TGRS.2013.2282172

Wagner, W., Hahn, S., Kidd, R., Melzer, T., Bartalis, Z., Hasenauer, S., . . . Schneider, S. (2013). The ASCAT soil moisture product: A review of its specifications, validation results, and emerging applications. Meteorologische Zeitschrift, 22(1), 5-33. doi:https://doi.org/10.1127/0941-2948/2013/0399

Wagner, W., Lemoine, G., Borgeaud, M., & Rott, H. (1999a). A study of vegetation cover effects on ERS scatterometer data. IEEE Transactions on Geoscience and Remote Sensing, 37(2), 938-948. doi:https://doi.org/10.1109/36.752212

Wagner, W., Lemoine, G., & Rott, H. (1999b). A Method for Estimating Soil Moisture from ERS Scatterometer and Soil Data. Remote Sensing of Environment, 70(2), 191-207. doi:https://doi.org/10.1016/S0034-4257(99)00036-X

Die approbierte gedruckte Originalversion dieser Dissertation ist an der TU Wien Bibliothek verfügbar.
The approved original version of this doctoral thesis is available in print at TU Wien Bibliothek.
TU Bibliothek Your knowledge hub WIEN

Wanders, N., Bierkens, M. F. P., de Jong, S. M., de Roo, A., & Karssenberg, D. (2014). The benefits of using remotely sensed soil moisture in parameter identification of large-scale hydrological models. Water Resources Research, 50(8), 6874-6891. doi:https://doi.org/10.1002/2013wr014639

Wang, J., Li, H., & Hao, X. (2010). Responses of snowmelt runoff to climatic change in an inland river basin, Northwestern China, over the past 50 years. Hydrology and Earth System Sciences, 14(10), 1979-1987.

Wang, L., Qu, J. J., Xiong, X., Hao, X., Xie, Y., & Che, N. (2006). A new method for retrieving band 6 of Aqua MODIS. IEEE Geoscience and Remote Sensing Letters, 3(2), 267-270.

Wang, X., Wang, J., Che, T., Huang, X., Hao, X., & Li, H. (2018). Snow cover mapping for complex mountainous forested environments based on a multi-index technique. IEEE journal of selected topics in applied earth observations and remote sensing, 11(5), 1433-1441.

Wang, X., Xie, H., & Liang, T. (2008). Evaluation of MODIS snow cover and cloud mask and its application in Northern Xinjiang, China. Remote Sensing of Environment, 112(4), 1497-1513. doi:10.1016/j.rse.2007.05.016

Wang, X., Xie, H., Liang, T., & Huang, X. (2009). Comparison and validation of MODIS standard and new combination of Terra and Aqua snow cover products in northern Xinjiang, China. Hydrological Processes: An International Journal, 23(3), 419-429.

Werth, S., & Güntner, A. (2010). Calibration analysis for water storage variability of the global hydrological model WGHM. Hydrology and Earth System Sciences, 14(1), 59-78. doi:https://doi.org/10.5194/hess-14-59-2010

Wolfe, R. E., Nishihama, M., Fleig, A. J., Kuyper, J. A., Roy, D. P., Storey, J. C., & Patt, F. S. (2002). Achieving sub-pixel geolocation accuracy in support of MODIS land science. Remote Sensing of Environment, 83(1-2), 31-49.

Xu, J., Zhang, F., Shu, H., & Zhong, K. (2017). Improvement of the Snow Depth in the Common Land Model by Coupling a Two-Dimensional Deterministic Ensemble Model with a Variational Hybrid Snow Cover Fraction Data Assimilation Scheme and a New Observation Operator. Journal of Hydrometeorology, 18(1), 119-138. doi:10.1175/jhm-d-16-0149.1

Yang, J., Jiang, L., Ménard, C. B., Luojus, K., Lemmetyinen, J., & Pulliainen, J. (2015). Evaluation of snow products over the Tibetan Plateau. Hydrological Processes, 29(15), 3247-3260.

Yang, X., Magnusson, J., Rizzi, J., & Xu, C.-Y. (2017). Runoff prediction in ungauged catchments in Norway: comparison of regionalization approaches. Hydrology Research, 49(2), 487-505. doi:https://doi.org/10.2166/nh.2017.071

Yang, X., Magnusson, J., Huang, S., Beldring, S., & Xu, C.-Y. (2020). Dependence of regionalization methods on the complexity of hydrological models in multiple climatic regions. Journal of Hydrology, 582, 124357. doi:https://doi.org/10.1016/j.jhydrol.2019.124357

Zhang, H., Zhang, F., Zhang, G., Che, T., Yan, W., Ye, M., & Ma, N. (2019). Ground-based evaluation of MODIS snow cover product V6 across China: Implications for the selection of NDSI threshold. Science of the Total Environment, 651, 2712-2726.

Die approbierte gedruckte Originalversion dieser Dissertation ist an der TU Wien Bibliothek verfügbar.
The approved original version of this doctoral thesis is available in print at TU Wien Bibliothek.
TU Bibliothek Your knowledge hub WIEN

Zhang, Y., Chiew, F. H., Zhang, L., & Li, H. (2009). Use of remotely sensed actual evapotranspiration to improve rainfall–runoff modeling in Southeast Australia. Journal of Hydrometeorology, 10(4), 969-980. doi:https://doi.org/10.1175/2009JHM1061.1

Zhang, Y., Chiew, F. H. S., Liu, C., Tang, Q., Xia, J., Tian, J., . . . Li, C. (2020). Can Remotely Sensed Actual Evapotranspiration Facilitate Hydrological Prediction in Ungauged Regions Without Runoff Calibration? Water Resources Research, 56(1), e2019WR026236. doi:https://doi.org/10.1029/2019WR026236

Zhang, Y., & Marcel, G. S. (2018). A High-Resolution Global Map of Soil Hydraulic Properties Produced by a Hierarchical Parameterization of a Physically-Based Water Retention Model. Retrieved from: https://doi.org/10.7910/DVN/UI5LCE

Zhang, Y., Schaap, M. G., & Zha, Y. (2018). A High-Resolution Global Map of Soil Hydraulic Properties Produced by a Hierarchical Parameterization of a Physically Based Water Retention Model. Water Resources Research, 54(12), 9774-9790. doi:https://doi.org/10.1029/2018wr023539

Die approbierte gedruckte Originalversion dieser Dissertation ist an der TU Wien Bibliothek verfügbar.
The approved original version of this doctoral thesis is available in print at TU Wien Bibliothek.
TU Bibliothek Your knowledge hub WIEN